Escola Tècnica Superior
d'Enginyeria Industrial de Barcelona
UNIVERSITAT POLITÈCNICA DE CATALUNYA

PhD Thesis

FORMULATION OF ANTICORROSIVE PAINTS EMPLOYING CONDUCTING POLYMERS

MIREIA MARTÍ BARROSO

Supervisors:

Dr. Elaine Armelin Diggroc

Dr. Carlos Alemán Llansó

BARCELONA, JUNE 2013

DEPARTAMENT D'ENGINYERIA QUÍMICA
GRUP D'INNOVACIÓ EN MATERIALS I ENGINYERIA MOLECULAR (IMEM)

Als que hi són i hi seran fins al final,
als que ja no hi són, però van ser-hi fins al final.

Acknowledgements

I am heartily thankful to my supervisors, Elaine Armelin and Carlos Alemán, for their encouragement, guidance and support from the start to the end of this project.

I also would like to thank specially Dr. A. Meneguzzi for his assistance with the Raman analysis, David Aradilla for the SEM measurements, Mª Teresa Casas for TEM microscopy and Dr. D.S. Azambuja and Georgina Fabregat for electrochemical measurements.

Lastly, I offer my gratitude to all of those who supported me during the completion of the project, especially to all IMEM's Group and Chemical Engineering Department, family, friends and workmates.

This work has been supported by MICINN (nowadays MINECO) and FEDER funds with projects MAT2009-09138 and MAT2012-34498, by ACC1Ó/CIDEM/COPCA with grant VALTEC08-2-0019 and by the ICREA ACADEMIA program.

Glossary

AIBN:	Azoisobutyronitrile
Alkyd-PAniEB/0.3:	Alkyd primer with 0.3 wt.% of polyaniline emeraldine base
Alkyd-PAniES/1:	Alkyd primer with 1 wt.% of polyaniline emeraldine salt
Alkyd-PTE/1:	Alkyd primer with 1 wt.% of poly[2,2'-(3-methylacetate) thiophene]
Alkyd-Zinc/10:	Alkyd primer with 10 wt.% of zinc phosphate
CP:	Conducting polymer
CPE:	Constant phase element
CPE_c:	Coating capacitance
CPE_{IL}:	Metal/coating interface capacitance
CPVC:	Critical pigment volume concentration
C_s:	System capacitance
DBSA:	Dodecylbenzene sulphonic acid
DFT:	Dry film thickness
DGEBA:	Diglycidyl ether of bisphenol A
DGEBF:	Diglycidyl ether of bisphenol F
DMSO:	Dimethyl sulfoxide
DSC:	Differential scanning calorimetry
E:	Electrode potential
E:	Elastic (or Young) modulus
EC:	Equivalent circuit
EIS:	Electrochemical impedance spectroscopy
EDX:	Energy dispersive X-ray
EP-0:	Epoxy primer supplied by Pinturas Hempel S.A. completely free of anticorrosive pigments and additives
EP/PAniEB-0.3:	EP-0 primer with 0.3 wt.% of PAni-EB
EP/PT3AME-0.3:	EP-0 primer with 0.3 wt.% of PT3AME

EP/PT3MDE-0.3:	EP-0 primer with 0.3 wt.% of PT3MDE
EP/$Zn_3(PO_4)_2$-10:	EP-0 primer with 10 wt.% of $Zn_3(PO_4)_2$
EPOXY-60:	Epoxy primer supplied by Pinturas Hempel S.A. with 60 wt.% of metallic zinc dust
EPOXY-60/PAni:	EPOXY-60 primer with 0.3 wt.% of PAni-ES
EPOXY-79:	Epoxy primer supplied by Pinturas Hempel S.A. with 79 wt.% of metallic zinc dust
EPOXY-79/PAni:	EPOXY-79 primer with 0.3 wt.% of PAni-ES
Epoxy-DMSO/PAni:	Epoxy coating formulated with DMSO as solvent and 0.3 wt.% of PAni-EB as anticorrosive additive
Epoxy-DMSO/PTE:	Epoxy coating formulated with DMSO as solvent and 1.0 wt.% of PTE as anticorrosive additive
Epoxy-DMSO/Zn:	Epoxy coating formulated with DMSO as solvent and 10 wt.% of zinc phosphate as anticorrosive additive
Epoxy-xylene/PAni:	Epoxy coating formulated with xylene as solvent and 0.3 wt.% of PAni-EB as anticorrosive additive
Epoxy-xylene/PTE:	Epoxy coating formulated with xylene as solvent and 1.0 wt.% of PTE as anticorrosive additive
Epoxy-xylene/Zn:	Epoxy coating formulated with xylene as solvent and 10 wt.% of zinc phosphate as anticorrosive additive
E_{OCP}:	Open circuit potential
ε_b:	Elongation at break
LbL:	Layer-by-layer
LCI:	Lowest Concentration of Interest
NMPy:	N-Methylpyrrole
PA:	Polyacetylene
PAni:	Polyaniline
PAni-EB:	Polyaniline emeraldine base
PAni-ES:	Polyaniline emeraldine salt
PNMPy:	Poly(*N*-methylpyrrole)

PPy:	Polypyrrole
PS:	Polystyrene
PSS:	PS sulfonated
PT3AME:	Poly(3-thiophen-3-yl-acrylic acid methyl ester)
PT3MDE:	Poly(2-thiophen-3-yl-malonic acid dimethyl ester)
PTE:	poly[2,2'-(3-methylacetate)thiophene]
PTh:	Polythiophene
PVC:	Pigment volume concentration
PVP:	Poly(N-vinylpyrrolidone)
Py:	Pyrrole
REACH:	Registration, Evaluation, Authorisation and Restriction of Chemical substances
R_c:	Coating resistance
RCS:	Refrigerated cooling system
R_{IL}:	Metal/coating interface resistance
R_p:	Polarisation resistance
R_s:	Resistance between working and reference electrodes
SCE:	Saturated calomel electrode
SEM:	Scanning electron microscopy
σ_{max}:	Tensile strength
T_c:	Crystallisation temperature
TEM:	Transmission electron microscopy
T_f:	Melting temperature
T_g:	Glass transition temperature
TGA:	Thermogravimetric analysis
Φ:	Water uptake
VOC:	Volatile organic compounds
XPS:	X-Ray photoelectron spectroscopy

Table of Contents

1

INTRODUCTION

The adverse effects of corrosion are evident in a range of industrial sectors encompassing processing of corrosive inorganic acids, pulp and paper industry, and production of food and beverages. However, the most severe and costly failures due to corrosion occur in seawater handling systems. Thus, seawater is one of the most corroded and most abundant naturally occurring electrolytes. The corrosion produced by seawater is reflected by the fact that most of the common structural metals and alloys are attacked by this liquid or its surrounding environments.

The seawater environments can be divided into five zones namely subsoil, continuously submerged, tidal, splash zone above high tidal and atmospheric zone,[1] the effects of corrosion being different from one zone to another. Early studies showed that in splash zone the stainless steels have usually satisfactory performance while, the carbon and low alloy steels do not.[2] Oxygen, biological activities, pollution, temperature, salinity and velocity are the major factors that affect the corrosion behavior materials in submerged zone. The corrosion behavior of conventional stainless steels indicates that pitting and crevice corrosion are the most usual mode of attack in this zone.[3,4]

This PhD Thesis is essentially devoted to develop new organic coatings by introducing conducting polymers (CPs) useful to protect steel from marine corrosion. In order to facilitate the complete understanding of the achieved results, this introductory chapter has been divided in three sections. The first is devoted to describe briefly the basic principles of the corrosion phenomenon, while the second summarizes the most effective procedures to protect metallic substrates from corrosion. Finally, the last section presents the main aspects of CPs as well as the more accepted mechanisms for the inhibition of corrosion in metallic substrates using this kind of materials.

1.1. Fundamentals of corrosion

When iron or steel is exposed to atmospheric oxygen in the presence of water, the well-known rusting process takes place. The metal is degraded to form ferric rust, a red-brown

compound, which is a sure sign of electrochemical oxidation of the underlying metal:[5]

$$4Fe + 3O_2 + 2H_2O \rightarrow 4FeOOH \qquad (1.1)$$

This electrochemical process is composed of two reactions: anodic iron oxidation and cathodic oxygen reduction. Thus, reaction 1.1 results in dissolution of iron and subsequent creation of iron hydroxide. Usually, FeOOH does not provide good protection of the underlying metal when exposed to the atmosphere. This is due to SO_2, which is a pollutant present in the air. This leads to the formation of H_2SO_4 which dissolves iron hydroxide and open pores in its structure,[6] which at latter stages may be filled up by $FeSO_4$. In solution iron dissolves as Fe^{2+} and partially oxidizes as Fe^{3+} and then precipitates as magnetite (Fe_3O_4):

$$Fe \rightarrow Fe^{2+} + 2e^- \qquad (1.2)$$

$$8FeOOH + Fe^{2+} + 2e^- \rightarrow 3Fe_3O_4 + 4H_2O \qquad (1.3)$$

Nearly all metals, with the exception of gold and platinum that are thermodinamically stable in room temperature air, will corrode in an oxidizing environment forming compounds such as oxides, hydroxides and sulphides. The degradation of metals by corrosion is a universal reaction, caused by the simple fact that the oxide of a metal has a much lower energy than the metal itself. For example, aluminium is attacked by oxygen to form the oxide as illustrated in reaction 1.4. This reaction is strongly exothermic, releasing -403 kcal per mole of oxide:

$$4Al + 3O_2 \rightarrow 2Al_2O_3 \qquad (1.4)$$

There are several forms of corrosion, also referred as modes or mechanisms of corrosion. Although they can be described using different terminologies, the one given here being among the most accepted. Although McKay and Worthington proposed eight forms of corrosion in their seminal 1936 book,[7] around fifteen different forms are currently found in the literature:[8-10]

a) *Uniform corrosion*. The surface effect produced by most direct chemical attacks (*e.g.* by an acid) is a uniform etching of the metal (Fig. 1.1a).

b) *Galvanic corrosion*. This is an electrochemical action of two dissimilar metals in presence of an electrolyte and an electron conductive path. It occurs when dissimilar metals are in contact (Fig. 1.1b).

c) *Concentration cell corrosion*. This occurs when two or more areas of a metal surface are in contact with different concentrations of the same solution (Fig. 1.1c).

d) *Pitting corrosion*. This localized corrosion occurs at microscopic defects on a metal surface. The pits are often found underneath surface deposits caused by corrosion product accumulation (Fig. 1.1d).

e) *Crevice corrosion*. This corrosion, which is also named contact corrosion, is produced at the region of contact of metals with metals or metals with non-metals. It may occurs at washers under barnacles, at sand grains, under applied protective films, and at pockets formed by threaded joints (Fig. 1.1e).

f) *Filiform corrosion*. This occurs on painted or plated surfaces when moisture permeates the coating. Long branching filaments of corrosion product extend out from the original corrosion pit and cause degradation of the protective coating (Fig. 1.1f).

g) *Intergranular corrosion*. This is an attachment on or adjacent to the grain boundaries of a metal or alloy (Fig. 1.1g).

h) *Stress corrosion cracking*. This is caused by the simultaneous effects of tensile stress and specific corrosive environment (Fig. 1.1h). Stresses may be due to applied loads, residual stresses from the manufacturing process, or a combination of both.

i) *Corrosion fatigue*. This is a special case of stress corrosion caused by the combined effects of cyclic stress and corrosion (Fig. 1.1i). No metal is immune from some reduction of its resistance to cyclic stressing if the metal is in a corrosive environment.

j) *Fretting corrosion*. This refers to corrosion damage at the asperities of contact surfaces (Fig. 1.1j). This damage is induced under load and in the presence of repeated relative surface motion, as induced for example by vibration.

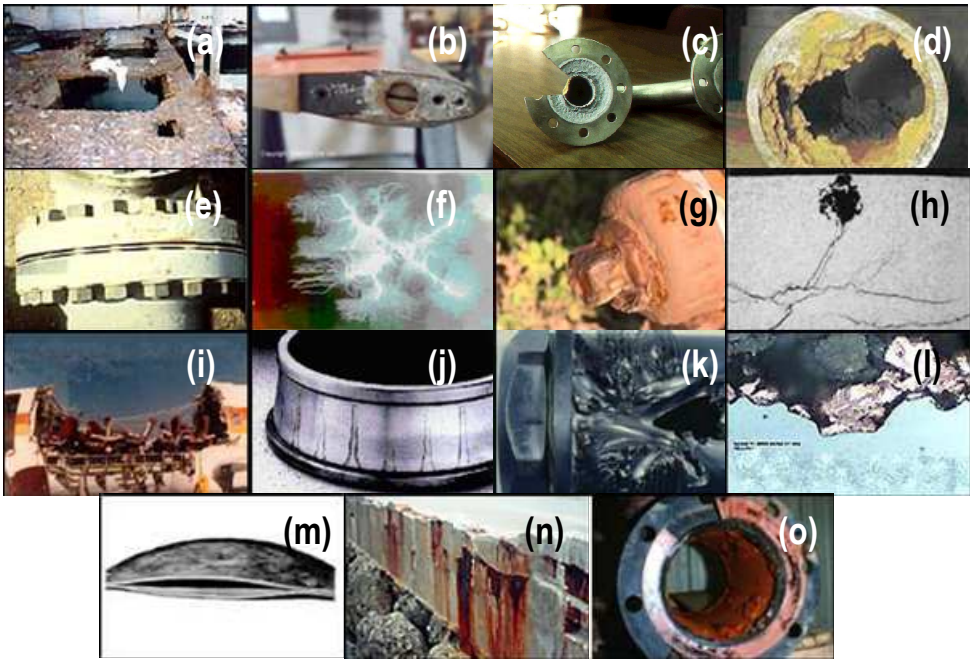

Figure 1.1. Examples to illustrate the different types of corrosion.

k) *Erosion corrosion*. This is the result of a combination of an aggressive chemical environment and high fluid-surface velocities (Fig. 1.1k).

l) *Dealloying*. This is a rare form of corrosion found in copper alloys, gray cast iron, and some other alloys. Dealloying occurs when the alloy loses the active component of the metal and retains the more resistant component in a porous "sponge" on the metal surface (Fig. 1.1l).

m) Hydrogen damage. Hydrogen embrittlement is a problem with high-strength steels, titanium, and some other metals (Fig. 1.1m). Control is by eliminating hydrogen from the environment or by the use of resistant alloys.

n) Corrosion in concrete. Concrete is a widely-used structural material that is frequently reinforced with carbon steel reinforcing rods, post-tensioning cable or prestressing wires. The steel is necessary to maintain the strength of the structure, but it is subject to corrosion (Fig. 1.1n).

o) Microbial corrosion. This corrosion is caused by the presence and activities of microbes (Fig. 1.1o). It can take many forms and can be controlled by biocides or by conventional corrosion control methods.

1.2. Corrosion prevention

Corrosion prevention aims at removing or reducing the effect of one or more of the conditions leading to corrosion using the following measures:

(1) Appropriate materials selection
(2) Change of environment
(3) Suitable design
(4) Electrochemical protection (*i.e.* cathodic and anodic protection)
(5) Application of coatings

The choice between these possibilities is usually based upon economic considerations, but in many cases aspects such as appearance, environment and safety must also be taken care of. Two or more of the five principles are commonly used at the same time. It is important to decide upon corrosion prevention at the design stage.

1.2.1. Materials selection

When selecting materials, each component must be considered with respect to design, manufacture and its effect on the total geometry.[11] However, it is also important that the materials in adjacent components are compatible. With regard to corrosion, compatibility often means that detrimental galvanic elements must be avoided. Not only the main structural materials, but also insulation and other secondary materials must be taken into account to prevent galvanic corrosion. In many cases it is possible to avoid other forms of corrosion by using a favourable combination of materials (*e.g.* to include a material that implies cathodic protection against uniform, selective, pitting, crevice or erosion corrosion on critical regions, even against stress corrosion cracking or corrosion fatigue). Not only do the

grades of structural materials have to be specified, but also the surface treatment and coatings.

The corrosion properties and other functional properties of materials depend on several external factors such as geometry, manufacture, surface conditions, environmental factors and mechanical load conditions. For each functional property these factors have to be evaluated. The final materials selection is often a result of compromises between various properties and their dependence on external factors.

The best tools for weighing the various aspects are quantitative expressions of properties and performance data valid under various conditions, such as corrosion rate and distribution, lifetime in corrosion fatigue, mechanical or electrochemical threshold values, compared with corresponding quantified requirements or service conditions (*i.e.* specified lifetime, actual stress intensity factors and functions, and corrosion potential).[8]

Environment	Material
Nitric acid	Stainless steels
Caustic solutons	Nickel and nickel alloys
Non-staining atmospheric exposure	Aluminium
Distilled water	Tin
Hot, strongly oxidizing solutions	Titanium
Concentrated sulfuric acid	Steel

Table 1.1. Some natural combinations of environment and material.[12]

As a general guideline for materials selection primarily dictated by corrosion aspects, the reason for the corrosion resistance of the respective material candidates may be used. For example, reducing environments are compatible with relatively noble metals or alloys (copper, lead, nickel and alloys based upon these metals). When metallic materials are to be used in oxidizing environment, on the other hand, their corrosion resistance must be based upon passivity (*e.g.* titanium and alloys that contain sufficient amounts of chromium). Irrespective of the mentioned rule, a metal is usually most corrosion resistant

when it contains the smallest possible amounts of impurities. Some “natural” combinations of environment and material are listed in Table 1.1.[12] In several cases, non-metallic materials such as polymers, rubbers, ceramics, wood or concrete must also be taken into consideration.

1.2.2. Change of environment

The environment may be changed in the following ways in order to reduce corrosion rates:

a) Decreasing (or increasing) the temperature.

b) Decreasing (or increasing) the flow velocity.

c) Decreasing (or increasing) the content of oxygen or aggressive species.

d) Adding inhibitors.

Regarding to the first three items, it should be emphasized that corrosion rates most often are reduced by reducing temperature, flow rates, or content of oxygen or aggressive species. On the other hand, the inhibitors can be arranged in groups based on which reaction (anodic or cathodic) they affect and how they influence upon the polarisation properties.

The *passivating inhibitors*, also called *passivators*, are usually inorganic. The oxidizing ones act by depolarizing the cathodic reaction (making it more efficient), or more frequently by introducing an additional cathodic reaction. When the concentration of inhibitor becomes high enough (higher than a critical value *c*), the cathodic current density at the primary passivation potential becomes higher than the critical anodic current density, and consequently the metal is passivated. However, if the inhibitor concentration is below the critical value, it is worse than no inhibitor at all. Examples of oxidizing inhibitors are chromates and nitrites.

Non-passivating inhibitors include both some anodic and the cathodic ones. The latter are exemplified by those that remove free oxygen by a reaction, as is the case for hydrazine and sodium sulphite:

$$N_2H_4 + O_2 \rightarrow N_2 + 2H_2O \quad (1.5)$$

$$2Na_2SO_3 + O_2 \rightarrow 2Na_2SO_4 \quad (1.6)$$

These inhibitors are effective in all environments where the oxygen reduction is the dominating cathodic reaction in the uninhibited state, such as in neutral natural waters. Conversely, other types must be used in strongly acid solutions. *Vapour phase inhibitors* can also be considered as adsorption inhibitors. These are used for protection of wrapped components temporarily. The inhibitor is placed together with the component(s) and acts due to its suitable low saturation pressure, leading to a sufficiently durable inhibitor condensate on the metal surface. By this, the effect of water and oxygen is prevented. It should be emphasized that these inhibitors may accelerate corrosion on some non-ferrous metals and alloys.

A large number of inhibitors for various metals and environments and their behaviour under different conditions are thoroughly dealt with in the literature.[11,13,14] Inhibitors are very important for corrosion prevention in oil and gas production plants, and in recirculation systems.

1.2.3. Suitable design

Design and materials selection are performed in connection with each other. In these processes the individual components, the interactions between them and the relation to other structures and the surroundings have to be taken into account. The various phases of the life cycle of the construction (*i.e.* manufacturing, storing, transport, installation, operation and service, maintenance, and destruction) should be considered. Some important general guidelines are:[15]

1. Design with sufficient corrosion allowance. Pipes, tanks, containers and other equipment are often made with a wall thickness twice the corrosion depth expected during the desired lifetime.

2. Design such that the components that are most liable to corrosion are easy to replace.

3. For structures exposed to the atmosphere: the design should allow easy drainage with ample supply of air. Alternatively, the opposite: hinder air transport to cavities by complete sealing. For components immersed in aqueous solutions there are similar extremes: efficient aeration should be secured (when this will cause passivation), or aeration should be prevented as far as possible.

4. Design in a way that makes drainage, inspection and cleaning easy.

5. Take the surroundings into account: make arrangements for minimizing the consequences of corrosion (*e.g.* where it may cause leakage).

6. Avoid high corrosion risk on load-bearing parts or on critical places by shifting the attack to less critical places.

7. Aim at simple geometry, and avoid heterogeneity and sharp changes in the system.

Detailed explanation of these and many other precautions are provided in reference 15.

1.2.4. Cathodic protection

The main principle of cathodic protection is to impress an external current on the material, which forces the electrode potential down to the immune region, or, for protection against localized corrosion, below a protection potential.[16] In other words, the material is made the cathode in an electrochemical cell. The external current can be produced in two different ways (Figure 1.2.):

a) By means of a less noble material in the form of sacrificial anodes, which are connected by metallic conductors to the structure to be protected.

b) By means of an external current source, usually a rectifier. A reference electrode may be used to control the rectifier potentiostatically.

Cathodic protection has been used for protection of ordinary structural steel in soil and seawater, more seldom (and under special conditions) for steel exposed to fresh water. Other materials can also be protected by cathodic protection, for instance to prevent localized corrosion on stainless steel and aluminium. Cathodic protection has in most cases

been applied in combination with a coating, with the intention to protect the steel on damaged areas of the coating. In recent decades the application of this technology has increased considerably in connection with the expanding offshore oil and gas exploration and production.[16]

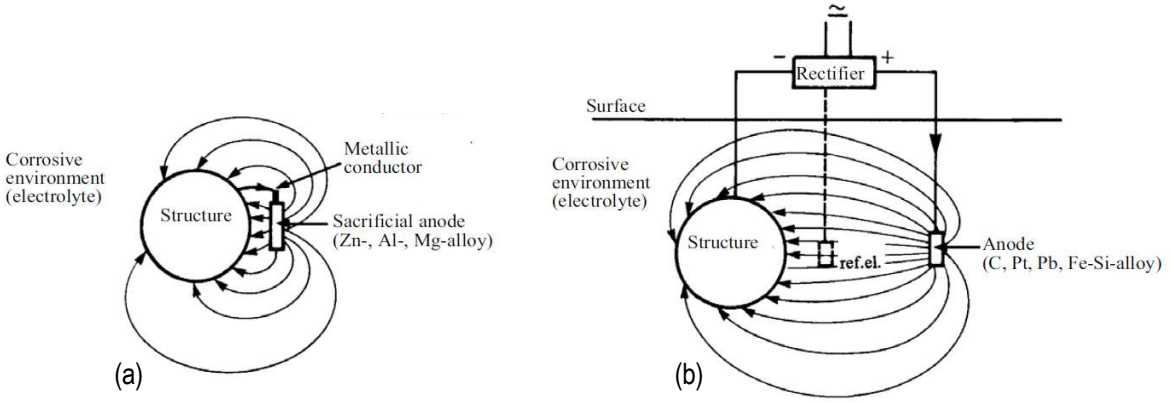

Figure 1.2. Cathodic protection by (a) sacrificial anodes and (b) impressed current.

1.2.5. Anodic protection

Anodic protection can be applied on materials with a well-defined and reliable passive region and low passive current density. The material is polarized in the anodic direction so that the potential is lifted to the passive region.[16] Figure 1.3 shows in principle the arrangement for internal protection of a steel tank by means of a potentiostat.

Anodic protection is used on objects such as steel tanks for storing and transport of sulphuric acid, apparatus made of stainless steels and titanium for treatment of various acids and salt solutions, and for aluminium exposed to water at high temperature. The method cannot be used in aggressive liquids that may cause localized corrosion or high passive current density. It may be used on 18/8 CrNi stainless steel exposed to 30 % H_2SO_4 + 1 % NaCl and on titanium exposed to hydrochloric acid solutions.[15] Pitting is avoided, in the former case because the sulphate ions counteract the chloride, in the latter case because the pitting potentials of titanium in the actual solutions are very high.

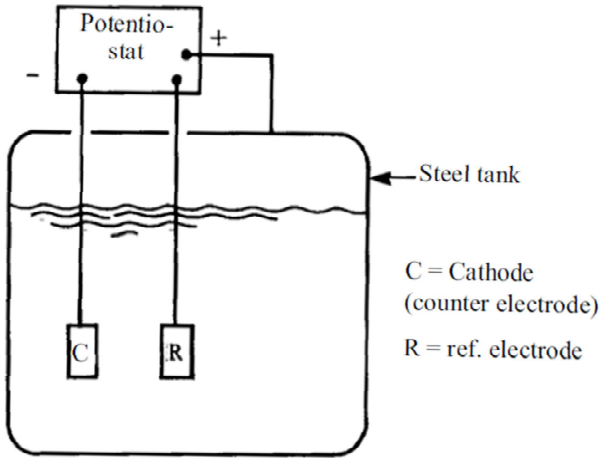

Figure 1.3. Internal anodic protection of a steel tank.

Anodic protection might be utilized much more than it has been so far, but the method must not be used under unfavourable conditions, because the anodic polarisation may cause a strong increase of the corrosion rate.

1.2.6. Corrosion protection by coating

Through the application of coatings, corrosion is prevented by one of the following three main mechanisms or by combination of two of them:

(i) Barrier effect, where any contact between the corrosive medium and the metallic material is prevented.

(ii) Cathodic protection, where the coating material acts as a sacrificial anode.

(iii) Inhibition/passivation, including cases of anodic protection.

1.2.6.1. Metallic coatings

In most cases of corrosion protection by metallic coatings, the purpose is to protect unalloyed or low-alloy steel, but there also exist many cases of other metals to be protected this way.[17] Metallic coatings can be divided in two groups: the *cathodic* coatings, which are more noble than the substrate, and the *anodic* ones, which are less noble than the

substrate (*i.e.* the coatings that have, respectively, a higher and a lower corrosion potential than the substrate in the environment in question). The cathodic coatings will most often act by the barrier effect only, but for some combinations of substrate and environment the substrate can also be anodically protected (on uncovered spots).[17] The anodic coatings, in addition to the barrier effect, will provide cathodic protection of possible "holidays" (*i.e.* spots or parts of the surface where the coating is imperfect and the substrate is exposed to the corrosive environment).[17] The normal major difference between a cathodic and an anodic coating is just the behavior at such a defect. This is illustrated in Figure 1.4. In the case of a cathodic coating (Figure 1.4a) the substrate is subject to galvanic corrosion in the coating defect. The corrosion may be rather intensive because the area ratio between the cathodic coating and the anodic spot of bare substrate usually is very high. In the other case (Figure 1.4b), only a cathodic reaction occurs on the bare substrate (it is protected cathodically), while the coating is subject to a corresponding galvanic corrosion distributed over a larger surface area. In order to protect the substrate, low porosity, high mechanical strength and continuous adhesion are even more necessary for a cathodic than for an anodic coating. Some examples of metallic coatings for steel are Ag, Ni, Cr and Pb, which are cathodic, while Zn and Cd are anodic in most environments.[17]

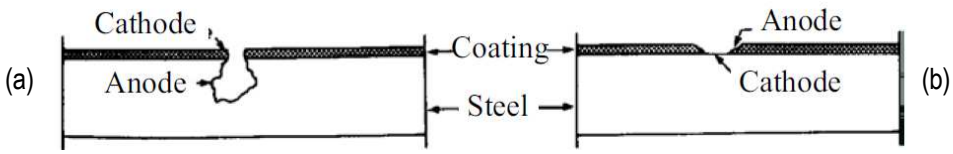

Figure 1.4. Localization of corrosion at a defect in a metal coating on steel: (a) cathodic and (b) anodic coatings.

1.2.6.2. Paint coatings

The use of paint coatings is the most common method for corrosion prevention. An anticorrosive paint is composed of a binder, pigments, a solvent/diluent, extenders and a variable number of other additives such as antioxidants, surface-active agents, driers, thickeners and antisettling agents.[16] A paint is primarily characterized by its pigment or by its binder. We distinguish between primers, which usually contain pigments causing some

inhibition or cathodic protection of the substrate, and paints for finishing coats, which contain colour pigments and extenders, which may improve the barrier effect of the coating system. The coats in thicker paint systems may be divided into primer, intermediate or body coats and topcoat. Recent development of thick film paints implies less need for distinction between intermediate coats and topcoat. An actual inhibiting type of pigment in primers is zinc phosphate,[16,18] while red lead and zinc chromate, which were earlier in widespread use, are seldom applied nowadays because of the risk of health injuries. Metallic zinc powders provide cathodic protection of the substrate if the zinc concentration is high enough. The pigments in the finishing coats provide colour and protect the binder from being damaged by ultraviolet sunlight. The most efficient barrier-acting pigment consists of aluminium flakes. The aluminium flakes increase the length of the diffusion path and are therefore assumed to increase the resistance to diffusion of water, oxygen and ions, but more recent investigations have shown that the effect and the mechanism depend strongly upon the type of binder. Other commonly used pigments in intermediate coats and topcoats are various forms of iron oxide. The binder may, for instance be bitumen (coal tar or asphalt), or linseed oil (natural materials), alkyd, chlorinated rubber, epoxy, vinyl, polyurethane etc. (synthetic organic materials), or silicate (inorganic). Some paints are hardened by reaction with oxygen in the air (oil and alkyd paints), others by evaporation of the solvent (*e.g.* chlorinated rubber) and a third group by a chemical reaction between two components (epoxy and polyurethane paints). Recently, a binder of polysiloxine has been introduced. There is also a growing interest for application of water-based paints (*e.g.* in marine environments).

For ships and marine structures zinc-rich primers are often recommended. It can be an organic zinc-epoxy or an inorganic zinc-ethyl-silicate primer. Zinc-rich primers are also used as so-called shop primers, or prefabrication primers, for temporary protection of semi-manufactured steel goods. After fabrication (*e.g.* of welded steel structures), the shop primer surface must be cleaned (degreased), and possible shop primer defects and weld joints have to be blast cleaned and coated with a primer before the whole structure is painted. Iron oxide is also used as a pigment in some shop primers. These must not be overpainted with a zinc-rich paint.

The main rule for painting previously painted steel is to use the same type of paint. If the old paint coating has turned out to be unsuitable in the actual environment, it should be removed before the structure is coated with a different type of paint. The cost of the paint itself forms often 15-20 % of the total cost of the painting operations including pre-treatment and application. It is important that the pretreatment and the type of paint are compatible. The advanced paints depend upon good pre-treatment to obtain the necessary adhesion to the substrate.[18]

A suitable film thickness and appropriate periods between application of the successive coats are important, but depend upon the type of paint. Data sheets from the paint producers give information about this. The thickness should be checked during the painting work. Other important properties are adhesion between old and new paint as well as resistance to detergents and mechanical wear. It can be mentioned that hardened two-component paints may be less suitable for over painting unless they are rubbed mechanically, but on the other hand they are resistant to detergents and mechanical wear.[18]

For barrier coatings, the resistance to transport of water, ions and oxygen is of crucial significance for protection of the substrate, and transport and absorption of these substances are also important factors in the deterioration of the coating.[19] The film resistance and the potential determine the cathodic reaction rate underneath the paint coating,[20] which interacts closely with two of the main deterioration mechanisms, namely blistering and cathodic disbanding.[21] A good barrier coating is generally characterized by low uptake of water, low conductivity, and low permeability of water and oxygen, but these properties do not give a direct expression of the durability of the coating.

1.2.6.3. Delamination of painted metals

The corrosion of coated metals in most cases starts in the coatings. At these sites the metal surface is exposed directly to the environment. Very often defects are created due to mechanical shocks, chemical attack of aggressive species or as a result of aging. Also they can be created during the production of the coating, for example as a result of inaccurate cleaning of the surface prior to painting. At these sites water and various ions present in the

environment may reach the bare metal surface and initiate the corrosion process. The mechanism of the corrosion in the defect is the same that in the case of uncoated metal. However, further progress of the corrosion leads to the delamination of the coating and the consequent detachment of the coating from the metal surface. This usually occurs through one of the following two general mechanisms: cathodic and anodic delamination.

The cathodic delamination occurs on ferrous metals and other alloys features conductive passive layers that are directly coated with organic coatings. The process leads to the breakage of the linking between the metal surface and the coating, inducing the loss of the protective properties of the coating. Cathodic delamination leads to the creation of blisters or to flanking off the paint from the metal surface.

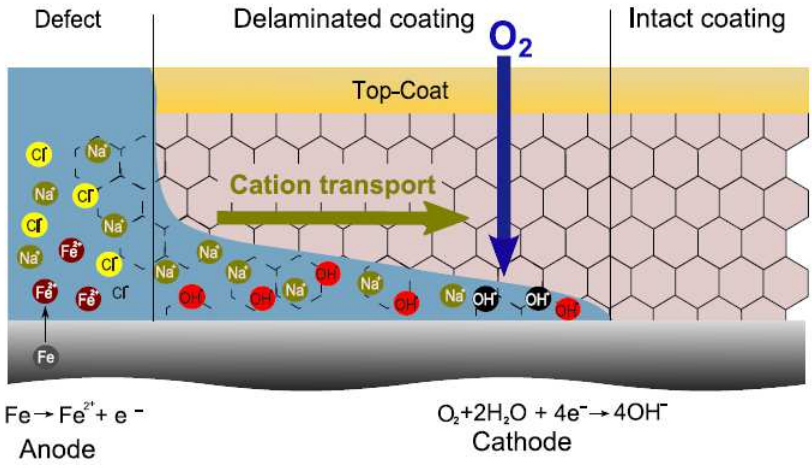

Figure 1.5. Scheme of the mechanism for cathodic delamination.

The electrochemical mechanism describing the cathodic delamination of coated steel was reported by Stratmann and co-workers,[22,23] and is illustrated in Figure 1.5. Coating defects are condensation centres in humid environments. Due to the impurities of the substrate and the ions present in the environment, water becomes an electrolyte. Furthermore, oxygen can be easily transported across the polymer layer. Therefore, cathodic oxygen reduction can occur under the paint, just at the edge of the defect where the contact with the electrolyte is ensured. Hence a galvanic element is formed, as the anodic reaction is inhibited at the intact interface. At the anodic defect sites the pH of the

solution is locally decreased while at cathodic sites it becomes alkaline. The detachment of the coating is caused by the cathodic reaction at the interface. Due to the oxygen reduction, radicals are created. The aggressive species attack and destroy the polymer structure, causing a decrease of its adhesion. The reaction is accompanied by a migration of cations from defects to the cathodic sites. For a weak interface, the migration of ions determines the rate of delaminating process.[23]

Anodic delamination starts in a similar way. At defects local electrodes are created and separated. However, the detachment of the paint is caused by the dissolution of the substrate, which leads to the creation of thin crevices along the metal/polymer interfaces.

1.3. Conducting polymers for corrosion protection

1.3.1. Introduction to conducting polymers

Since the discovery of intrinsically CPs in the late 1970 by Heeger, MacDiarmid and Shirakawa, for which they were awarded with the Nobel prize,[24-26] the unique combination of physical and chemical properties of these materials has drawn the attention of scientists and engineers from many different fields or research. The major feature which made CPs so promising is that they are organic materials with both electronic and electrochemical properties.[27] Among the many technological possibilities of CPs, some examples that deserve consideration are their application as conductometric transducers to measure changes in enzymatic conversion,[28,29] electroluminescent light emitting diodes,[30,31] actuators for biomimetic propulsions,[32] nanometric and micrometric supercapacitors,[33,34] bioactive matrices for tissue engineering [35,36] and electrobactericide films.[37]

Polyacetylene (PA) was the first CP discovered in 1970's. In the reduced state this polymer shows only semiconducting properties but after treatment in iodine vapour, its conductivity increases by more than fifteen orders of magnitude and reach a value in the range of 10^4-10^6 S/cm, which is comparable to that of metals.[38] Spectroscopic measurements confirmed that PA undergoes oxidation, which leads to the transformation of neutral polymer chains into polycarbocations. In order to maintain the charge neutrality of

the polymer matrix, the above reaction is accompanied by a simultaneous incorporation of anions into the polymer matrix. However, application of this polymer meets serious difficulties due to its very low stability when exposed to air, its conductivity decreasing very rapidly because of the destruction of the conjugated structure. Although some strategies to improve the stability of PA have been proposed,[39] the low durability still remains a significant disadvantage of this CP.

Due to extensive research in the area of CPs, another group of materials was discovered. Heterocyclic CPs: polypyrrole (PPy), polyfuran and polythiophene (PTh) can be easily prepared by electrochemical or chemical oxidation of pyrrole,[27] furane[40] and tiophene,[41,42] respectively. Also, other aromatic systems such as aniline[43] and azulene,[44] were found to undergo a polymerisation resulting in a CP [*i.e.* polyaniline (PAni) and polyazulene, respectively]. The chemical structure of the most representative heterocyclic CPs is depicted in Figure 1.6.

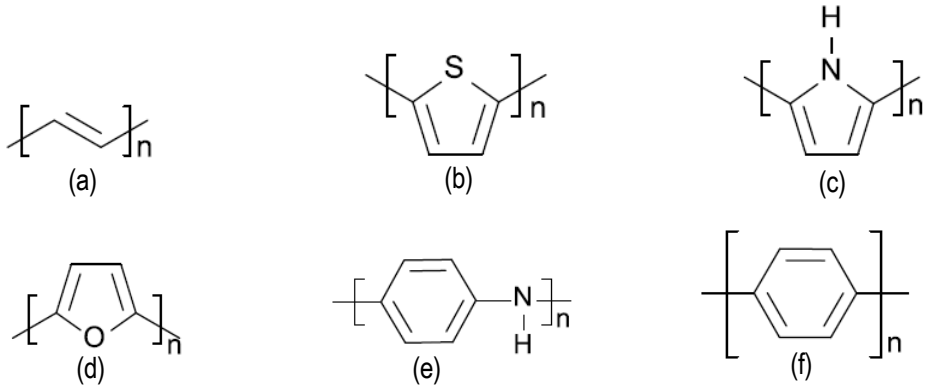

Figure 1.6. Chemical structure of heterocyclic CPs: (a) polyacetylene (PA); (b) polythiophene (PTh); (c) polypyrrole (PPy); (d) polyfurane; (e) polyaniline (PAni); and (f) poly(p-phenylene).

1.3.2. Electronic structure of conducting polymers

PA has been taken as an example to illustrate fundamentals of electronic structure of CPs, because of its simplicity. The PA chain consists of single and double bonds that are situated in an alternated sequence. Figure 1.7a shows the degenerated ground state of PA.

When the two structures coexist in a single polymer chain, a defect called “soliton” results where the two structures meet (Figure 1.7b). This defect consists of a single unpaired electron with overall charge equals to zero. By controlled addition of p-doping anions which consume free electrons, the neutral soliton transforms into a positive soliton (Figure 1.7c). In contrast, the n-doping of PA results in a negative soliton (Figure 1.7d). Both positive and negative solitons are stable because the charge spreads over several monomer units.[45] Solitons may move along the polymer chain by successive alternation of neighbor single bonds. Solitons may exchange electrons between neighbor chains according to “intersoliton hoping” mechanism. Two neutral solitons which are present in a single chain may recombine, which results in the elimination of defects in the chain. A charged soliton together with a neutral one can form an energetically preferred state called polaron. Chemically a polaron can be considered a radical cation. Polarons may also recombine to create a bipolaron, which is a double charged defect. Polarons and bipolarons are delocalized over several monomer units.

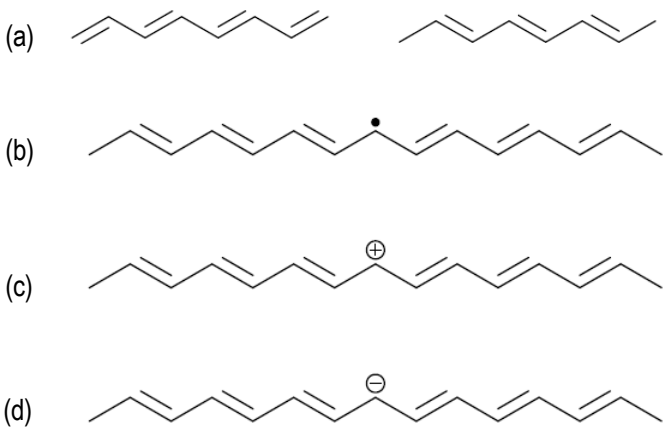

Figure 1.7. (a) Degenerated states of polyacetylene with reversed order of alternated bonds; (b) neutral soliton; (c) positive soliton; and (d) negative soliton.

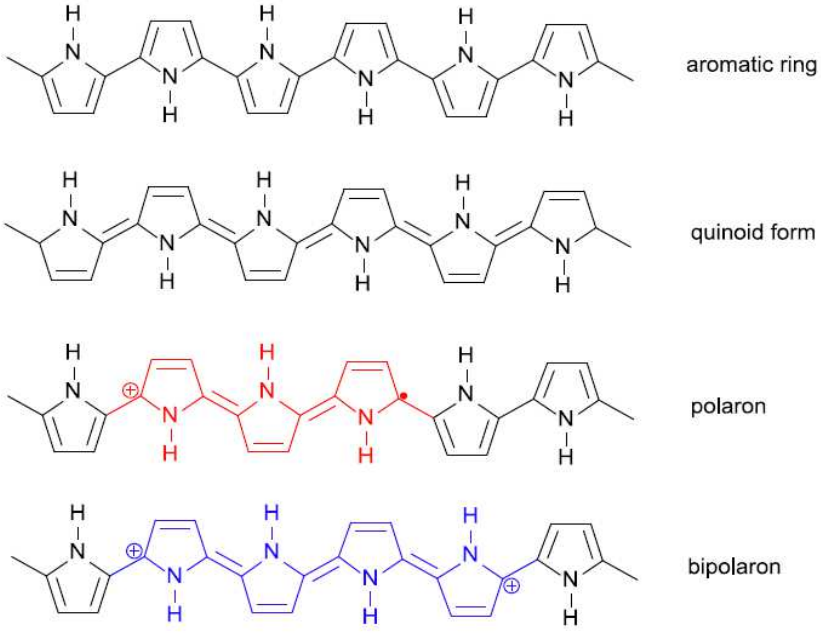

Figure 1.8. Forms of the polypyrrole chain.

Heterocyclic CPs do not have a degenerated state. In the reduced form, they exist as chain of aromatic rings connected by long bonds (Figure 1.8). Another form showing an alternated bond sequence is the quinoid one, in which aromatic rings are connected by double bonds. However, this form is unstable and immediately transforms into the aromatic one. In such structure, formation of two single polarons is not energetically favourable and, therefore, polaron defects are created. At sufficiently high doping levels the polarons recombine into bipolarons.

1.3.3. Inhibition of corrosion by conducting polymers

CPs as materials which have already showed some anticorrosion behavior became a natural candidate for further research. The models usually employed to describe the corrosion protection imparted by CPs are essentially three:

1) The *ennobling mechanism* is based on the assumption that the CP acts as an oxidizer, maintaining the metal in the passivity domain. This mechanism could induce the

oxidation of the free metal surface at small defects in the passive layer. However, some works report that this mechanism only applies in chloride free solutions.[46,47] Wessling claimed that ennobling mechanism also improves the passivity of the oxide layer at the polymer/metal interface, inhibiting electrochemically driven delamination.[48] However, this effect has been found to be negligible.[49]

2) An alternative mechanism is that, the electrons produced during the metal oxidation at the defect area can go into the polymer and dislocate the oxygen reduction process from the metal/polymer interface. This would hinder the coating detachment caused by interfacial oxygen radicals.[50,51]

3) The *self-healing mechanism* proposed by Kendig[52] is based on the assumption that doping anions with corrosion inhibiting properties inside the polymer matrix are released during the reduction of the polymer and migrate to the corresponding defect. Thus, the inhibitor anion could significantly decrease the corrosion rate and the CP would act as a store for corrosion inhibitors, which supplies them immediately just after the corrosion defect appears. The efficacy of the inhibition is strongly dependent of the concentration of doping anions.

These mechanisms are based on the unique properties of CPs. Furthermore, all these mechanisms can contribute simultaneously to the substrate protection. It should be emphasized that many properties of CPs, such as the ionic and electronic conductivity, type and concentration of doping anion, etc., can be controlled during the polymerisation process. Thus, it is possible to adjust the properties of the coating as required by each mechanism, even though it is a serious danger that some of the properties demanded by a given mechanism are unwanted for the other/s.

In recent years the IMEM group of the Universitat Politécnica de Catalunya has investigated the influence of different CPs (*i.e.* PTh,[53,54,56,58,59] PPy[54,56,57,59] and PAni[55-59] derivatives) on the protection against corrosion when they are used as additives of conventional organic coatings. In addition to chemical nature of the CP, the effect of other factors such as the strategy used to add the CP to the paint, the resin used in the

formulation of the paint, the level of dispersion of the CP in the paint, etc, were examined. Results showed that, in general, the incorporation of CP produces a benefit in the performance of the coating, even though other important conclusions were reached from such studies. More specifically, the improvement achieved for epoxy paints was higher than that obtained for alkyd and polyurethane formulations. In general, the corrosion inhibition induced by PTh derivatives and PAni was higher than that of PPy derivatives. The interval of effective concentrations for the CP was found to range from 0.3 % w/w to 1.0 % w/w. Furthermore, it was found that, in order to the take the maximum profit of the CP as corrosion inhibitor, it is essential to achieve a good dispersion of the additive in the paint. This is usually achieved by incorporating the CP dispersed in an organic solvent (*e.g.* xylene) into the paint during its formulation. In addition, corrosion tests evidenced that some PTh derivatives and PAni act not only as corrosion inhibitors but also as adhesion promoters.

1.4. References

[1] F. L. LaQue, "Marine corrosion and prevention", p. 116, John Wiley and Sons, Inc., New York, 1975.

[2] D. B. Anderson and R. W. Ross Jr., "Protection of steel piling in marine splash and spray zone-Metallic sheathing concept", Proceeding of the 4th International Congress on Marine Corrosion and Fouling, France, 461-473, 1976.

[3] T. Hodgkies and S. Rigas, “A comparison of the corrosion resistance of some higher-alloy stainless steels in seawater at 20-100 °C”, *Desalination*, 1983, **44**, 283-294.

[4] D. A. ShiXer, “Understanding material interactions in marine environments to promote extended structural life”, *Corros. Sci.*, 2005, **47**,2335-2352.

[5] U. R. Evans, “Electrochemical mechanism of atmospheric rusting”, *Nature*, 1965, **206**, 980-982.

[6] N.-G. Vannerberg and T. Sydberger, “Reaction between SO_2 and wet metal surfaces”, *Corros. Sci.*,1970, **10**, 43-49.

[7] R. J. McKay and R. Worthington, “Corrosion resistance of metals and alloys”, Reinhold Publishing, New York, 1936.

[8] H. H. Uhlig, “Corrosion and corrosion control”, Jon Wiley and Sons, Inc., New York, 1936.

[9] C. P. Dillon, “Forms of corrosion recognition and prevention” (Nace Handbook 1), N A C E International, Houston, 1982.

[10] P. E. Schwitzer and P. A. Schwitzer, “Encyclopedia of corrosion technology”, CRC Press, New York, 2004.

[11] P. R. Roberge, “Handbook of corrosion engineering”, McGraw-Hill, New York, 1999.

[12] M. G. Fontana and N. D. Green, “Corrosion engineering”, McGraw-Hill, New York, 1986.

[13] Corrosion Inhibitors, Book B559, EFC 11. London: Institute of Materials, 1994.

[14] L. L. Shreir, R. A. Jarman and G. T. Burstein, “Corrosion” Vol. 1, 3rd Ed. Oxford: Butterworth-Heinemann, 1994.

[15] V. R. Pludek, “Design and corrosion control”, The MacMillian Press, 1977.

[16] E. Bardal, “Corrosion and protection”, Springer-Verlag, London 2004.

[17] L. L. Sheir, R. A. Jaman and G. T. Burnstein, “Corrosion”, Vol. 2, 3rd Ed., Oxford: Butterworth.

[18] ISO-Standard 12944 – 2, 1988. Paint and varnishes. Corrosion protection of steel structures by protective paint systems. Part 2, 1998.

[19] M. Stratmann, R. Feser and A. Leng, “Corrosion protection by organic films”, *Electrochim. Acta*, 1994, **39**, 1207-1214.

[20] U. Steinsmo and E. Bardal, “Factors limiting the cathodic current on painted steel”, *J. Electrochem. Soc*., 1989, **136**, 3588-3594.

[21] O. Knudsen and U. Steinsmo, “Effect of cathodic disbonding and blistering on current demand for cathodic protection of coated steel”, *Corrosion*, 2000, **56**, 256-264.

[22] A. Leng, H. Streckel and M. Stratmann, “The delamination of polymeric coatings from steel. Part 1: Calibration of the Kelvinprobe and basic delamination mechanism”, *Corr. Sci*., 1998, **41**, 547-578.

[23] A. Leng, H. Streckel and M. Stratmann, "The delamination of polymeric coatings from steel. Part 2: First stage of delamination, effect of type and concentration of cations on delamination chemical analysis", *Corr. Sci*., 1998, **41**, 579-597.

[24] A. J. Heeger, "Nobel Lecture: Semiconducting and metallic polymers. The fourth generation of polymeric materials", *Rev. Mod. Phys*., 2001, **73**, 681-700.

[25] A. G. MacDiarmid, "Nobel Lecture: "Synthetic metals": A novel role for organic polymers", *Rev. Mod. Phys*., 2001, **73**, 701-712.

[26] H. Shirakawa, "Nobel Lecture: The discovery of polyacetylene film – the dawning of an era of conducting polymers", *Rev. Mod. Phys*., 2001, **73**, 713-718.

[27] T. A. Skoteheim and J. R. Reynolds "Handbook of conducting polymers", 3rd edition, CRC Press, Boca Raton, 2007.

[28] S. Geetha, R. K. Chepuri, M. Rao, D. C. Vijayan and D. C. Trivedi, "Biosensing and drug delivery by polypyrrole", *Anal. Chim. Acta*, 2006, **568**, 119-125.

[29] A. Malinauskas, R. Garjonyté, R. Mazeikiene and I. Jurevieiute, R. K. Chepuri, M. Rao, D. C. Vijayan, D. C. Trivedi, "Electrochemical response of ascorbic acid and electrogenerated polymer modified electrodes for electroanalytical applications", *Talanta*, 2004, **64**, 121-129.

[30] J. H. Burroughes, D. D. C. Bradley, A. R. Brown, R. N. Marks, K. Mackay, R. H. Friend, P. L. Burns and A. B. Holmes, "Light-emitting diodes based on conjugated polymers", *Nature*, 1990, **347**, 539-541.

[31] D. Braun, "Semiconducting polymer LEDs", *Mater. Today*, 2000, **5**, 33-39.

[32] T. F. Otero and M. T. Cortés, "Artificial mucles with tactile sensitivity", *Adv. Mater*., 2003, **15**, 279-282.

[33] D. Aradilla, F. Estrany and C. Alemán, "Symmetric supercapacitors based on multilayers of conducting polymers", *J. Phys. Chem*. C, 2011, **115**, 8430-8438.

[34] D. Aradilla, F. Estrany, E. Armelin and C. Alemán, "Ultraporous poly(3,4-ethylenedioxythiophene) for nanometric electrochemical supercapacitor, *Thin Solid Films*, 2012, **520**, 4402-4409.

[35] E. Armelin, A. L. Gomes, M. M. Pérez-Madrigal, J. Puiggalí, L. Franco, L. J. del Valle, A. Rodríguez-Galan, J. S. de C. Campos, N. Ferrer-Anglada and C. Alemán,

"Biodegradable free-standing nanomembranes of conducting polymer:polyester blends as bioactive platforms for tissue engineering", *J. Mater. Chem*., 2012, **22**, 585-594.

[36] L. J. del Valle, F. Estrany, E. Armelin, R. Oliver and C. Alemán, "Cellular adhesión, proliferation and viability on conducting polymer substrates", *Macromol. Biosci*., 2008, **8**, 1144-1151.

[37] B. Teixeira-Dias, L. J. del Valle, D. Aradilla, F. Estrany and C. Alemán, "A conducting polymer/protein composite with bactericidal properties", *Macromol. Mater. Eng*., 2012, **297**, 427-436.

[38] M. Nechtstein, F. Devreux, R. L. Greene, T. C. Clarke and G. B. Street, "One-dimensional spin diffusion in polyacetylene, (CH)x", *Phys. Rev. Lett*., 1980, **44**, 356-359.

[39] H.Naarman, "Electronic properties of conjugated polymers", *Springer series in Solid State Sciences*, Vol. **76**, 1987, p. 12.

[40] G. Tourillon and F. Garnier, "New electrochemically generated organic conducting polymers", *J. Electroanal. Chem*., 1982, **135**, 173-178.

[41] R. J. Waltman, J. Bargon and A. F. Diaz, "Electrochemical studies of some conducting polythiophene films", *J. Phys. Chem*., 1983, **87**, 1459-1463.

[42] T. Yamamoto, K. Sanechika and A. Yamamoto, "Preparation of thermostable and electric-conducting poly(2,5-thienylene)", *J. Polym. Sci., Polym. Lett. Ed*., 1980, **18**, 9-12.

[43] E. Genoes and C. Tsintavis, "Redox mechanism and electrochemical behavior of polyaniline deposits", *J. Electroanal. Chem*., 1985, **195**, 109-128.

[44] A. F. Diaz, J. Castillo, K. K. Kanazawa, J. A. Logan, M. Salmon and O. Fajardo, "Conducting poly-N-alkylpyrrole", *J. Electroanal. Chem*., 1982, **133**, 233-239.

[45] J. L. Bredas, R. R. Chance and R. Silbey, "Comparative theoretical study of the doping of conjugated polymers: Polarons in polyacetylene and polyparaphenylene", *Phys. Rev*., Part B, 1982, **26**, 5843-5854.

[46] J. Reuk, A Ópik and K. Idla, "Corrosion behavior of polypyrrole coated mild steel", *Synth. Met*., 1999, **102**, 1392-1393.

[47] P. T. Nguyen, U. Rammelt, W. Plieth, S. Richter, M. Plötner, W.-J. Fischer, N. Kiriy, K. Potje-Kamloth and H.-J. Adler, "Experiments with organic field transistors based on polythiophene and thiophene oligomers", *Electrochim. Acta*, 2005, **50**, 1757-1763.

[48] B. Wessling, "Corrosion prevention with an organic metal (polyaniline): Surface ennobling passivation, corrosion test results", *Mater. Corr*., 1996, **47**, 439-445.

[49] R. J. Holness, G. Williams, D. A. Worsley and H. N. McMurray,"Polianiline inhibition of corrosion-driven organic coating cathodic delamination on iron", *J. Electrochem. Soc*., 2005, **152**, B73-B81.

[50] P. J. Kinlen, D. C. Silverman and C. R. Jeffereys, "Corrosion protection using polyaniline coating formulations", *Synth. Met*., 1997, **85**, 1327-1332.

[51] T. D. Nguyyen, M. Keddam and H. Takenouti, "Device to study electrochemistry of iron at a defect of protective coating of electronic conducting polymer", *Electrochem. Solid-State Lett*., 2003, **6**, B25-B28.

[52] M. Kendig, M. Hon and L. Warren, "Smart corrosion inhibiting coatings", *Prog. Org. Coat*., 2003, **47**, 183-189.

[53] C. Ocampo, E. Armelin, F. Liesa, C. Alemán, X. Ramis and J. I. Iribarren, "Application of a polythiophene derivative as anticorrosive additive for paints", *Prog. Org. Coat*. 2005, **53**, 217-224.

[54] J. I. Iribarren, E. Armelin, F. Liesa, J. Casanovas and C. Alemán, "On the use of conducting polymers to improve the resistance against corrosion of paints based on polyurethane", *Mater. Corros*., 2006, **57**, 683-689.

[55] E. Armelin, C. Ocampo, F. Liesa, J. I. Irribarren, X. Ramis and C. Alemán, "Study of epoxy and alkyd coatings modified with emeraldine base form of polyaniline", *Prog. Org. Coat*., 2007, **58**, 316-322.

[56] E. Armelin, R. Oliver, F. Liesa, J. Iribarren, F. Estrany and C. Alemán, "Marine paint formulations: Conducting polymers as anticorrosive additives", *Prog. Org. Coat*., 2007, **59**, 46-52.

[57] E. Armelin, R. Pla, F. Liesa, X. Ramis, J. I. Iribarren, "Corrosion protection with polyaniline and polypyrrole as anticorrosive additives for epoxy paint", *Corros. Sci*., 2008, **50**, 721-728.

[58] J. I. Iribarren, C. Ocampo, E. Armelin, F. Liesa and C. Alemán, "Poly(3-alkylthiophene)s as anticorrosive additive for paints: Influence of the main chain stereoregularity", *J. Appl. Polym. Sci*., 2008, **108**, 3291-3297.

[59] E. Armelin, A. Meneguzzi, C. A. Ferreira and C. Alemán, “Polyaniline, polypyrrole and poly(3,4-ethylenedioxythiophene) as additives of organic coatings to prevent corrosion”, *Surf. Coat. Technol*., 2009, **203**, 3763-3769.

2

OBJECTIVES

The objectives of this PhD Thesis are the following:

1) *Test the performance of nanostructured particles of an electroactive CP as anticorrosive additive for solvent-borne epoxy formulations*. For this purpose, hollow microspheres of poly(*N*-methylpyrrole) (PNMPy) with a shell thickness of ~30 nm have been prepared using the layer-by-layer (LbL) self-assembly technique and characterized using different spectroscopic and structural methods. In order to examine the anticorrosive capabilities of these microspheres, a two components epoxy formulation has been prepared by incorporating a very low concentration (0.3-1.0 wt.%) of PNMPy. The compatibility between the PNMPy and the solvent-borne epoxy paint has been investigated by microscopy.

2) *Investigate the partial replacement of zinc dust used as anticorrosive additive in marine epoxy primers by a small concentration of an organic CP.* The 79 wt.% of zinc dust of a commercial paint for marine use has been reduced to 60 wt.% without detrimental effects in the protecting properties by adding 0.3 wt.% of polyaniline emeraldine salt (Pani-ES). The purpose of such modification in the paint formulation is to provide important benefits to manufacturers by reducing the health risks, meeting the new regulations and reducing both the formulation cost and paint weight.

3) *Extend the use of CPs as anticorrosive additives to alkyd primers, evaluating their performance by comparison with zinc phosphate.* Specifically, zinc phosphate has been replaced in a commercial alkyd primer by PAni-ES, polyaniline emeraldine base (PAni-EB) and poly[2,2'-(3-methylacetate)thiophene] (PTE). The coating adherence, water uptake, permeability and resistance of the commercial and modified primers have been examined after a few hours and 3, 7, and 30 days of immersion in an aggressive NaCl 3.5 wt.% aqueous solution.

4) *Evaluate the performance of soluble PTh derivatives as anticorrosive additives of epoxy coatings.* The anticorrosive performance of epoxy coatings modified by adding PTh derivatives bearing two carboxylate groups per repeat unit has been compared with that of paints formulated with zinc phosphate and PAni-EB. Specifically, two PTh derivatives, which

involve acrylic acid methyl ester and malonic acid dimethyl ester as substitutents at the 3-position of the thiophene ring, have been tested.

5) *Development and characterization of novel epoxy coatings based on DMSO as green solvent and free of zinc anticorrosive pigment.* Novel anticorrosive epoxy coatings based on environmentally friendly dimethyl sulfoxide (DMSO) solvent and free of metallic compounds as anticorrosive pigment have been formulated. The latter have been replaced by a small concentration of organic additives based on CPs (PAni-EB and PTE), as non-toxic anticorrosive pigments. The properties and performance of the new coatings have been compared with those of conventional coatings based on xylene as solvent and zinc phosphate as anticorrosive additive.

3

METHODS

A short description of the methods and techniques used to carry out the research tasks is given in this chapter.

3.1. FTIR spectroscopy

In most cases FTIR spectra were recorded on a FTIR 4100 Jasco spectrophotometer, localized at the Chemical Engineering Department at UPC, with a resolution of 4 cm^{-1} (transmittance mode) in a wavenumber range of 4000-600 cm^{-1}. Samples were placed in an attenuated total reflection accessory (top-plate) with thermal control and a diamond crystal (Speac-Teknokroma model MKII Golden Gate Heated Single Reflection Diamond ATR).

Figure 3.1. Image of the FTIR spectrometer and reflection accessory used in this work.

Some tests were performed using a Bomem Michelson MB100 FTIR spectrophotometer, from Thermodynamics Department at UPC, with a resolution of 4 cm^{-1} (absorbance mode) and the same attenuated total reflection accessory.

In general the goal of FTIR spectroscopy is to measure, how well a sample absorbs or transmits infrared radiation. Specifically, a beam of light (electromagnetic radiation) in the infrared wavelength region impinges on the sample and the wavelength/frequency is scanned. Some of the radiation is absorbed by the sample and some of it is passed through (transmitted). The resulting spectrum represents the molecular absorption and transmission, creating a molecular fingerprint of the sample. This fingerprint depends on the chemical groups existing in the samples, different molecular structures producing different

infrared spectra. Such characteristic makes the FTIR technique a very useful tool for the chemical identification of polymeric materials.

3.2. Raman spectroscopy

When needed, Raman spectroscopy was performed with a Dilor Jobin Yvon dispersive spectrometer equipped with a 1024 diodes multichannel detector using He/Ne laser (20 mW) with 633 nm of excitation wavelength. The spectral interval ranged from 1200 to 2000 cm^{-1}.

In Raman spectroscopy, a light beam of fixed wavelength (monochromatic light) from a laser source undergoes inelastic scattering as it interacts with the sample material. Inelastic scattering means that the frequency of photons in monochromatic light changes upon interaction with a sample. Photons of the laser light are absorbed by the sample and then re-emitted. The frequency of the reemitted photons is shifted up or down in comparison with original monochromatic frequency, which is called the Raman Effect. This shift provides information about vibrational, rotational and other low frequency transitions in molecules.

3.3. UV-vis-NIR reflectance spectroscopy

Measurements were performed on a UV/Vis-NIR Shimazu 3600 spectrophotometer, which contains a tungsten halogen visible source, a deuterium arc UV source, a photomultiplier tube UV-Vis detector, and an InGaAs photodiode and cooled PbS photocell NIR detectors. The wavelength range is 185-3300 nm. We worked in the reflectance mode, which was done using the integrating sphere accessory (Model ISR-3100). The interior of the sphere is coated with a highly diffuse BaO reflectance standard. The total reflectance measured by this device will be both specularly reflected and diffusely reflected light. Single-scan spectra were recorded at a scan speed of 60 nm/min using the UVProbe 2.31 software.

The UV/visible radiation causes electronic transitions within a molecule, promoting bonding and non-bonding electrons from a ground state to a high energy state (*i.e.* electron are promoted to less stable antibonding orbitals). The molecule then loses this excess energy by rotation and vibrational relaxation.

In principle the technique is similar to IR spectroscopy, so when a sample of an unknown compound is exposed to light, certain functional groups within the molecule absorb light of different wavelengths in the UV or visible or NIR region. UV-VIS-NIR spectroscopy is used for qualitative and quantitative analysis of materials.

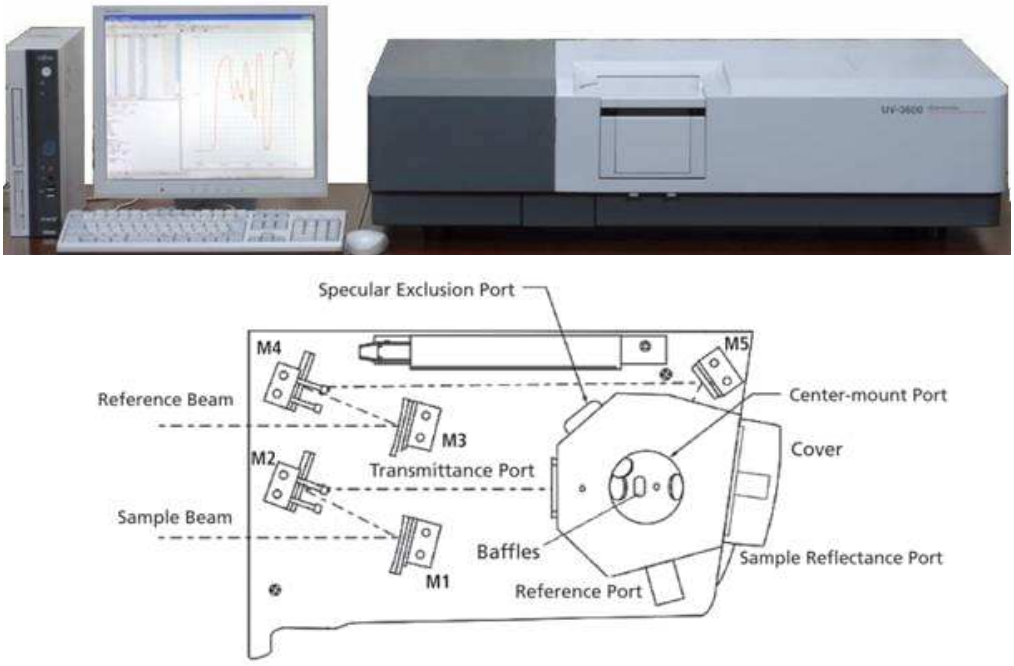

Figure 3.2. UV-vis-NIR spectrophotometer and basic optical layout for a double beam integrating sphere, localized at the Center for Research in NanoEngineering (CRnE-UPC).

3.4. X-Ray photoelectron spectroscopy

X-Ray photoelectron spectroscopy (XPS) analyses were performed in a PHI 5500 Multitechnique System instrument (from Physical Electronics) equipped with a monochromatic Al Kα X-Ray source (1486.6 eV, 350 W), placed perpendicular to the analyzer axis and calibrated using the 3d5/2 line of Ag with a full width at half maximum (FWHM) of 0.8 eV. The X-ray spot size was 650 μm. The pass energy was set at 150 and 40 eV for the survey and the narrow scans, respectively. Charge compensation was achieved with a combination of electron and argon ion flood guns. The energy and emission

current of the electrons were 4 eV and 0.35 mA, respectively. For the argon gun, the energy and the emission current were 0 eV and 0.1 mA, respectively. The partial pressure for the argon flood gun was $2 \cdot 10^{-8}$ mbar. Data acquisition and processing were achieved with the Advantage Software. Spectral calibration was determined by setting the main C 1s component at 285 eV. The surface composition was determined using the manufacturer's sensitivity factors.

Each element produces a characteristic set of XPS peaks at characteristic binding energy values, enabling the identification of each element existing inside or on the surface of the analyzed material. These characteristic peaks correspond to the electron configuration of the electrons within the atoms, (*e.g.*, 1s, 2s, 2p and 3s) The number of detected electrons in each of the characteristic peaks is directly related to the amount of element within the irradiated area (volume).

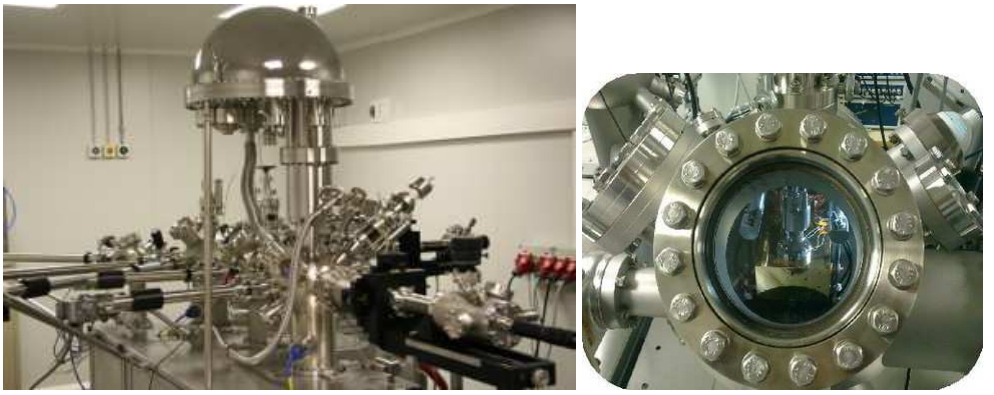

Figure 3.3. X-ray photoelectron spectroscopy chamber with a nine channel detector and SPM 150 Aarhus chamber equipped with ultra-high vacuum conditions (<10-10mbar), localized at the Center for Research in NanoEngineering (CRnE-UPC).

3.5. Scanning electron microscopy and energy dispersive X-ray spectroscopy

Scanning electron microscopy (SEM) and energy dispersive X-ray spectroscopy (EDX) studies were carried out using a Focused Ion Beam Zeiss Neon 40 scanning electron microscope equipped with an EDX system and operating at 30 kV.

SEM uses a focused beam of high-energy electrons to generate a variety of signals at the surface of solid specimens. Accelerated electrons carry significant amounts of kinetic energy, and this energy is dissipated as a variety of signals produced by electron-sample interactions when the incident electrons are decelerated in the solid sample. These signals include secondary electrons, backscattered electrons, diffracted backscattered electrons, photons, visible light and heat. Secondary electrons and backscattered electrons are commonly used for imaging samples: secondary electrons are most valuable for showing morphology and topography on samples, backscattered electrons are most valuable for illustrating contrasts in composition in multiphase samples (*i.e.* for rapid phase discrimination) and photon are used for elemental analysis and continuum X-rays.

Figure 3.4. Focused Ion Beam Zeiss Neon 40 scanning electron microscope, localized at the Center for Research in NanoEngineering (CRnE-UPC).

3.6. Transmission electron microscopy

TEM images were collected with a Philips TECNAI 10 electron microscope operating at 80 kV. Bright field micrographs were taken with an SIS MegaView II digital camera.

Figure 3.5. Philips TECNAI 10 electron microscope localized at the Chemical Engineering Department of UPC.

The TEM microscope operates on the same basic principles as the light microscope but uses electrons instead of light. What can be seen with a light microscope is limited by the wavelength of light. TEM uses electrons as light source and their much lower wavelength makes it possible to get a resolution a thousand times better than with a light microscope.

3.7. Optical Microscopy

The coating surfaces were observed using an Olympus BX-5 light polarizing microscope, operating in reflection mode with an Olympus C3030Z digital camera coupled, localized in the CRnE.

A polarizing microscope is a special microscope that uses polarized light for investigating the optical properties of specimens. Transverse wave light with directional vibration is called polarized light. A polarizing plate (polarizing filter) or polarizing prism is often used as the device to change natural light to linearly polarized light.

There are two types of polarizing microscopes: transmitted light models and incident light models. Figure 3.6 shows the basic construction of a transmitted light polarizing microscope.

Figure 3.6. External view of a transmitted light polarizing microscope (BX-P).

3.8. Differential Scanning Calorimetry

Differential scanning calorimetry (DSC) was performed using a TA Instruments Q100 series equipped with a refrigerated cooling system (RCS) operating at temperatures from -90 to 550 °C and employing a heating rate of 10 °C/min. Experiments were conducted under a flow of dry nitrogen with a sample weight of approximately 5 mg and calibration was performed with indium.

DSC is a thermoanalytical technique in which the difference in the amount of heat required to increase the temperature of a sample and a reference is measured as a function of temperature. Both the sample and reference are maintained at nearly the same temperature throughout the experiment. Usually the temperature program for a DSC analysis is designed such that the sample holder temperature increases linearly as a function of time. The reference sample should have a well-defined heat capacity over the range of temperatures to be scanned.

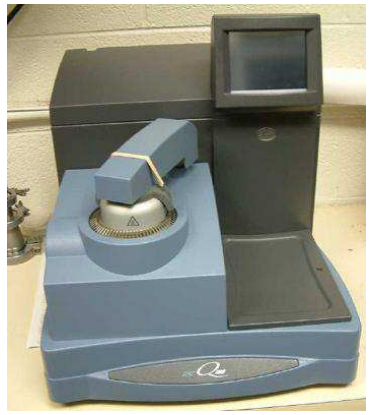

Figure 3.7. Differential Scanning Calorimeter (TA Instruments Q100), localized at the Chemical Engineering Department of UPC.

3.9. Thermogravimetry

Thermogravimetric analyses (TGA) were mainly carried out with a Perkin Elmer TGA-6 thermobalance at a heating rate of 10 °C/min under nitrogen atmosphere and a temperature range from 30 to 850 °C. In some occasions TGA were carried out with a Q50 thermogravimetric analyzer of TA Instruments at a heating rate of 20 °C/min under nitrogen atmosphere and a temperature range from 20 to 600 °C.

Figure 3.8. Q50 thermogravimetric analyzer of TA Instruments localized at the Chemical Engineering Department at UPC.

TGA is a type of testing that is performed on samples to determine changes in weight in relation to changes in temperature. TGA is commonly employed in research and testing to determine characteristics of materials such as polymers, to determine degradation temperatures, absorbed moisture content of materials, the level of inorganic and organic components in materials and solvent residues.

3.10. Stress-strain assays

The mechanical properties of the paints were evaluated through stress-strain assays with a Zwick Z2.5/TN1S testing machine. Regular films were prepared by evaporation at room temperature of the volatile organic solvent or by casting and after post-curing. Plate samples with a length of 30 mm and a width of 3 mm were cut out from paint films and used. The deformation rate was 10 mm/min. All the mechanical parameters reported in this work were obtained by averaging the results obtained from ten independent measurements.

This kind of stress-strain assays consist on hold the sample using hydraulic grips and apply a determined deformation rate until breaking in order to determine mechanical characteristics like Young's modulus, tensile strength and elongation at break.

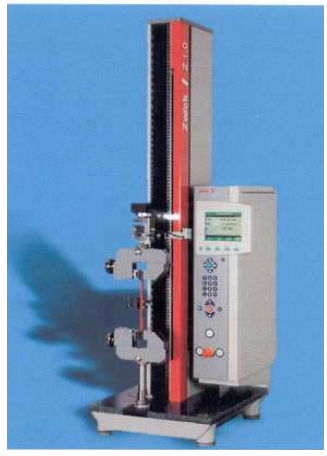

Figure 3.9. Zwick Z2.5/TN1S stress-strain assays testing machine, localized in the Chemical Engineering Department at UPC.

3.11. Electrochemical Impedance Spectroscopy

EIS was performed as a function of time in aqueous 3.5 wt.% NaCl solution at open circuit potential (E_{OCP}). Stainless steel and platinum electrodes were used as counter electrodes while the silver|silver chloride (Ag|AgCl) electrode were used as reference electrode in all cases. EIS measurements were performed in potentiostatic mode at the E_{OCP}. The amplitude of the EIS perturbation signal was 10 mV, the frequency ranged from 10^5 to 10^{-2} Hz taking 70 frequencies per decade with a potentiostat Autolab PGSTAT 302N.

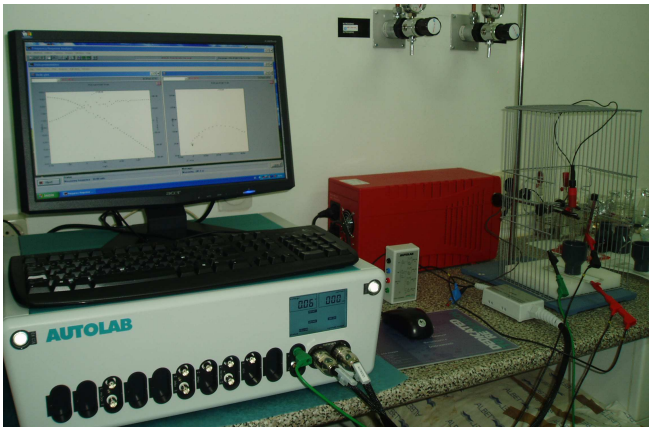

Figure 3.10. Potentiostat Autolab PGSTAT 302N, localized at the Chemical Engineering Department of UPC.

Electrochemical systems such as coated surfaces or corroding metals often behave like simple electronic circuits.[1-5] Within the framework of ac waveforms, a few simple circuit elements and a simple, but useful, combination of them can be examined. This equivalent circuit model provides a simple way of understanding complicated electrochemical systems by associating a real physical process to each circuit component. The Randles cell (Figure 3.11) is a simple but useful combination of a capacitor and two resistors. This electrical circuit can be used to represent a coating or a corroding metal, although the values and meanings of the components are different.

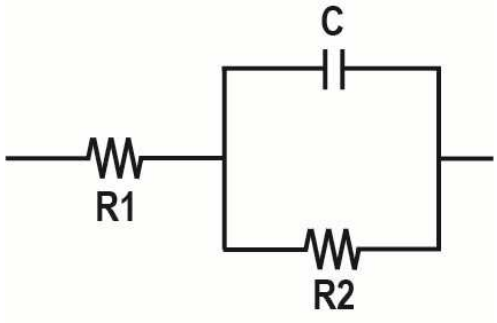

Figure 3.11. The Randles cell equivalent circuit.

When this equivalent circuit model is applied to a coating immersed in an electrolyte, R1 represents the resistance of the electrolyte solution between the reference electrode tip and the surface of the coating. The value of R1 is usually a few ohms if the concentration of electrolyte's salt is small. The capacitor, C, represents the coating and can be characterized by the thickness and dielectric constant of the coating material. Finally, the resistor, R2, corresponds to the resistance of the coating. It is also a property of the material of the coating and varies with the thickness and composition of the coating.

The same equivalent circuit can also be applied to a bare corroded metal in an electrolyte solution. Once again R1 is associated with the electrolyte resistance. However, in such system the capacitor, C, is associated with the double layer capacitance (C_{dl}) of the metal/electrolyte interface. The value of C is generally between 10 and 100 μF/cm^2. In system the resistor R2 is related with the polarisation resistance.

3.12. Accelerated Corrosion Assays

Corrosion studies were performed using the home-made equipment (Figure 3.12) developed and patented in our laboratory.[6] This device is prepared to perform accelerated immersion assays in an aggressive solution medium, which consists of an aqueous solution of NaCl (3.5 wt.%, pH=6.6) or $NaHSO_3$ (3 wt.%, pH=3.5) stored in a plastic or glass container, through controlled cycles. The operating conditions of each programmed cycle were: (i) immersion of coated steel sheets (15 min); (ii) wring out (30 min); (iii) drying stage with bulbs (230 V – 100 W; 10 min); and (iv) cooling time at room temperature (5 min).

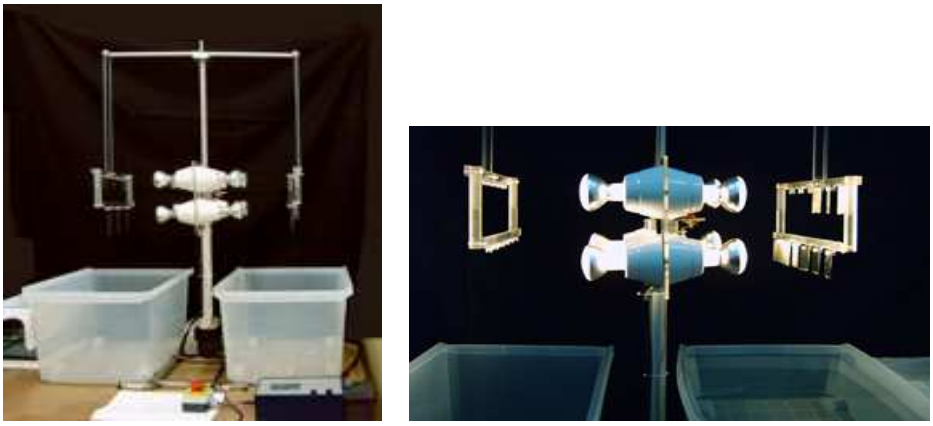

Figure 3.12. Accelerated corrosion assays home-made equipment.

Rectangular steel panels were coated with the studied modified and unmodified paints by immersion and were dried on air. They were sealed on the edges and around the hole used for securing the pieces to the equipment. Before coating the panels were previously degreased with acetone and polished with zirconium balls following the standard method *UNE-EN-ISO 8504: Preparation of steel substrates before application of paints and related products-Surface preparation methods*. [7]

The dry film thickness was measured with a machine model Uno-Check Fe or with a Mega-Check pocket NFE both from Neurtek S.A.

The corrosion of the steel was continually monitored and evaluated at regular time intervals by both visual and microscopy inspections according to the standard methods:

ASTM D714: Standard Test Method for Evaluating Degree of Blistering of Paints. [8]

ASTM D1654: Standard Test Method for Evaluation of Painted or Coated Specimens. [9]

UNE-EN-ISO 4624: Paints and varnishes: Pull-off Test for Adhesion, ISO 4624:2002. [10]

3.13. References

[1] J. R. Macdonald, Impedance Spectroscopy; Emphasizing Solid Materials and Systems, Wiley Interscience, 1987.

[2] A. J. Bard and L. R. Faulkner, Electrochemical Methods; Fundamentals and Applications, Wiley Interscience, 2000.

[3] D. A. Jones, Principles and Prevention of Corrosion, Prentice Hall, 1995.

[4] J. R. Scully and D. C. Silverman, and Kendig, M.W. (Ed.), Electrochemical Impedance: Analysis and Interpretation, ASTM, West Conshohocken, PA, 1993.

[5] R. Cottis and S. Turgoose, Electrochemical Impedance and Noise, NACE International, Houston, TX, 1999.

[6] F. Liesa, C. Alemán, E. Armelin and J. I. Iribarren, F.; ES Patent No. P200502713, 2005.

[7] UNE-EN-ISO 8504: Preparation of steel substrates before application of paints and related products-Surface preparation methods.

[8] ASTM D714: Standard Test Method for Evaluating Degree of Blistering of Paints.

[9] ASTM D1654: Standard Test Method for Evaluation of Painted or Coated Specimens.

[10] UNE-EN-ISO 4624: Paints and varnishes: Pull-off Test for Adhesion, ISO 4624:2002.

4

NANOSTRUCTURED CONDUCTING POLYMER FOR CORROSION INHIBITION

Part of the work described in this chapter was published in *J. Mater. Chem.*, 2010, **20**, 10652-10660

This chapter describes the ability of poly(N-methylpyrrole) to form nanostructures and the performance of such nanostructures when act as anticorrosive additive of organic coatings. Poly(N-methylpyrrole) hollow particles of controlled thickness have been prepared using the Layer-by-Layer assembly technique and polystyrene core-shell particles as template, which are subsequently eliminated to yield free-standing hollow microspheres with layer thickness of 30 nm. The morphology and composition of these structures have been evaluated by scanning electron microscopy, transmission electron microscopy, FTIR, Raman and X-ray photoelectron spectroscopies. Results demonstrate that intact hollow spheres can be obtained controlling the number of polymer deposition cycles. Furthermore, the protection against corrosion imparted by this nanostructured conducting polymer has been examined when this material is used to replace the inorganic anticorrosive additives typically employed in the formulation of conventional epoxy paints.

4.1. Introduction

Organic/inorganic nanocomposites, which are obtained by combining organic and inorganic materials, have attracted significant attention, novel materials with advanced structures being produced by the layer-by-layer (LbL) templating technique.[1-5] The LbL method has become one of the more employed route to sequential deposition of a broad range of templates, *e.g.* molecules (proteins, dyes, lipids, polymers, etc), biological cells and nanoparticles with inorganic compounds.[6-8] The general process involves the sequential deposition of species onto various templates, which are subsequently removed to yield free-standing structures. This technique offers two main possibilities for the generation of self-assembled monolayered films: (a) use solid planar substrates or (b) use core-shell particles. Since the pioneering studies of Decher[1-5] many research groups have successfully used this technology to prepare nanoscale materials. In this sense, we can emphasize the brilliant research developed by Caruso and co-workers with complex systems based on polymer capsules. The recent reviews written by Caruso *et. al.*[6-8] presents the new advances on the LbL assembly technique, as well as the future research directions using planar, colloidal and naturally occurring templates.

One of the critical steps of this LbL approach is the removal of the templating substrate, which is necessary to obtain the free-standing nanostructured material. Thus, non-desirable morphologies and functions may be obtained after the template removal because of the substrate rupture. Fortunately, after almost twenty years since the LbL self-assembly was firstly introduced by Decher and Hong,[1-5] such limitations have been partially or totally overcome as is reflected by the wide number of innovative materials reported in the last few years (*e.g.* nanofilms, microspheres, nanotubes, macroparticles, porous particles and biomimetic structures).[9] Many of the nanostructured materials currently under development are based on the CPs deposition in a core-shell particle. The major part of the works is related to PPy and PAni systems.[10-17] However, in the last years, poly(*N*-methylpyrrole) (PNMPy) has attracted the attention of the researchers since its environmental stability and positive oxidation potential are higher than those of PPy.[18] Thus, despite the electrical conductivity of PNMPy electrodeposited films is lower than that of the PPy one, the former material has been postulated as a good alternative to replace PPy in some applications, like sensors,[19-24] batteries[25,26] or capacitors,[27,28] and drug delivery systems.[29,30]

In this chapter, we report the preparation and characterization of nanostructured PNMPy and its performance to act as anticorrosive additives in epoxy paints. More specifically, we present the fabrication of hollow microspheres of controlled nanolayer thickness using the LbL procedure and polystyrene (PS) core-shell particles as template. The surface composition and morphology of these PNMPy nanostructures, which were doped with chloride and dodecylbenzenesultonate ions, have been analyzed using spectroscopy techniques (FTIR, Raman and UV-vis-NIR), X-Ray photoelectronspectroscopy, scanning electron microscopy (SEM) and transmission electron microscopy (TEM). In order to determine its efficacy in inhibiting corrosion, a small concentration of this CP has been added to a solvent-borne epoxy paint. Unfortunately, the dispersion of nanostructured PNMPy in the epoxy formulations was deficient, microspheres agglomerating when they enter in contact with the xylene-based paint. This undesirable behaviour limits the applicability of PNMPy microspheres as anticorrosive additive.

4.2. Methods

4.2.1. Materials

Pyrrole (Py) and N-methylpyrrole (NMPy) 99 % were purchased from Aldrich and were used freshly distilled. Styrene was purchased from Aldrich and was purified after passing through an activated neutral alumina column. Poly(N-vinylpyrrolidone) (PVP) with M_w=360.000 g/mol, α-azoisobutyronitrile (AIBN), iron (III) chloride hexahydrate 97 % (ACS reagent) and dodecylbenzene sulphonic acid (DBSA) 70 wt.% were also purchased from Aldrich and used as received. All solvents or acid solutions were purchased from Panreac S.A., while aqueous solutions were prepared using doubly distilled deionized water.

4.2.2. Preparation of polystyrene microspheres

PS microspheres were prepared following the procedure described by Lascelles *et. al*.[10] In a three-necked round flask provided with magnetic stirring and a condenser, PVP stabilizer (3.8 g) dissolved in isopropyl alcohol (180 mL) was heated until 70 °C for 1 h under nitrogen atmosphere. Then, a solution of AIBN (0.25 g) and styrene monomer (25 g) was added dropwise to the reaction vessel. The mixture was vigorously stirred at 70 °C for 24 h, and after this it was left to cooling at room temperature. The very fine white resulting emulsion was centrifuged several times, and washed repeatedly with deionized water to remove the PVP stabilizer excess. The chemical composition of the PS samples was evaluated with FTIR spectroscopy, while the size of the latex particles was determined by SEM and TEM.

4.2.3. Preparation of PS sulfonated microspheres

Concentrated sulphuric acid (98 %, 11 mL) was introduced in a 30 mL centrifuge tube. PS microparticles (10 % in deionized water, 3 mL) were added dropwise under magnetic stirring. The sulfonation reaction was allowed to take place at 40 °C during 24 h under reflux. When the vessel cooled to the room temperature, the solution was centrifuged and

the solid was washed several times with an excess of ethanol. A white fine powder, made of PS sulfonated (PSS) core/shell particles, was obtained after drying under vacuum for 48 h.

4.2.4. Preparation of PNMPy/PSS and PPy/PSS microspheres

PSS microparticles (0.06 g) were dispersed in 3.5 mL of deionized water in a 30 mL centrifuge tube. A solution of 0.02 mL of NMPy and 1.5 mL of ethanol was introduced into the PSS suspension under magnetic stirring. After 15 min, 0.1 g of $FeCl_3 \cdot 6H_2O$ and 2 mL of deionized water were added. The polymerisation process took place at room temperature during 24 h. The resulting powder was washed by centrifugation, with an excess of deionized water and with ethanol. Finally the sample was dried under vacuum for 48 h. In order to reach a suitable PNMPy thickness in PNMPy/PSS microspheres, this polymerisation step was repeated three times. The same procedure was used to obtain PPy/PSS core-shell systems. The complete synthesis procedure, including the doping of the PNMPy/PSS and PPy/PSS microspheres and the extraction of the PSS core to obtain hollow spheres (see next subsections), is displayed in Figure 4.1.

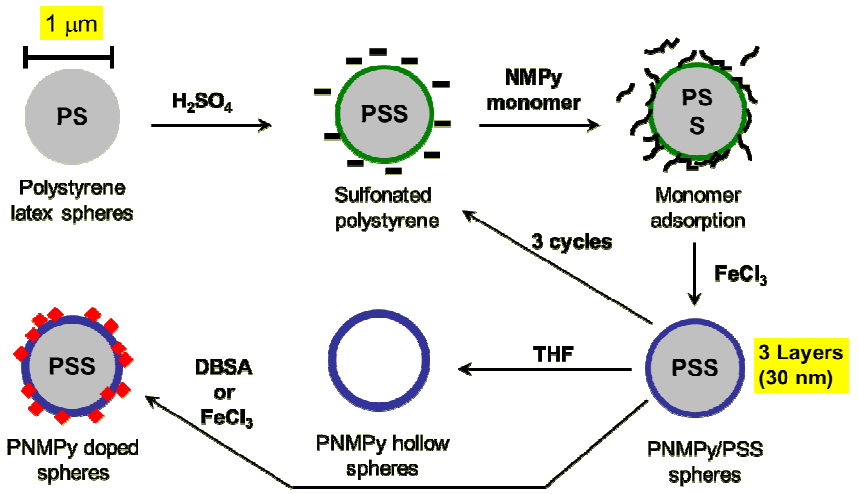

Figure 4.1. Scheme showing the synthesis of doped and hollow PNMPy spheres.

4.2.5. Doping process of PNMPy/PSS and PPy/PSS core-shell microspheres

PNMPy/PSS core-shell microspheres (0.02 g) were mixed with 0.05 mL of DBSA and 0.5 mL of ethanol, the mixture being stirred at 40 °C under nitrogen atmosphere for 2 h. After this, it was washed by centrifugation with an excess of deionized water, and dried under vacuum for 48 h.

Another portion of PNMPy/PSS core-shell microspheres (0.015 g) was mixed with 0.5 mL of $FeCl_3 \cdot 6H_2O$ at room temperature under magnetic stirring and nitrogen atmosphere for 20 h. The mixture was washed by centrifugation with an excess of ethanol and with deionized water (several times), and dried under vacuum for 48 h. The same process was followed for the doping of the PPy/PSS core-shell systems.

4.2.6. Preparation of PNMPy hollow microspheres

The PNMPy/PSS core-shell microspheres were dispersed into tetrahydrofuran (THF) under magnetic stirring for 48 h at room temperature. The resulting mixture was washed by centrifugation, and the final product was dried in vacuum at 40 °C for 24 h. The chemical composition and the morphology of the polymer microspheres were characterized by spectroscopic techniques.

4.2.7. Analytical Techniques

FTIR and Raman spectroscopy. FTIR spectra were recorded on a FTIR 4100 Jasco spectrophotometer. Samples were placed in an attenuated total reflection accessory (Top-plate) with a diamond crystal (Specac model MKII Golden Gate Heated Single Reflection Diamond ATR). Raman spectroscopy was performed with a Dilor Jobin Yvon dispersive spectrometer equipped with a 1024 diodes multichannel detector using a He/Ne laser (20 mW) with 633 nm of excitation wavelength. The spectral interval ranged from 1200 to 2000 cm^{-1}.

UV-vis-NIR reflectance spectroscopy. The instrument utilized was a UV/Vis-NIR Shimadzu 3600 spectrophotometer, which contains a tungsten halogen visible source, a deuterium arc UV source, a photomultiplier tube UV-Vis detector, and an InGaAs photodiode and cooled PbS photocell NIR detectors. The wavelength range is 185-3300 nm. We worked in the reflectance mode, which was done using the integrating sphere accessory (Model ISR-3100). The interior of the sphere is coated with a highly diffuse BaO reflectance standard. The total reflectance measured by this device will be both specularly reflected and diffusely reflected light. Dried microspheres were mounted into the $BaSO_4$ powder sample holder and pressed with a glass block. The standard white $BaSO_4$ was packed in the same way, being used as the reference sample. Single-scan spectra were recorded at a scan speed of 60 nm/min using the UVProbe 2.31 software.

X-Ray photoelectron spectroscopy. X-Ray photoelectron spectroscopy (XPS) analyses were performed in a PHI 5500 Multitechnique System instrument (from Physical Electronics) equipped with a monochromatic Al Kα X-Ray source (1486.6 eV, 350 W), placed perpendicular to the analyzer axis and calibrated using the 3d5/2 line of Ag with a full width at half maximum (FWHM) of 0.8 eV. The X-ray spot size was 650 μm. The pass energy was set at 150 and 40 eV for the survey and the narrow scans, respectively. Charge compensation was achieved with a combination of electron and argon ion flood guns. The energy and emission current of the electrons were 4 eV and 0.35 mA, respectively. For the argon gun, the energy and the emission current were 0 eV and 0.1 mA, respectively. The partial pressure for the argon flood gun was $2 \cdot 10^{-8}$ mbar. These standard conditions of charge compensation resulted in a negative but perfectly uniform static charge. Data acquisition and processing were achieved with the Advantage Software. Spectral calibration was determined by setting the main C 1s component at 285 eV. The surface composition was determined using the manufacturer's sensitivity factors.

TEM and SEM Microscopy. SEM studies were carried out using a Focused Ion Beam Zeiss Neon 40 scanning electron microscope equipped with an energy dispersive X-ray (EDX) spectroscopy system and operating at 30 kV. The samples were mounted on a double-sided adhesive carbon disc and sputter-coated with a thin layer of gold to prevent

sample charging problems. TEM images were collected with a Philips TECNAI 10 electron microscope operating at 80 kV. Bright field micrographs were taken with an SIS MegaView II digital camera. A solution containing PS, sulfonated PS, PNMPy/PSS core-shell and PNMPy hollow spheres (1mg/10μL in water) were cast onto a carbon coated copper-grids (300 mesh) and the solvent was allowed to evaporate.

4.3. Results and Discussion

4.3.1. Chemical composition and morphology of the conducting polymer microspheres

Characterization of CPs by spectroscopy is a difficult task compared to the conventional and insulating polymers, due to the charge of inorganic particles present in the polymer chains after the oxidative chemical polymerisation. This task becomes worse when the concentration of CP is very low, as occurs in the structures investigated in this work: PSS microspheres coated with nanolayers of PNMPy or PPy. In this study we discuss the most usual spectroscopic techniques for the characterization of the CPs adapted to these systems.

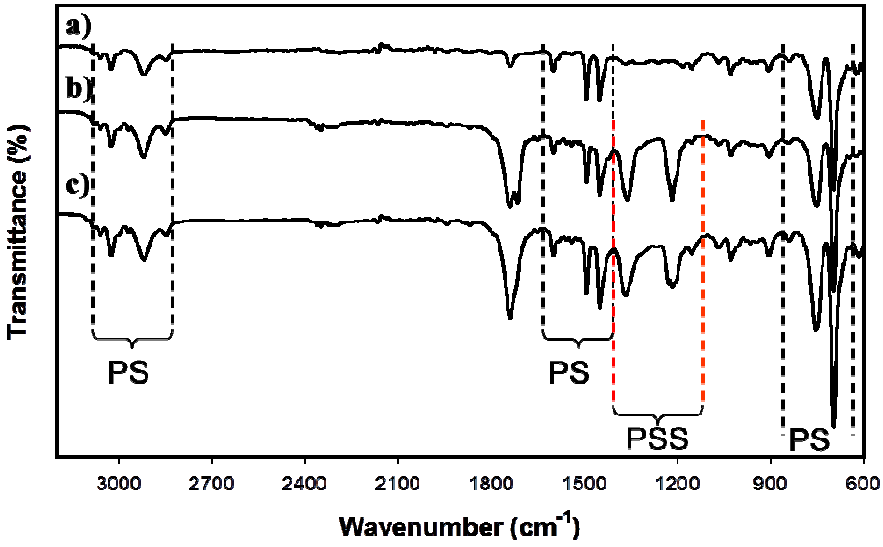

Figure 4.2. FTIR-ATR spectra of (a) PS, (b) PSS and (c) PNMPy/PSS particles.

Figure 4.2 compares the FTIR spectra of (a) PS microspheres, (b) PSS microspheres and (c) PNMPy/PSS microspheres. The mean peaks of PS (Figure 4.2a) are observed at 3032 and 2933 cm^{-1} (C-H aromatic and aliphatic stretching), 1494 and 1454 cm^{-1} (C=C aromatic stretching), 1032 and 916 cm^{-1} (C-H in-plane and out-of-plane bending), and two intense absorption bands at 759 and 698 cm^{-1} (substituted benzene rings). The sulfonation reaction produces two new intense peaks at 1369 and 1220 cm^{-1} (Figure 4.2b), which correspond to the asymmetric and symmetric SO stretching vibrations, respectively, indicating that the success of the reaction.[31]

Infrared spectroscopy is one of the most employed techniques for identification of organic compounds. However, despite many works describe the characterization of PTh and PPy derivatives using this spectroscopic method,[10,11] the application of this technique to our system present serious limitations. Figure 4.2c displays the IR spectrum of three-layered PNMPy coating a PSS sphere, where the major absorption bands correspond to the PSS material. Thus, the FTIR-ATR technique is not sensitive enough to monitor the presence of 30 nm of PNMPy coating the surface of the PSS particles. The use of FTIR-RAS (Reflection Absorption Spectroscopy) spectrometer housing with an angle specular reflectance accessory, which is very sensible to colloid particles and nanostructured materials with thin layers like those studied in this work,[32,33] has been considered as an alternative. However, the deposition of the PNMPy/PSS microspheres on a polished surface for FTIR-RAS analysis was difficult. On the other hand, detailed evidence of the degradation processes affecting the polymerisation of NMPy can be appreciated in the FTIR-ATR spectra of the neutral material, which show a strong band from C=O carbonyl groups (at 1740 cm^{-1}) produced by the polymer oxidation. This overoxidation of PPy and PNMPy has already been described in the literature.[18,34]

On the other hand, RAMAN spectroscopy has proved to be a useful technique for studying CP nanostructures, especially when they are in the doped state. The bands corresponding to the polymer are increased by the Raman resonant effect; while the bands of the dopant molecules are not in resonance conditions.[18] Therefore, we examined the presence of the PNMPy and PPy in microspheres doped systems with Raman spectroscopy.

Figure 4.3 compares the Raman spectra of PNMPy-$FeCl_3$, PNMPy-DBSA, PPy-$FeCl_3$ and PPy-DBSA materials. The PNMPy core-shell was characterized by Raman analysis with the observation of strong bands at 1578 cm^{-1} (C_α=C_β ring stretching), 1425 and 1327 cm^{-1} (C-N antisymmetrical stretching) and 1170 cm^{-1} (C-H in plane deformation and ring stretching) referred to doped species.

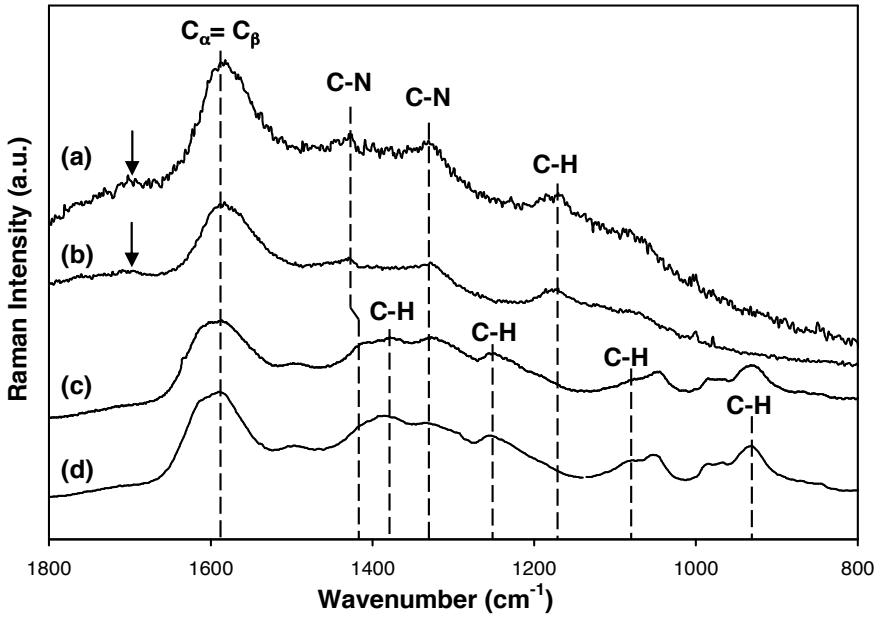

Figure 4.3. Raman spectra of (a) PNMPy-FeCl3, (b) PNMPy-DBSA, (c) PPy-FeCl3, and (d) PPy-DBSA core-shell particles. Inset arrow indicates the C^{α}=C^{β} bond-stretching vibration associated to the loss of symmetry in the molecule due to the irreversible oxidation of the Py ring (see Figure. 4.4). Exciting radiation: 632.8 nm.

Interestingly, the peaks assigned to the C_β-H bending vibrations at 1080-1040 cm^{-1} and the C_β=C_β stretching are not detected in the Raman spectra of the PNMPy microspheres. The disappearance of peaks usually indicates loss of symmetry in the molecule.[35] In this case we attribute such disappearance to the polymer backbone overoxidation of the position C-H (β) in the Py aromatic ring (see inset arrow on Figure 4.3a and 4.3b, and scheme showed in Figure 4.4). The origin of these CO groups is the oxidative process

undergone by some five-membered rings during the preparation of the PNMPy. The peaks are also quite broad presenting much noise, which is due to both the very thin layer of CP coat (30 nm) and the interactions with the dopant counterions.

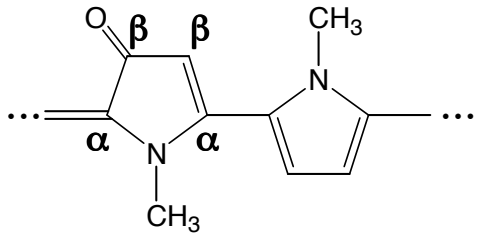

Figure 4.4. Scheme of Poly(N-methylpyrrole) backbone overoxidated.

On the other hand, it is worth noting that when polymer chains are partially doped some peaks should be duplicated. This is evidenced for PPy doped spheres in Figures 4.3c and 4.3d, which show not only a duplicated stretching mode of the C=C bonds at *ca.* 1600 cm^{-1} but also two additional bands at 1080 cm^{-1} (C-H in plane deformation) and 1380 cm^{-1} (ring stretching). These features should be attributed to the partially oxidized PPy backbone, as is indicated also by the presence of bipolaron (932 and 1080 cm^{-1}) and polaron (980 and 1045 cm^{-1}) C-H deformation and bending peaks. However, no relevant difference was found between the Raman spectra of the PNMPy microspheres doped with $FeCl_3$ and DBSA, or similarly between the spectra of the two PPy systems. This is in agreement with the loss of Raman resonance effect in the dopant molecules discussed above.

Another interesting observation provided by the Raman analyses is the absence of absorption bands related with the PS molecules. This allowed us to confirm that the template was completely coated by the CP in all the prepared microspheres doped systems. Furthermore, the spectra displayed in Figure 4.3 are consistent with those reported in the literature.[36-38]

The nanometric layer of the CP coating the microsphere has been characterized using UV-vis spectroscopy, which is a very sensitive technique. The UV-vis reflectance spectrum is depicted in the Figure 4.5. Control experiments on samples with the uncoated PS microspheres revealed almost 100 % reflectance in the range from 300 to 800 nm. Thus,

they are fine powder with white-milk colour and no absorption on the UV-visible region. However, the PS microspheres coated with PNMPy became a dark powder with significantly lower reflectance (*i.e.* higher absorbance), this feature being consistent with the well-coated core-shell particles found by Raman spectroscopy.

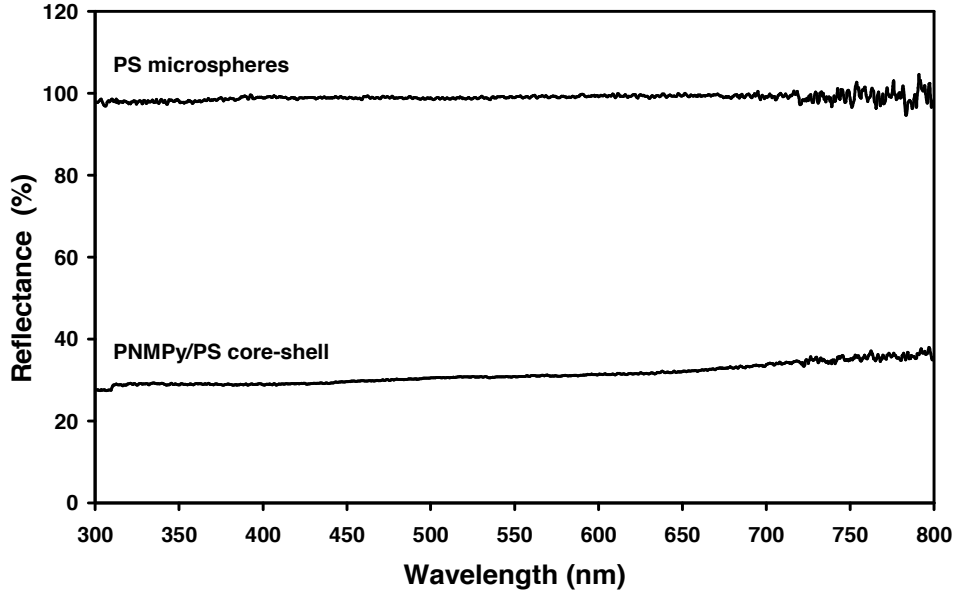

Figure 4.5. UV-vis reflectance spectra obtained for uncoated PS microspheres and for PNMPy/PS core-shell particles. The lower reflectance of the latter reflects an increase of the light absorption by the PNMPy-coated PS core-shell particles.

The CP composition of the coated PS microspheres was further characterized with XPS analysis. Elemental analyses showed the characteristic peaks of various elements with different binding energies corresponding to: Cl 2p (200.8 eV), C 1s (284.9 eV), N 1s (399.1 eV) and O 1s (532.2 eV). PNMPy XPS data reveals additional peaks compared to PS microspheres, as can be seen in Figure 4.6. These peaks indicate that the CP is partially doped by chloride anions and undergone partial surface oxidation by the high level of oxygen atoms. The presence of Cl 2p signals, which was already observed by Lascelles *et. al.*[10] for PPy coated PS particles, is observed when $FeCl_3$ oxidant is employed in the chemical polymerisation process. On the other hand, the presence of oxygen is consistent

with the FTIR spectrum of the PNMPy/PSS core-shell particles showed in the Figure 4.2c. The surface chemical composition determined by XPS for the coated PS studied in this work is: 87.65 % C, 10.17 % N, 2.18 % Cl (considering C+N+Cl=100 %). The C/N ratio of PNMPy is 8.618 and the Cl/N ratio is 0.21; which is comparable with the doping level typically accepted for PPy.

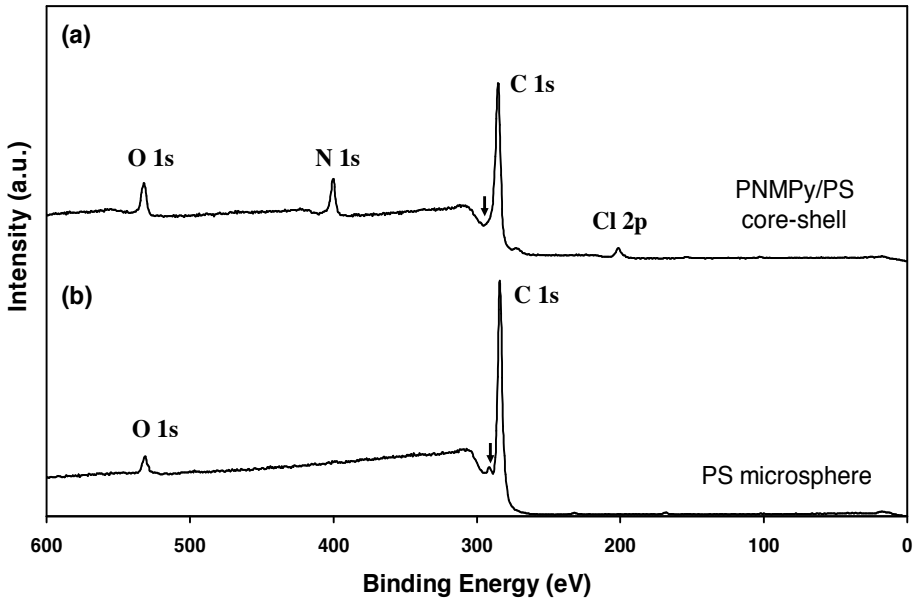

Figure 4.6. XPS survey spectra of: (a) PNMPy/PSS core-shell microspheres prepared by LbL self-assembly deposition and with core thickness of 30 nm; and (b) PS uncoated microspheres used as template.

High resolution spectra of C 1s, N 1s and Cl 2p are displayed in Figure 4.7 for both uncoated PS and PNMPy/PSS coated particles. As it can be seen, no signal associated to the aromatic ring of PS is observed in the spectra of the coated microspheres (Figure 4.7a), *i.e.* π-π^* shake-up satellite peaks at 291.5-293.0 eV are not detected in the C 1s region. This indicates that the core-shell is well covered by 30 nm thickness of PNMPy. There is no evidence of Fe atoms (708-720 eV) at the surface of the material, indicating that the material is well purified after the polymerisation process. The overall of the XPS results obtained in this work are in excellent agreement with those reported by Lascelles *et. al.*[10] and by Yang *et. al.*[14] for PPy/PS microspheres.

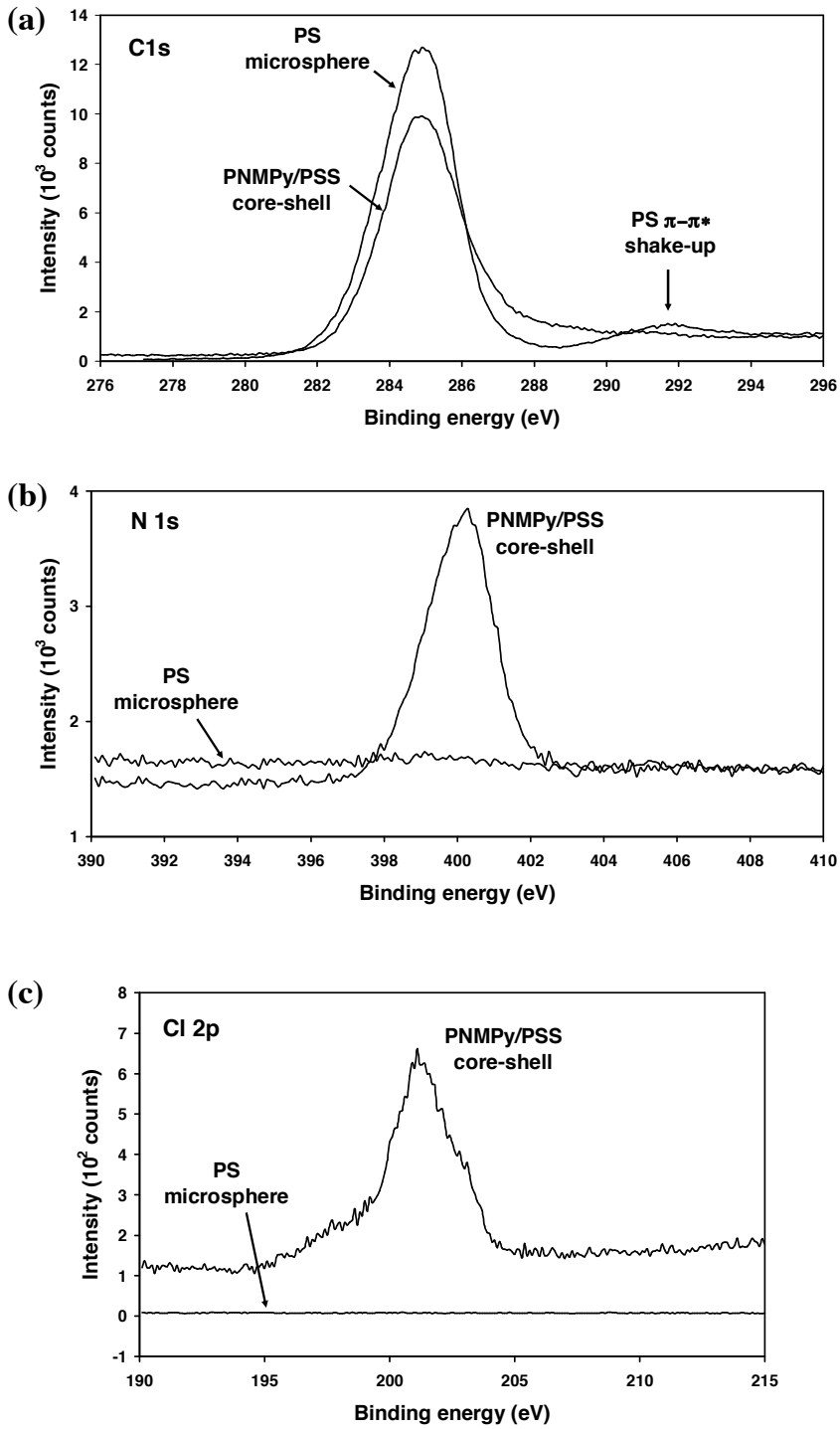

Figure 4.7. High resolution XPS spectra of PNMPy/PSS core-shell and PS uncoated microspheres: (a) C 1s region; (b) N 1s region; and (c) Cl 2p region.

Regarding to the overall procedure used to prepare nanolayers of CP, which is illustrated in Figure 4.1, solid PS spheres with an average diameter of 1.0±0.3 μm were obtained using the synthesis procedure developed by Lascelles *et. al.*[10] The SEM and TEM micrographs displayed in Figure 4.8 (Scheme A) indicate that all the PS particles are spherical and their size distribution is homogeneous.

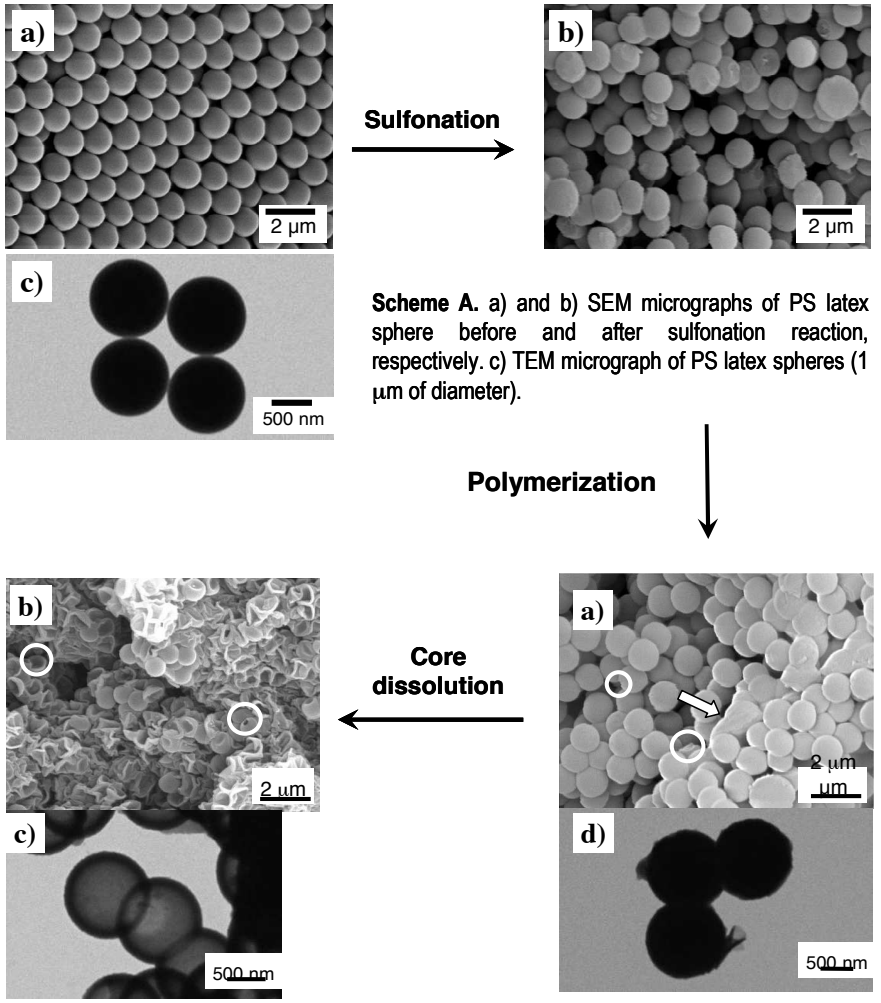

Scheme A. a) and b) SEM micrographs of PS latex sphere before and after sulfonation reaction, respectively. c) TEM micrograph of PS latex spheres (1 μm of diameter).

Scheme B. a) and b) SEM micrographs of spherical PNMPy/PSS particles and the "*broken egg-shells*" morphology observed after PS core dissolution. The imperfections or defects in PNMPy spheres were detected only when the shell was very thin (~10 nm). c) and d) TEM micrographs of "*caved-in*" and intact hollow PNMPy particles after three polymerization cycles (~30 nm).

Figure 4.8. Morphology of the PNMPy core-shell and hollow spheres, which have been prepared according to the LbL synthesis depicted in the Figure 4.1.

Figures 4.8 and 4.9 show the versatility of the process in forming composite multilayers of PNMPy. The shell thickness of the hollow spheres as well as their shape and stability depend on the number of polymerisation cycles, as it was discussed previously. Thus, intact hollow spheres were obtained when the shell thickness was increased with three PNMPy layer depositions (Figure 4.8b and 4.8d, Scheme B). Accordingly, the LbL self-assembly technique provides a successful pathway for the fabrication of nanostructured PNMPy in its doped and undoped states, as well as hollow-sphere structures. Thus, the LbL procedure should be considered as an excellent method to mimic vesicles or capsules using CPs.

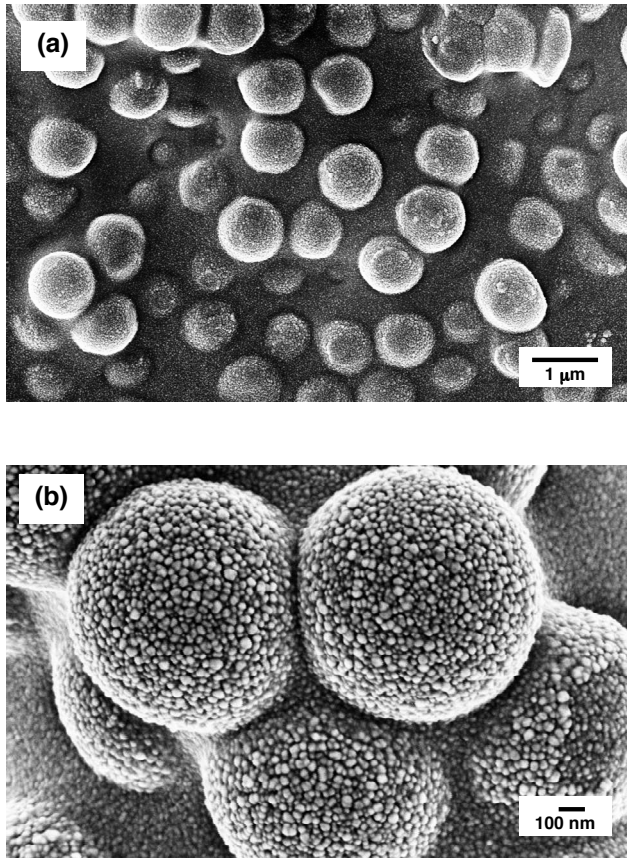

Figure 4.9. (a) SEM image of PNMPy/PSS core-shell. Intact microspheres are observed after three controlled polymer deposition cycles (when the shell thickness is about 30 nm). (b) High resolution SEM image showing the highly rough and porous surface of the PNMPy microspheres.

The PNMPy/PS overlayer thickness average is 9±1.8 nm for one polymerisation step, taken by TEM microscopy and assuming that the coating is uniform. After three polymerisation cycles the PNMPy shell thickness increased to 30±2.5 nm. Microspheres with thinner thickness undergo deformations when high vacuum conditions are applied in the SEM microscope (Figure 4.8a and 4.8b, Scheme B), and some particles coalesce together. These features are fully consistent with the observations reported by Yang *et. al.*,[39] who examined the influence of the PS sulfonation time on the shell thickness of polyaniline microspheres using SEM and TEM.

Figure 4.9 shows the SEM image of PNMPy/PSS core-shell in which intact microspheres are observed after three controlled polymer deposition cycles (the shell thickness is about 30 nm) as well as the SEM image at 100 nm showing the highly rough and porous surface of the PNMPy microspheres obtained by LbL technique. The surface of the PNMPy microspheres is more roughness than that of the PPy ones,[39] and indeed the porosity of the bulk is higher in the former than in the latter. Previous studies on PPy and PNMPy confirm these observations.[40,41] Due to the high porosity of PNMPy, the THF solvent molecules used to extract the PS core are able to diffuse into the template, which is easily removed without damage the spherical shape of the PNMPy (Figure 4.8c, Scheme B). On the other hand, Figure 4.9b evidences that the PS template is completely covered. Finally, energy dispersive EDX spectroscopy analyses revealed the presence of chloride anions in the doped PNMPy/PSS core-shell particles as well as a very low amount of iron.

4.3.2. On the use of conducting polymer microspheres as anticorrosive additive of organic coatings.

In order to evaluate the anticorrosive properties imparted by spherical PNMPy microparticles, the LbL self-assembly synthesis was scaled to prepare the required amount of CP. The purification procedure was the same than used for small quantity (section 4.2.4). A bicomponent solvent-borne epoxy formulation was prepared according to the following composition: 20 % by weight of epoxy resin (Epikote 1001X75, Resolution Europe-Brenntag), 5 % by weight of titanium dioxide (white oxined, Europigments), 1 % by weight of

PNMPy/PSS microspheres, 20 % by weight of barite (barium sulfate, Comindex S.A.), 12 % by weight of talc (Talco Industrial FF, T3Química), 0.23 % by weight of Aerosil 200 (Degussa AG), 1 % by weight of Antiterra U (BYK Chemie), 0.7 % by weight of BYK-500 and BYK-525 (BYK Chemie) and 19 % by weight of a mixture of solvents containing butanol, methyl-isobutyl-ketone and xylene (Panreac Química). The foregoing components were mixed and dispersed at 15000 rpm for 15 minutes with a Dispermat disperser model TU APS 250. After the mixing and dispersion, the formulation is ground in a batch mill provided with zirconium oxide balls to reduce the particle size below 50 micrometers. This process led to obtain part A of the epoxy paint. Part B, which corresponded to the polyamineamide hardener, was added to the Part A in the composition of 12 % by weight. The epoxy/amine ratio was 1.4-1.6 and the PVC/CPVC ratio (Pigment volume concentration / Critical pigment volume concentration ratio) was maintained at 0.65-0.70. 1 % by weight of PNMPy/PSS microspheres was added after dispersion in the appropriated solvent.

The PNMPy microspheres, contrary to what happens with poly[2,2'-(3-methylacetate)thiophene] (PTE) and similar to what occurs with polyaniline emeraldine base (PAni-EB) discussed in next chapters, had an enormous tendency to agglomerate. The PNMPy microspheres did not act as anticorrosive microparticles, despite we tried to disperse it in various solvents and tried to reduce their particle size. In order to achieve homogenous dispersions, electroactive PNMPy/PSS core-shell particles were added in a very low concentration (0.3 wt.%) in the vehicle (epoxy resin + solvents). The resulting dispersion showed dark spots above the coating surface after drying process, showing a clear phase separation from the homogenous coating surface, as is illustrated in Figure 4.10. Among the solvents unsuccessfully used to disperse PNMPy/PSS core-shell microspheres, chloroform, dichloromethane, tetrahydrofuran and dimethylsulfoxide deserve special mention because they are frequently employed in the formulation of paints.

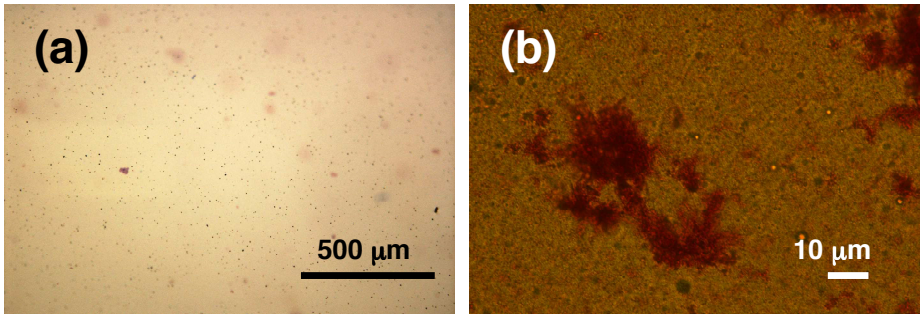

Figure 4.10. (a) Optical micrograph showing a great amount of conducting polymer particles in the epoxy coating surface, (b) Optical micrograph showing high magnification of agglomerated PNMPy/PSS microspheres inside the epoxy coating.

This behavior has been attributed to the high charge density at the microsphere surface, which causes a high electrostatic repulsion repelling the polar solvent molecules. The SEM micrographs of an epoxy film with PNMPy/PSS microspheres, prepared in xylene by solvent casting and without apply the Dispermat disperser mixing, are shown in Figure 4.11. Micrographs allow appreciate the fingerprint left by the agglomerated microspheres after detached from the coating surface by the high vacuum applied in the microscopy chamber. This represents another evidence of the microspheres repelled the epoxy solvent molecules, corroborating their incompatibility with the solvent-borne epoxy formulation. Similar results were previously obtained using PPy as anticorrosive additive.[42]

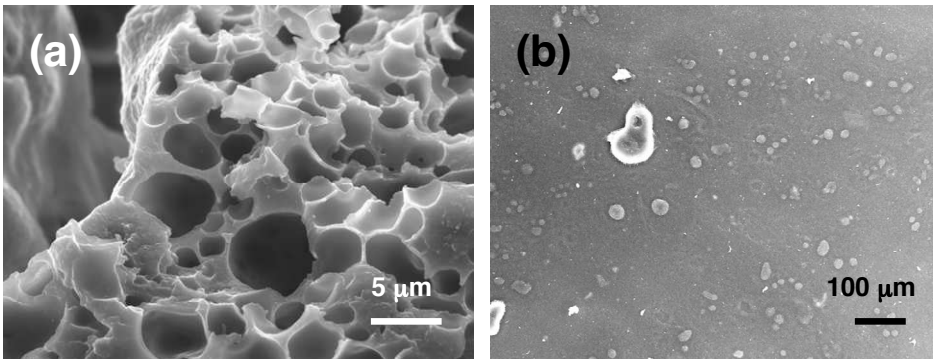

Figure 4.11. (a) SEM image of an epoxy film with a high concentration (> 1 wt.%) of PNMPy/PSS microspheres. The unsuccesful dispersion of the nanostructured CP in the epoxy resin is evidenced. (b) SEM image of an epoxy coating showing individual and agglomerated PNMPy/PSS core-shell particles onto the surface.

4.4. Conclusions

This chapter reports an innovative study about the performance of a nanostructured CP to act as anticorrosive additive in the formulation of conventional organic coatings. We presented a comprehensive study about the synthesis of PNMPy microspheres that have been prepared using the LbL self-assembly strategy. The LbL templating technique has been proved to be a highly versatile method to produce nanostructured PNMPy. Raman and XPS spectroscopies are excellent tools for characterization of nanolayers made of CPs. After the successful preparation and characterization of PNMPy/PSS core-shell microspheres, we have examined the ability of this CP to protect steel from corrosion. Unfortunately, this nanostructured CP has been found to be incompatible with the epoxy resins typically used in the formulation of solvent-borne organic primers. Thus, PNMPy/PSS microspheres tend to agglomerate giving place to the apparation of dark spots at the coating surface and precluding their application as anticorrosive additive. This behavior has been attributed to the high charge density at the microsphere surface.

4.5. References

[1] G. Decher, “Fuzzy nanoassemblies: Toward layered polymeric multicomposites“, *Science*, 1997, **277**, 1232-1237.

[2] F. Caruso, R. A. Caruso and H. Möhwald, “Nanoengineering of inorganic and hybrid hollow spheres by colloidal templating“, *Science*, 1998, **282**, 1111-1114.

[3] E. R. Kleinfeld and G. S. Ferguson, “Stepwise formation of multilayered nanostructural films from macromolecular precursors“, *Science*, 1994, **265**, 370-373.

[4] E. Donath, G. B. Sukhorukov, F. Caruso, S.A. Davis and H. Möhwald, “Novel hollow polymer shells by colloid-templated assembly of polyelectrolytes“, *Angew. Chem. Int. Ed.*, 1998, **37**, 2201-2205.

[5] F. Caruso, H. Lichtenfeld, M. Giersig and H. Möhwald, “Electrostatic self-assembly of silica nanoparticle-polyelectrolyte multilayers on polystyrene latex particles“, *J. Am. Chem. Soc.*, 1998, **120**, 8523-8524.

[6] B. Städler, A. D. Price, R. Chandrawati, L. Hosta-Rigau, A. N. Zelikin and F. Caruso, "Polymer hydrogel capsules: en route toward synthetic cellular systems", *Nanoscale*, 2009, **1**, 68-73.

[7] Y. Wang, A. S. Angelatos and F. Caruso, "Template synthesis of nanostructured materials via layer-by-layer assembly", *Chem. Mat.,* 2008, **20**, 848-858.

[8] J.F. Quinn, A.P.R. Johnston, G.K. Such, A. N. Zelikin and F. Caruso, "Next generation, sequentially assembled ultrathins films: beyond electrostatics", *Chem. Soc. Rev.,* 2007, **36**, 707-718.

[9] P. Hammond, "Form and function in multilayer assembly: New applications at the nanoscale", *Adv. Mat.*, 2004, **16**, 1271-1293.

[10] S. F. Lascelles, S. P. Armes, P. A. Zhdan, S. J. Greaves, A. M. Brown, J. F. Watts, S. R. Leadley and S. Y. Luk, "Surface characterization of micrometre-sized, polypyrrole-coated polystyrene latexes: Verification of a 'core-shell' morphology", *J. Mat. Chem.*, 1997, **7**, 1349-1355.

[11] X. Feng, C. Mao, G. Yang, W. Hou and J. J. Zhu,"Polyaniline/Au composite hollow spheres: Synthesis, characterization, and application to the detection of dopamine", *Langmuir*, 2006, **22***,* 4384-4389.

[12] C. Mangeney, S. Bousalem, C. Connan, M. J. Vaulay, S. Bernard and M. M. Chehimi, "Latex and hollow particles of reactive polypyrrole: preparation, properties, and decoration by gold nanospheres", *Langmuir*, 2006, **22**, 10163-10169.

[13] X. Yang, T. Dai, M. Wei and Y. Lu, "Polymerization of pyrrole on a polyelectrolyte hollow-capsule microreactor", *Polymer*, 2006, **47***,* 4596-4602.

[14] F. Yang, Y. Chu, S. Ma, Y. Zhang and J. Liu, "Preparation of uniform silica/polypyrrole microspheres and polypyrrole hollow microspheres by the template of modified silica particles using different modified agents", *J. Coll. Interf. Sci.*, 2006, **301**, 470-478.

[15] H. Yang, W. Jiang and Y. Lu, "Fabrication and characteristic of conductive and ferromagnetic hollow composite microcapsules", *Mat. Lett.*, 2007, **61**, 2789.

[16] T. Yao, Q. Lin, K. Zhang, D. Zhao, H. Lv, J. Zhang and B. Yang, "Preparation of SiO_2@polystyrene@polypyrrole sandwich composites and hollow polypyrrole capsules with movable SiO_2 spheres inside", *J. Coll. Interf. Sci.*, 2007, **315**, 434-438.

[17] C. Zhou, J. Han, G. Song and R. Guo, "Fabrication of poly(aniline-*co*-pyrrole) hollow nanospheres with Triton X-100 micelles as templates", *J. Pol. Sci.Part A: Pol. Chem.*, 2008, **46**, 3563-3572.

[18] L. H. Dall'Antonia, M. E. Vidotti, S. I. Córdoba de Torresi and R. M. Torresi, "A new sensor for ammonia determination based on polypyrrole films doped with dodecylbenzenesulfonate (DBSA) ions", *Electroanalysis*, 2002, **14**, 1577-1586.

[19] D. T. McQuade, A. E. Pullen and T. M. Swager, "Conjugated polymer-based chemical sensors", *Chem. Rev.*, 2000, **100**, 2537-2574.

[20] J. Liu, Y. Lin, L. Liang, J. A. Voigt, D. L. Huber, Z. R. Tian, E. Coker, B. Mckenzie and M. J. Mcdermott, "Templateless assembly of molecularly aligned conductive polymer nanowires: A New Approach for Oriented Nanostructures", *Chem. Eur. J.*, 2003, **9**, 604-611.

[21] J. X. Huang, S. Virji, B. H. Weiller and R. B. Kaner, "Polyaniline nanofibers: facile synthesis and chemical sensors" *J. Am. Chem. Soc.*, 2003, **125**, 314-5.

[22] J. X. Huang, S. Virji, B. H. Weiller and R. B. Kaner, "Nanostructured polyaniline sensors", *Chem. Eur. J.*, 2004, **10**, 1314-1319.

[23] S.Virji, J. X. Huang, R. B. Kaner and B. H. Weiller, "Polyaniline nanofiber gas sensors: examination of response mechanism", *Nano Lett.*, 2004, **4**, 491-496.

[24] L. Jiang, H. K. Jun, Y. S. Hohb, J. O. Lim, D. D. Lee and J. S. Huh, "Sensing characteristics of polypyrrole–poly(vinyl alcohol) methanol sensors prepared by in situ vapor state polymerization", *Sens. Actuators B*, 2005, 105, 132-137.

[25] S. Y. Chew, Z. P. Guo, J. Z. Wang, J. Chen, P. Munroe, S. H. K. Ng, L. Zhao and H. K. Liu, "Novel nano-silicon/polypyrrole composites for lithium storage", *Electrochem. Commun.*, 2007, **9**, 941-946.

[26] M. Sun, S. Zhang, T. Jiang, L. Zhang and J. Yu, "Nano-wire networks of sulfur–polypyrrole composite cathode materials for rechargeable lithium batteries", *Electrochem. Commun.*, 2008, **10**, 1819-1822.

[27] M. Hughes, M. S. P. Shaffer, A. C. Renouf, C. Singh, G. Z. Chen, D. J. Fray and A. H. Windle, "Electrochemical capacitance of nanocomposite films formed by coating aligned arrays of carbon nanotubes with polypyrrole" *Adv. Mater.*, 2002, **14**, 382-385.

[28] A. S. Saraç, H. Geyik, E. A. Parlak and M. Serantoni, "Electrochemical composite formation of thiophene and *N*-methylpyrrole polymers on carbon fiber microelectrodes: Morphology, characterization by surface spectroscopy, and electrochemical impedance spectroscopy", *Prog. Org. Coat.*, 2007, **59**, 28-36.

[29] S. C. Wuang, K. G. Neoh, E. T. Kang, D. W. Pack and D. E. Leckband, "Polypyrrole nanospheres with magnetic and cell-targeting capabilities", *Macromol. Rapid Commun.*, 2007, **28**, 816.

[30] B. C. Thompson, S. E. Moulton, J. Ding, R. Richardson, A. Cameron, S. O'Leary, G. G. Wallace and G. M. Clark, "Optimising the incorporation and release of a neurotrophic factor using conducting polypyrrole", *J. Control. Releas.*, 2006, **116**, 285-294.

[31] B. Stuart, Infrared spectroscopy: Fundamentals and applications, New York, Ed. John Wiley & Sons Ltd., 2004, Chapter 6, 117-198.

[32] N. Kato, P. Schuetz, A. Fery and F. Caruso, "Thin multilayer films of weak polyelectrolytes on colloid particles"**,** *Macromolecules*, 2002, **35**, 9780-9787.

[33] X. Shi, A. L. Briseno, R. J. Sanedrin and F. Zhou, "Formation of uniform polyaniline thin shells and hollow capsules using polyelectrolyte-coated microspheres as templates", *Macromolecules*, 2003, **36**, 4093-4098.

[34] A. Cambra, M. I. Redondo and M. J. Gonzalez-Tejera, "Influence of counter-ion concentration on properties of electrochemically generated poly-*N*-methylpyrrole (PNMPy/ClO_4)", *Synth. Met.*, 2003, **139**, 21-27.

[35] K. P. R. Nilsson, J. Rydberg, L. Baltzer and O. Inganäs, "Twisting macromolecular chains: Self-assembly of a chiral supermolecule from nonchiral polythiophene polyanions and random-coil synthetic peptides", *Proc. Natl. Acad. Sci. USA*, 2004, **101**, 11197-11202.

[36] M. Li, J. Yuan and G. Shi, "Electrochemical fabrication of nanoporous polypyrrole thin films", *Thin Solid Films*, 2008, **516**, 3836-3840.

[37] F. Chen, G. Shi, M. Fu, L. Qu and X. Hong, "Raman spectroscopic evidence of thickness dependence of the doping level of electrochemically deposited polypyrrole film", *Synth. Met.*, 2003, **132**, 125-132.

[38] M. Li, Z. Wei and L. Jiang, "Polypyrrole nanofiber arrays synthesized by a biphasic electrochemical strategy", *J. Mat. Chem.*, 2008, **18**, 2276-2280.

[39] Y. Yang, Y. Chu, F. Yang and Y. Zhang, "Uniform hollow conductive polymer microspheres synthesized with the sulfonated polystyrene template", *Mat. Chem. Phys.*, 2005, **92**, 164-171.

[40] C. Alemán, J. Casanovas, J. Torras, O. Bertran, E. Armelin, R. Oliver and F. Estrany, "Cross-linking in polypyrrole and poly(N-methylpyrrole): Comparative experimental and theoretical experimental studies", *Polymer*, 2008, **49**, 1066-1075.

[41]. D. Aradilla, F. Estrany, R. Oliver, E. Armelin and C. Alemán, "Morphology and growing of nanometric multilayered films formed by alternated layers of poly(3,4-ethylenedioxythiophene) and poly(N-methylpyrrole)", *Thin Solid Films*, 2010, **518**, 4203–4210.

[42] E. Armelin, A. Meneguzzi, C.A. Ferreira and C. Alemán. "Polyaniline, polypyrrole and poly(3,4-ethylenedioxythiophene) as additives of organic coatings to prevent corrosion." *Surf. Coat. Technol.*, 2009, **203**, 3763-3769.

5

PARTIAL REPLACEMENT OF METALLIC ZINC DUST IN HEAVY DUTY PROTECTIVE COATINGS BY CONDUCTING POLYMER

The work described in this chapter was published in *Prog. Org. Coat.*, 2010, **69**, 26-30

The aim of this work is to show that the high concentration of metallic zinc dust typically used in marine epoxy primers can be significantly reduced by introducing a small concentration of conducting polymer as auxiliary anticorrosive additive. Specifically, in this work we show that the concentration of the anticorrosive inorganic pigment can be reduced from 79 to 60 wt.% by adding 0.3 wt.% of polyaniline emeraldine salt. Initially, the influence of this modification in the structural, thermal and mechanical properties of the coating has been examined. After this, accelerated corrosion assays in an aggressive solution medium have been developed. The protection imparted by the unmodified and modified paint formulations has been determined using the standard method ASTM D 1654-79.

5.1. Introduction

Metallic substrates are usually protected from aggressive environments through organic coatings (paints). In order to achieve long-term corrosion inhibition, a high concentration of anticorrosive pigments is added to the formulation of such coatings. Consequently, corrosion inhibitors, which are of inorganic nature (*e.g.* metallic zinc dust, $Zn_3(PO_4)_2$ and metal oxides) are constantly released into the environment. Paints formulated with some heavy metals (*e.g.* chromates) have been severely limited and phased out in the last years due to their detrimental effects on both environmental and human health.[1] Zinc and its compounds, while of significantly lower toxicity to humans than chromates, have been recognized as toxic to aquatic life.[2] By this reason environmental regulations to decrease the use of zinc containing compounds as additive anticorrosive are becoming stricter every day, and their reduction in regulated paints will be implemented in next years.[3]

In recent years conducting polymers (CPs) have received attention because their electrochemical properties are suitable to protect active metals from corrosion.[4,5] Within this field, CPs can be used in different ways, some of them being recently reviewed.[6] These can be summarized as follows: (1) CPs can be directly deposited on the metal surface acting as a protecting primer alone,[7] even although significant improvements have been obtained when a relatively small concentration of inorganic pigment is added;[8-10] (2) CPs can be combined with conventional topcoats providing better corrosion protection than conventional

primer-topcoat systems with inorganic corrosion inhibitors;[11-13] (3) in some cases CPs blended with conventional resins have been found to improve the protection imparted by the resins alone;[14,15] and finally (4) we proposed to modify paint formulations by adding a very low concentration of CPs (~ 0.3 wt.%).[16-25]

In recent years we have tested the reliability of polyaniline (PAni),[18,20,21,23-25] polythiophene (PTh)[16,17,29,22,24] and polypyrrole (PPy)[21,22,24] derivatives as anticorrosive additives. For this purpose, a low concentration of CP was added to different marine and industrial primers frequently used for corrosion protection in aggressive environments (*i.e.* epoxy, polyurethane and polyalkyd formulations containing inorganic anticorrosive pigments that were kindly supplied by industrial manufacturers). Accelerated corrosion assays showed that the addition of a small concentration of CP usually improves the resistance of the paint, the inhibition of corrosion increasing with the miscibility between the CP and the paint. Furthermore, in some cases (*e.g.* PAni) the CP was found to act as an adhesion promoter. On the other hand, in a recent study we used CPs as anticorrosive additives of a paint formulation that was completely free of inorganic pigments and additives.[18] The addition of PAni emeraldine salt (PAni-ES) (0.3 wt.%) dispersed in xylene provided an excellent corrosion protection. Specifically, accelerated corrosion assays, in which steel panels coated with the modified paint were exposed in 3.5 % NaCl solution for 720 h, evidenced that this polymer works as both a corrosion inhibitor and an adhesion promoter.

In this work we present a different view of our technology. Thus, we focus on the partial replacement of zinc based anticorrosive compounds by a small concentration of an organic CP. Specifically, we examine if the addition of 0.3 wt.% of PAni-ES to a marine epoxy primer formulation allows reduce the content of metallic zinc dust from 79 wt.% to 60 wt.% without detrimental effects in its protecting properties. This modification of the paint formulation is expected to provide important benefits to manufacturers: (i) significant reduction of the health risks (*i.e.* CPs are non-toxic materials[25]); (ii) derived marked advantages by being proactive in meeting the new regulations; and (iii) reduction of the formulation cost and paint weight.

5.2. Methods

The two epoxy primers used in this work were supplied by Pinturas Hempel S.A., manufacturers of paints for marine and protective use. They consist on epoxy primers, hereafter denoted EPOXY-79 and EPOXY-60, which only differ in the concentration of anticorrosive additive: 79 and 60 wt.% of metallic zinc dust, respectively. The paints are composed of the epoxy resin Epikote 3011 (Hexion) and Craymid 115 (Cray Valley), both mixed in a stoichiometric amount, and a mixture of alcoholic solvents and aromatic hydrocarbons. PAni-ES was purchased from Aldrich (CAS nº: 650013). PAni-ES (0.3 wt.%) was added to the mixtures of the resin base and hardener, and stirred mechanically until homogeneous dispersions were reached. The modified paints have been denoted as EPOXY-79/PAni and EPOXY-60/PAni. A naval steel (St F111) was employed as metallic substratum for corrosion experiments.

Films for the structural, thermal and mechanical characterization of the paints were prepared by evaporation at room temperature of the volatile organic solvents contained in the formulations. The structural characterization of the coating films was performed using a Bomem Michelson MB100 FTIR spectrophotometer with a resolution of 4 cm^{-1} in the absorbance mode. The samples were placed in an attenuated total reflection accessory with thermal control and a diamond crystal (Golden Gate Heated Single Reflection Diamond ATR, Specac-Teknokroma). Thermogravimetric analyses were carried out with a Perkin Elmer TGA-6 thermobalance at a heating rate of 10 °C/min under nitrogen atmosphere and a temperature range from 30 to 850 °C. The mechanical properties of the paints were evaluated through stress-strain assays with a Zwick Z2.5/TN1S testing machine. Plate samples with a length of 30 mm, a width of 3 mm and a thickness of 100-250 μm were cut out from paint films and used. The deformation rate was 10 mm/min. All the mechanical parameters reported in this work were obtained by averaging the results obtained from ten independent measurements.

Corrosion tests were performed on rectangular metal panels of 40 × 50 × 1 mm^3 containing a hole with a diameter of 6.5 mm. Before coating, steel panels were polished, degreased with acetone and stored in dry atmosphere. The paints were applied by

immersion of the metallic pieces in the primer/solvent/hardener with the manufacturer recommended mixing ratio. The thickness of the films yielded using this procedure was measured using a machine model Uno-Chek Fe from Neurtek S.A. company.

Corrosion studies were performed using the home-made equipment developed in our laboratory.[23] This device is prepared to perform accelerated immersion assays in an aggressive solution medium, which consists of an aqueous solution of NaCl (3.5 wt.%, pH=6.6) stored in a plastic container, through controlled cycles. The operating conditions of each programmed cycle were: (i) immersion of coated steel sheets (15 min); (ii) wring out (30 min); (iii) drying stage with bulbs (230 V – 100 W; 10 min); and (iv) cooling time at room temperature (5 min). Painted panels were sealed on the edges and around the hole used for securing the pieces. The samples were scribed and tested for a total exposure time of 720 h (720 accelerated corrosion cycles). The corrosion of the steel was monitored by both visual and microscopy inspections as described on the standard method ASTM D 1654-79. The coating surfaces were observed using an Olympus BX-5 light polarizing microscope, operating in reflection mode with an Olympus C3030Z digital camera coupled. Photographs and micrographs of the samples were taken before exposure to the aggressive solution as well as throughout the corrosion assays.

5.3. Results and Discussion

5.3.1. Characterization of dry paints

In order to obtain modified paints with homogeneous surface and good adherence, we improved the dispersion between PAni-ES and both EPOXY-79 and EPOXY-60 by dissolving the CP in the minimum volume of xylene before mix. This solvent is commonly used by coating's companies and was found to improve significantly the properties of the modified paints.[18] PAni-ES (0.3 wt.%) dissolved in xylene was added to the formulation of each paint and stirred mechanically until homogeneous dispersions were reached. The thickness of the films obtained after one coat, which were smooth and uniform in all cases, were 71±15 and 94±18 μm for EPOXY-79/PAni and EPOXY-60/PAni, respectively,

and 71±12 and 76±16 μm for the corresponding unmodified formulations. These values are close to the thickness recommended by the manufacturer for EPOXY-79 and EPOXY-60: 80 μm. As was reported previously, PAni-ES improved significantly the adherence of the paint to the metal substrate,[18,24] which contributed to impart corrosion resistance.

The FTIR absorption spectra of the modified and unmodified paints are compared in Figure 5.1. The spectra recorded for EPOXY-79 and EPOXY-60 were very similar, which was an expected result. On the other hand, the addition of a small concentration of PAni-ES is not appreciable by FTIR spectroscopy, which is consistent with previous studies.[18,20,21,23-25] The absence of terminal epoxy groups, typically found at 917 cm^{-1}, indicates that in all cases the curing process was successfully completed. The more important bands correspond to: hydroxyl groups (3500-3200 cm^{-1}), C-H vibration (2966, 2927, 2868 and 2858 cm^{-1}), aromatic C=C (1608, 1510 cm^{-1}), aromatic ether (1247 cm^{-1}) and C-H out-of-plane bending (829 cm^{-1}).

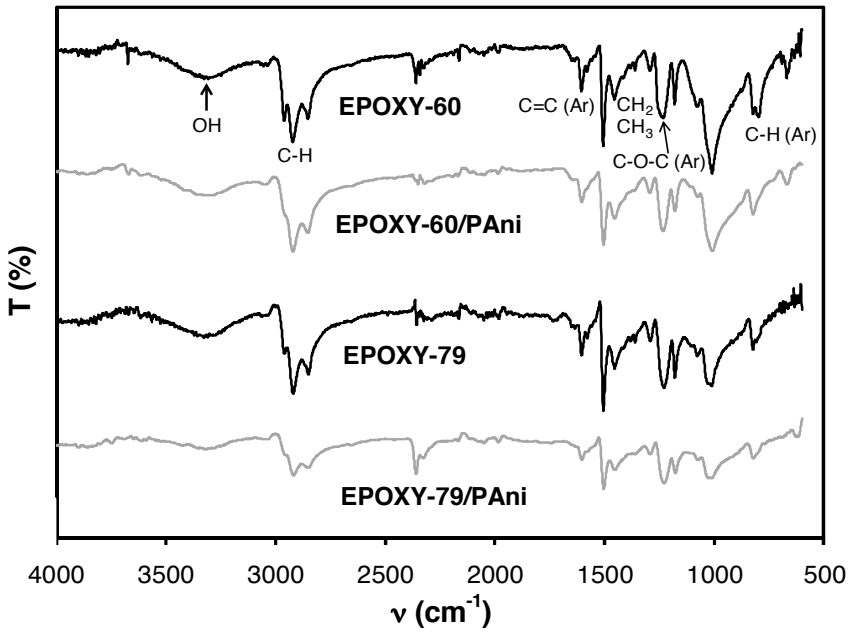

Figure 5.1. Infrared absorption spectra of the epoxy paints without (control samples) and with PAni-ES.

The thermal stability of the four coatings was studied by thermogravimetry, the resulting curves being compared in Figure 5.2. The thermal behavior is not influenced by the addition of PAni-ES. Thus, in all cases thermal decomposition starts at around 300 °C and char-yielded at 850 °C indicates a high percentage of inorganic additives contained in these paint formulations, *i.e.* 75, 79, 81 and 78 % for EPOXY-60, EPOXY-60/PAni, EPOXY-79 and EPOXY-79/PAni, respectively.

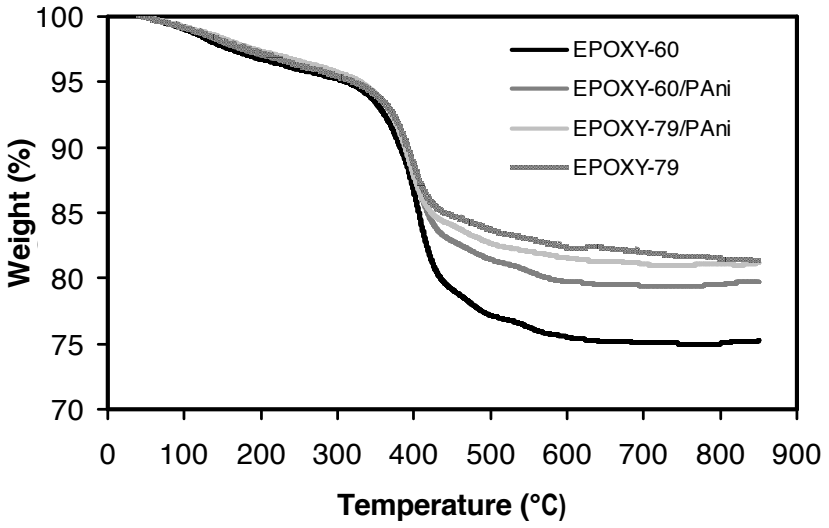

Figure 5.2. Thermogravimetric curves of the two epoxy paints without (control samples) and with PAni-ES.

Mechanical properties, which are listed in Table 5.1, indicate that the coatings studied in this work are brittle materials with relatively high Young modulus (*E*) and low elongation at break (ε_b). The latter must be attributed to the high content of inorganic anticorrosive pigments. The Young's modulus varied between 331 and 645 MPa, while tensile strength (σ_{max}) ranged between 2 and 13 MPa. The addition of PAni-ES to the EPOXY-79 formulation induced a reduction of all the mechanical characteristics. However, the modification of the EPOXY-60 paint with 0.3 wt.% of PAni-ES enhanced both the Young modulus and the tensile strength. The overall of these results clearly reflects that the mechanical resistance of the epoxy coating under study increases when 19 % of metallic

zinc dust is replaced by 0.3 wt.% of PAni-ES, *i.e.* EPOXY-79 transforms into EPOXY-60/PAni.

Coating	Description	*E* (MPa)	σ_{max} (MPa)	ε_b (%)
EPOXY-60	60 wt.% of Zn dust	331	2	8
EPOXY-60/PAni	60 wt.% of Zn dust +0.3 wt.% PAni-ES	645	13	2
EPOXY-79	79 wt.% of Zn dust	614	10	2
EPOXY-79/PAni	79 wt.% of Zn dust +0.3 wt.% PAni-ES	446	2	1

Table 5.1. Tensile properties of the coatings studied in this work.

5.3.2. Accelerated corrosion assays

The samples coated with the unmodified and modified epoxy paints are displayed in Figure 5.3 before, during and after the accelerated corrosion assays. As it was expected, the resistance against corrosion of the unmodified paints improves with the concentration of metallic zinc dust, being considerably higher for the EPOXY-79 control samples than for the EPOXY-60 ones. Thus, for the latter coating the rust throughout the scribe was evident after 120 h of exposure on the NaCl solution, whereas for the EPOXY-79 the rust formed after 720 cycles was very scarce. The addition of PAni-ES increased the resistance against corrosion in all cases. It is particularly remarkable that no rust was detected in samples coated with EPOXY-79/PAni after 720 accelerated corrosion cycles. Furthermore, PAni-ES also was very effective when added to the EPOXY-60 preventing corrosion near the scratch line before 240 h. Thus, apparently the corrosion resistance of EPOXY-60/PAni was significantly higher than that of EPOXY-60, at least until 480 h of exposure. This was confirmed by examining the scrapped test panels, which are displayed in Figure 5.4. The scrapped panels were used to evaluate the corrosion resistance according to the ASTM Standard Methods D-1654, *i.e.* through the progress of rust, which is determined by the loss of adherence near to the scribe mark, and the area corroded under the film.

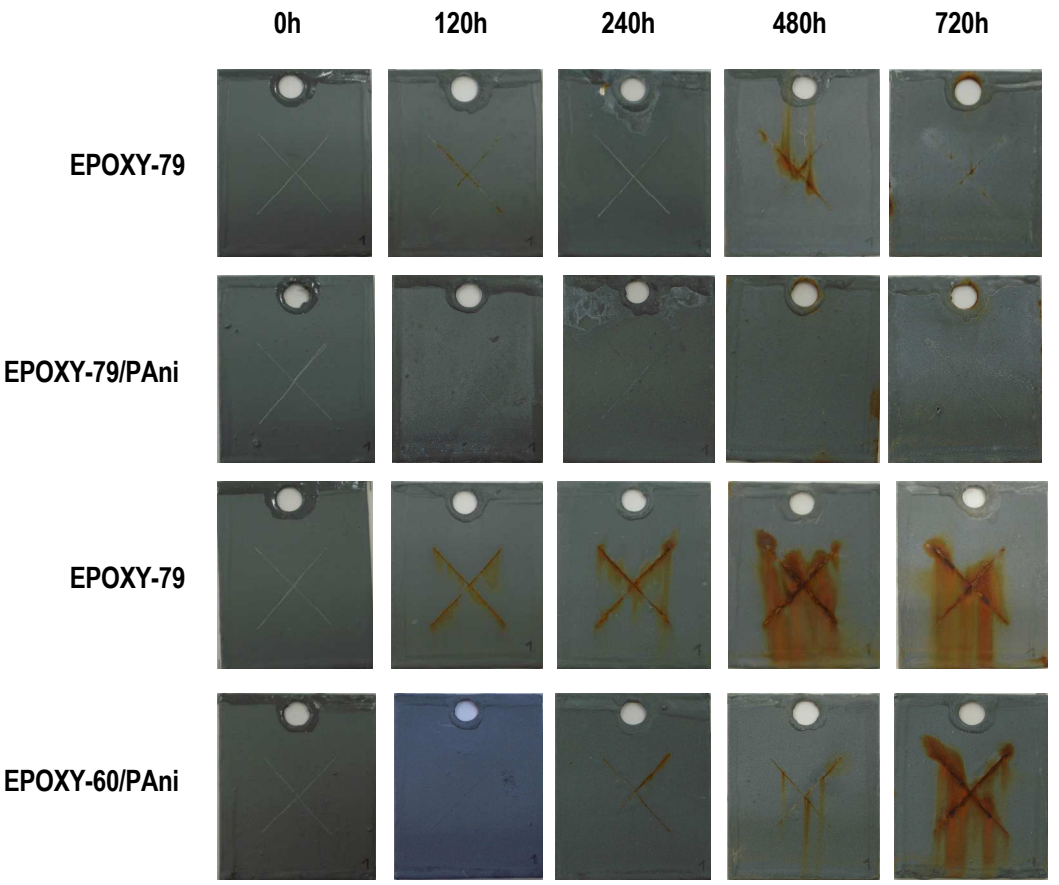

Figure 5.3. Test panels of the epoxy coatings without conducting polymer (controls) and modified with PAni-ES (0.3 wt.%) before and after 120, 240, 480 and 720 accelerated corrosion cycles (see text). The dimensions of the rectangular steel panels were: 40 × 50 × 1 mm^3, the diameter of the hole for securing being 6.5 mm.

Figure 5.5 represents the progression of rust from scribe against time (*i.e.* number of corrosion cycles). As it was expected, the loss of adherence increases with the number of cycles in all cases. The addition of PAni-ES to the paint with lowest content of zinc dust, EPOXY-60, enhances the adherence, while the opposite behavior is detected when the CP is added to the EPOXY-79. Thus, the high concentration of metallic anticorrosive pigment does not allow this protecting action of PAni-ES in the latter coating. The evolution of the corroded area under the film *vs.* time according to the ASTM D-1654 is displayed in Figure 5.6. It is worth noting that the progress of corrosion was very small for the

EPOXY-79/PAni coating (*i.e.* the corroded area was 1.1 % after 720 corrosion cycles). This represents a significant improvement with respect to the unmodified paint EPOXY-79, which showed a corroded area of 16.3 % after the same number of cycles. However, the most remarkable result corresponds to the EPOXY-60/PAni that shows not only better results than the EPOXY-60 but also a behavior similar to that of the EPOXY-79. Thus, the corroded area after 720 h was 14.1 %. Another interesting feature is that the corroded area increases very rapidly for the EPOXY-60 coating (*i.e.* it is 16.3 % and 27.2 % after 150 and 720h, respectively). This poor behavior is clearly corrected by the addition of PAni-ES, which should be attributed in part to the enhancement of the adherence provoked by the CP (Figure 5.5).

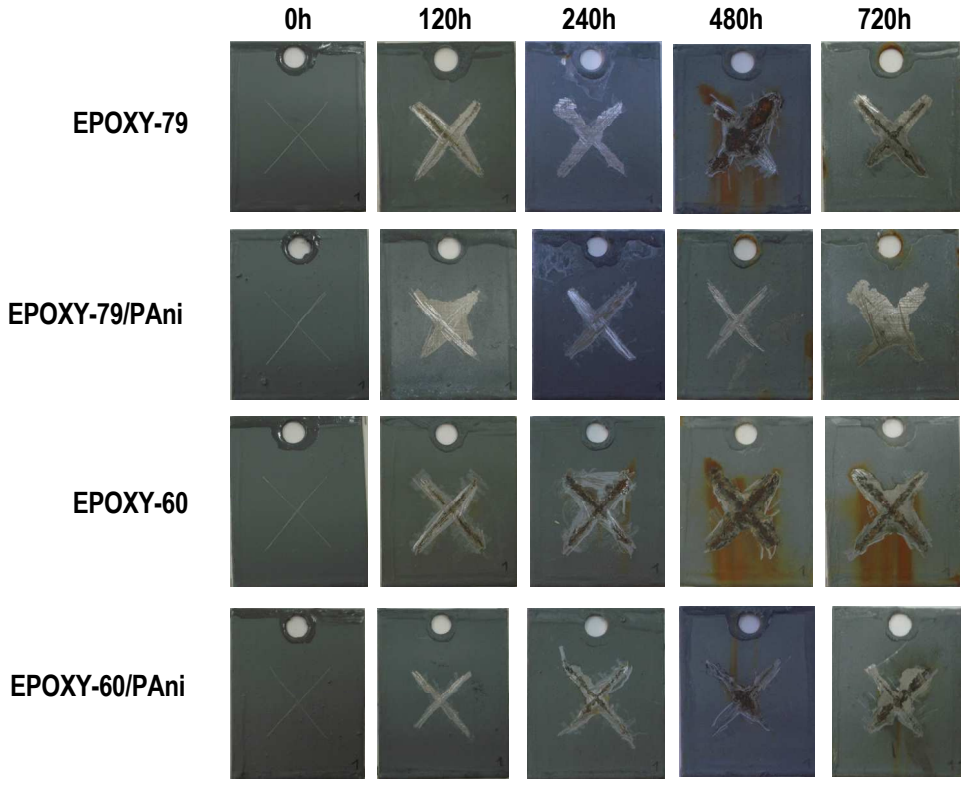

Figure 5.4. Scrapped test panels of the epoxy coatings without conducting polymer (controls) and modified with PAni-ES (0.3 wt.%) before and after 120, 240, 480 and 720 accelerated corrosion cycles (see text). The dimensions of the rectangular steel panels were: 40 × 50 × 1 mm^3, the diameter of the hole for securing being 6.5 mm.

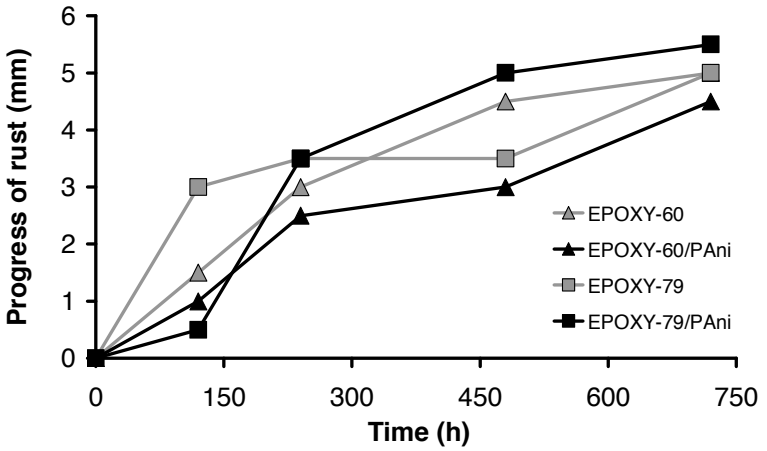

Figure 5.5. Progression of rust from scribe vs. time in the EPOXY-60, EPOXY-60/PAni, EPOXY-79 and EPOXY-79/PAni panels, according to the ASTM Standard Method D-1654.

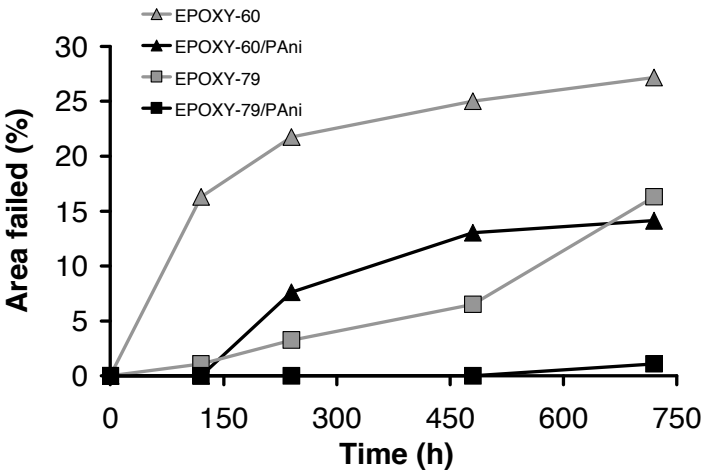

Figure 5.6. Progression of the corrosion area vs. time in the EPOXY-60, EPOXY-60/PAni, EPOXY-79 and EPOXY-79/PAni panels, according to the ASTM Standard Method D-1654.

Figure 5.7 shows optical micrographs of the unmodified and modified coatings before and after 720 accelerated corrosion cycles. The initial samples of the four paints show a rough surface. Moreover, identification of PAni-ES is not possible in the EPOXY-60/PAni

and EPOXY-79/PAni coating reflecting an excellent dispersion of the CP. It is worth noting that the roughness increases with the number of corrosion cycles reflecting the degradation of the surface. Interestingly, after 720 h the degradation undergone by the EPOXY-79 and EPOXY-60/PAni surfaces was very similar.

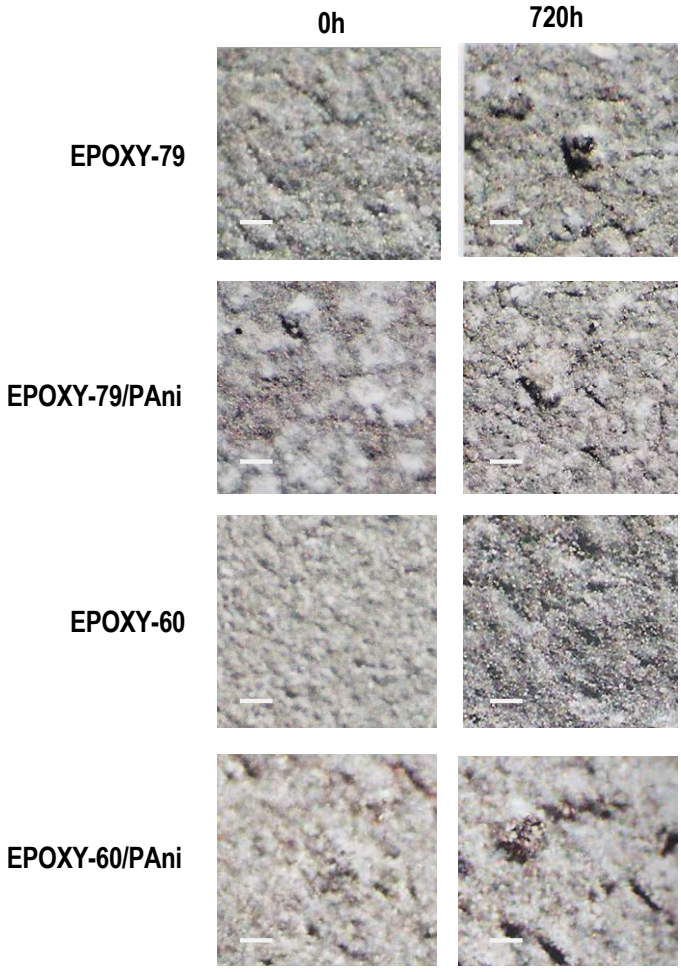

Figure 5.7. Optical micrographs of the EPOXY-60, EPOXY-60/PAni, EPOXY-79 and EPOXY-79/PAni before and after 720 accelerated corrosion cycles. Scale bar: 100 μm.

5.3.3. Protection mechanism

The ability of CPs to intercept electrons at carbon steel surfaces and to transport them was illustrated and discussed in early studies.[27-29] On the other hand, zinc dust pigment protects steel sacrificially if the concentration is high enough to facilitate the contact between metallic particles. However, such high concentration also produces a significant reduction of the mechanical and adherence properties of the coating. Current environmental regulations tend to decrease the use metallic inorganic pigments typically used in organic coatings. This work presents an approach based on the combination of a low concentration of CP, as an auxiliary anticorrosive additive, and zinc dust. Specifically, 0.3 wt.% of PAni-ES was dispersed in an epoxy primer to partially replace the inorganic anticorrosive pigment, *i.e.* the concentration of metallic zinc dust was reduced from 79 wt.% to 60 wt.%. Results obtained in this study combined with those previously achieved,[18,20,21,23-25] in which PAni-ES was added to other paint formulations, *i.e.* both containing and free of anticorrosive pigments and additives, allow us propose the protection mechanism imparted by this CP.

The oxidation state of the Zn particles plays an important role in the first stage of the mechanism. Thus, diffusion of oxygen and water oxidizes neutral zinc giving place to a passivating zinc oxide layer. This barrier film prevents dissolved oxygen from reaching the metal surface and receiving electrons. As a result of the oxidation of Zn^0 to Zn^{+2}, two electrons are released and these flow through the coating films. PAni-ES, which is the doped form of PAni, captures the electrons from the oxidation reaction and reduces to the neutral form of PAni (*i.e.* PAni-EB). On the other hand, it should be remarked the important role of the chloride ions in the pitting corrosion, this attack being characterized by the easy penetration of the Cl^- across the crystalline structure of the protective oxide. This type of corrosive attack generates local galvanic cells with a high unfavorable surface reaction between cathodic and anodic areas. However, in this case the chloride anions induce the conversion of PAni-EB to PAni-ES completing the autocatalytic cycle. It is worth noting that this cycle, which stabilizes the potential of the iron in the ferrous form Fe^{2+} in the passive region and the zinc in the active, is possible because of the co-existence of both zinc dust and PAni-ES as anticorrosive additives. Moreover, accelerated corrosion assays evidenced

that the addition of a small content PAni-ES allow reduce significantly the content of zinc dust in the paint. Thus, the electrochemically properties of the CP induce a protecting redox cycle in which the reversible transformation PAni-ES into PAni-EB is essential.

5.4. Conclusions

Immersion testes in an aggressive medium showed that metallic zinc dust of the EPOXY-79 coating can be partially replaced by 0.3 wt.% of PAni-ES without any detrimental effect in the protecting properties. Moreover, the incorporation of the CP enhances the adherence properties of the coating, this effect being consistent with previous studies using PAni-ES. The partial substitution of the inorganic anticorrosive pigment produces a change in the protection mechanism. Thus, coatings with a high concentration of zinc dust pigment protect steel sacrificially, this effect being possible because of the contact between metallic particles. In contrast, the combination zinc dust with PAni-ES, which acts as an auxiliary anticorrosive additive, is based on an autocatalytic cycle controlled through the reversible transformation between the doped and neutral forms of the CP. The results presented in this work provide a significant advance towards the new environmental regulations to decrease the use of zinc containing compounds as anticorrosive pigments.

5.5. References

[1] Europe's environment. The fourth assessment. N° 1 (2007) - Chapter 5, Sec.2, page 228. [http://www.eea.europa.eu/].

[2] Y. Shao, C. Jia, G. Meng, T. Zhang and F. Wang, “The role of a zinc phosphate pigment in the corrosion of. scratched epoxy-coated steel”, *Corros. Sci.*, 2009, **51**, 371-379.

[3] U.S. Environmental Protection Agency (EPA Regulations, July 9th, 2009) [http://www.epa.gov/iris/subst/0426.htm].

[4] J. I. Martins, T. C. Reis, M. Bazzaoui, E. A. Bazzaoui and L. I. Martins, “Polypyrrole coatings as a treatment for zinc-coated steel surfaces against corrosion”, *Corros. Sci.*, 2004, **46**, 2361-2381.

[5] N. A. Ogurtsov, A. A. Pud, P. Kamarchik and G. S. Shapoval, “Corrosion inhibition of aluminum alloy in chloride mediums by undoped and doped forms of polyaniline”, *Synth. Met.*, 2004, **143**, 43-47.

[6] E. Armelin, R. Oliver, F. Liesa, J. I. Iribarren, F. Estrany and C. Alemán, “Marine paint formulations: Conducting polymers as antiocorrosive additives”, *Prog. Org. Coat.*, 2007, **59**, 46-52.

[7] D. E. Tallman, G. Spinks, A. Dominis, G. G. Wallace and D. E. Tallman, “Electroactive conducting polymers for corrosion control: Part 1. General introduction and a review of non-ferrous metals”, *J. Solid State Electrochem.*, 2002, **6**, 73-84.

[8] D. M. Lenz, M. Delamar and C. A. Ferreira, “Improvement of the anticorrosion properties of polypyrrole by zinc phosphate pigment incorporation”, *Prog. Org. Coat.*, 2007, **58**, 64-69.

[9] T. Schauer, A. Joos, L. Dulog and C. D. Eisenbach, “Protection of Iron against corrosion with polyaniline primer”, *Prog. Org. Coat.*, 1998, **33**, 20-27.

[10] O. Zubillaga, F. J. Cano, I. Azkarate, I. S. Molchan, G. E. Thompson, A. M. Cabral and P. J. Morais, “Corrosion performance of anodic films containing polyaniline and TiO_2 nanoparticles on AA3105 aluminium alloy”, *Surf. Coat. Technol.*, 2008, **202**, 5936-5942.

[11] V. J. Gelling, M. M. Wiest, D. E. Tallman, G. P. Bierwagen and G. G.Wallace, “Studies of poly(3-octyl pyrrole) and poly(3-octadecyl pyrrole) on aluminum 2024 T-3 alloy”, *Prog. Org. Coat.*, 2001, **43**, 149-157.

[12] C. A. Ferreira, S. Aeiyach, A. Coulaud, and P. C. Lacaze, “Appraisal of the polypyrrole/cataphoretic paint bilayer system as a protective coating for metals”, *J. Appl. Electrochem.*, 1999, **29**, 259-263.

[13] J. H. Huh, E. J. Oh and J .H. Cho, “Investigation of corrosion protection of iron by polyaniline blend coatings”, *Synth. Met.*, 2003, *137*, 965-966.

[14] J. I. Iribarren, F. Cadena and F. Liesa, “Corrosion protection of carbon steel with thermoplastic coatings and alkyd resins containing polyaniline as conductive polymer”, *Prog. Org. Coat.*, 2005, **52**, 151-160.

[15] S. Ahmad, S. M. Ashraf and U. Riaz, “Corrosion studies of polyaniline/cocnut oil poly(esteramide urethane) coatings”, *Polym. Adv. Technol.*, 2005, **16**, 541-548.

[16] C. Ocampo, E. Armelin, F. Liesa, C. Alemán, X. Ramis, and J.I. Iribarren, "Application of a polythiophene derivative as anticorrosive additive for paints", *Prog. Org. Coat.*, 2005, **53**, 217-224.

[17] F. Liesa, C. Ocampo, C. Alemán, E. Armelin, R. Oliver and F. Estrany, "Application of electrochemically produced and oxidized poly(3,4-ethylenedioxythiophene) as anticorrosive additive for paints: Influence of the doping level", *J. Appl. Polym. Sci.*, 2006, **102**, 1592-1599.

[18] E. Armelin, R. Pla, F. Liesa, X. Ramis, J.I. Iribarren and C. Alemán, "Corrosion protection with polyaniline and polypyrrole as anticorrosive additives for epoxy paint", *Corros. Sci.*, 2008, **50**, 721-728.

[19] J. Iribarren, C. Ocampo, E. Armelin, F. Liesa and C. Alemán, "Poly(3-alkylthiophene)s as anticorrosive additive for paints: Influence of the main chain stereoregularity", *J. Appl. Polym. Sci.*, 2008, **108**, 3291-3297.

[20] E. Armelin, C. Ocampo, F. Liesa, J.I. Iribarren, X. Ramis and C. Alemán, "Study of epoxy and alkyd coatings modified with emeraldine base form of polyaniline", *Prog. Org. Coat.*, 2007, **58**, 316-322.

[21] J.I. Iribarren, E. Armelin, F. Liesa, J. Casanovas and C. Alemán, "On the use of conducting polymers to improve the resistance against corrosion of paints based on polyurethane resins", *Mater. Corros.*, 2006, **57**, 683-688.

[22] E. Armelin, R. Oliver, F. Liesa, J.I. Iribarren, F. Estrany and C. Alemán, "Marine paint fomulations: Conducting polymers as anticorrosive additives", *Prog. Org. Coat.*, 2007, **59**, 46-52.

[23] J.I. Iribarren, F. Liesa, F. Cadena and L. Bilurbina, "Urban and marine corrosion", *Mater. Corr.*, 2004, **55**, 689-394.

[24] E. Armelin, A. Menneguzzi, C. A. Ferreira and C. Alemán, "Polyaniline, polypyrrole and poly(3,4-ethylenedioxythiophene) as additives of organic coatings to prevent corrosion", *Surf. Coat. Technol.*, 2009, **203**, 3763-3769.

[25] E. Armelin, C. Alemán and J. I. Iribarren, "Anticorrosion performances of epoxy coatings modified with polyaniline: A comparison between the emeraldine base and salt forms", *Prog. Org. Coat.*, 2009, **65**, 88-93.

[26] T. Schauer, A. Joos, L. Dulog and C.D. Eisenbach, “Protection of iron against corrosion with polyaniline primers”, *Prog. Org. Coat.*, 1998, **33**, 20-27.

[27] W.-K. Lu, R.L. Elsenbaumer and B. Wessling, “Corrosion protection of mild steel by coatings containing polyaniline”, *Synth. Met.*, 1995, **71**, 2163-2166.

[28] B. Wessling, “Scientific and Commercial Breakthrough for Organic Metals”, *Synth. Met.*, 1997, **85**, 1313-1318.

[29] T.D. Nguyen, T.A. Nguyen, M.C. Pham, B. Piro, B. Normand and H. Takenouti, “Mechanism for protection of iron corrosion by an intrinsically electronic conducting polymer”, *J. Electroanal. Chem.*, 2004, **572**, 225-234.

6

EVALUATION OF AN ENVIRONMENTALLY FRIENDLY ANTICORROSIVE PIGMENT FOR ALKYD PRIMER

The work described in this chapter was published in *Prog. Org. Coat.*, 2012, **73**, 321-329

An alkyd formulation containing zinc phosphate (10 wt.%) was prepared and subsequently modified replacing the latter anticorrosive additive by a very low concentration of conducting polymer. Specifically, three modified paints, which contain polyaniline emeraldine base (undoped form), polyaniline emeraldine salt (doped form) and an eco-friendly polythiophene derivative (partially oxidized), were formulated. The properties and corrosion resistance of the four alkyd coatings have been characterized. Among the three modified paints, the one containing polythiophene shows the best adherence and the highest corrosion resistance. This has been attributed to the fact that the miscibility of the polythiophene derivative with the alkyd formulation is better than that of polyaniline. Furthermore, accelerated corrosion assays and electrochemical impedance spectroscopy measurements revealed that the corrosion resistance of the paint with polythiophene is several orders of magnitude higher than that with zinc phosphate. The polythiophene derivative has been found to induce the formation of a passivating and well-adhered layer between the coating and the surface, preventing the access of chloride anions and oxygen to the substrate.

6.1. Introduction

Alkyd-based coatings have been widely applied in the protection of metallic substrates against corrosion due to their low cost and high efficacy in moderate corrosive media (*e.g.* industrial environments).[1,2] Two of the main characteristics of these organic coatings are their good adhesion, which prevents coating delaminating, and their ease of application in painting, both being responsible of their frequent use as maintenance painting.

Classical anticorrosive alkyd primers usually contain inhibitors based on hexavalent chromium, lead compounds and zinc phosphate derivatives,[3-5] the latter being the most widespread at present time due to its ability for steel passivation in acidic media.[4-6] Although zinc phosphate derivatives provide good results, in some cases their anticorrosive performance is lower than that of chromates.[7] This has been attributed to the fact that the former additive promotes the coating permeability. Nowadays, particular attention has been paid to the use of zinc phosphate in organic coatings. Some authors[8,9] have pointed out that

phosphate-based pigments are not environmentally benign as was claimed in many reports. Accordingly, Lima-Neto *et. al.*[8] proposed that zinc phosphate should be classified as "not hazardous" for the human health but "very toxic" for the aquatic environment. However, some zinc derivatives have been found not only to contaminate the environment but also to cause health problems to humans.[10] In order to avoid such problems, the European Community has restricted the use of zinc through a regulation (Directive 76/464 EEC, codified as 2006/11/EEC),[11] giving place to intense research aimed to find out alternative pigments for the replacement of zinc phosphate. Currently, research on both zinc-free inorganic pigments (mainly based on magnesium, aluminium or calcium) and pigments based on organic molecules with low toxicity is receiving special attention. Within this context, organic CPs have been claimed to present better anticorrosive behaviour than zinc phosphate.[12-23]

Since the pioneering work of Mengoli *et al.*,[24] many CP-containing primers have been developed using PAni [9,12,16,20], which is consequence of the good stability, low cost, low toxicity and good electrochemical properties of this organic material.[25] Nevertheless, PAni shows a high tendency towards aggregation when it is in contact with the paint solvent. Overcoming of this limitation is not easy because of the poor solubility of PAni in common solvents. In order to develop high-performance paints using CPs as corrosion inhibitor, the achievement of good and homogeneous dispersions on the resin formulation is essential. This is a non-trivial task, even though some strategies to obtain such dispersions have been proposed. For example Ikkala and co-workers[26] successfully developed a method to disperse PAni-EB in different epoxy resin hardeners. The applicability of other CPs, like PTh and PPy derivates, as protective systems remains much less studied. Within this context, the first description of the anticorrosive behaviour offered by some polythiophene derivatives, which shows better dispersion than PAni, was reported by some of us.[27-31] PThs are promising candidates because their oxidizing strength (E *vs* SCE: from +0.8 V to +1.2 V) is higher than those of PAni (E *vs* SCE: from +0.4 V to +1.0 V) and PPys (E *vs* SCE: from -0.1 V to +0.3 V) [25]. Recently, we patented the use of a simple PTh ester (hereafter denoted PTE), which showed better protecting abilities than zinc phosphate compounds, for

application as anticorrosive pigment to low volatile organic compounds (VOC) solvent-based epoxy and alkyd formulations.[32]

In this study we examine the performance as anticorrosive pigments of three different CPs and zinc phosphate when they are used in a commercial alkyd primer recommended for the protection of steel surfaces in contact with industrial or urban atmospheres. Accordingly, our final aim is the identification of a satisfactory substitute for classical zinc-containing corrosion inhibitors. Specifically, very small weight percentages of PAni-EB, PAni-ES and PTE, which showed good dispersion in organic solvents like xylene or organochlorides, were employed. Moreover, such three CPs are considered "eco-friendly" additives due to both their very low concentration in the paint formulation and their non-toxic behaviour when in contact with cells, as was evidenced in previous studies.[33-35] In order to compare the properties (*e.g.* coating adherence, water uptake, permeability, and resistance) of conventional alkyd films with those of the primer modified with a CP or zinc phosphate, adhesion tests, accelerated corrosion studies and electrochemical impedance spectroscopy (EIS) assays were performed.

6.2. Methods

6.2.1. Materials

The alkyd resin was supplied by Cray Valley Spain. PAni-ES (catalog number: 650013; 2-3 wt.% in xylene) and PAni-EB (catalog number: 476706; solid) were purchased from Aldrich, whereas PTE was synthesized in our laboratory according to the experimental procedure described by Osada and co-workers.[36] All pigments and additives were purchased from different suppliers, like Panreac Química or Europigments. Corrosion experiments were performed using DIN CK15 (AISI/SAE 1015) steel panels (120 x 40 mm) as metallic substratum.

6.2.2. Preparation of alkyd paints

Alkyd paints were prepared on a Dispermat TU dispersion equipment at 15000 rpm for 20 minutes using a milling system APS 250 that reduced the size of the particles to less than 40 μm.

Four different formulations were prepared and compared: (i) alkyd primer containing zinc phosphate 10 wt.% (Alkyd-Zinc/10); (ii) alkyd primer containing 1.0 wt.% of PAni-ES in xylene (Alkyd-PAniES/1); (iii) alkyd primer containing 0.3 wt.% of PAni-EB (Alkyd-PAniEB/0.3); and (iv) alkyd primer containing 1.0 wt.% of PTE (Alkyd-PTE/1). Alkyd-Zinc/10 was prepared mixing phenolic alkyd resin (29 wt.%), a mixture of inert pigments and additives (39.3 %), including calcium carbonate as extender, a mixture of alcoholic solvents and aromatic hydrocarbons (31.7 %) and zinc phosphate (10 wt.%). The preparation of the alkyd paints (ii) to (iv) was similar to that of (i), 10 wt.% of zinc phosphate being replaced by the CPs with concentrations varying from 0.3 to 1.0 wt.%. The exact alkyd paint formulation is not revealed due to the patent confidentiality.[32]

Dispersion required 45 minutes at the above-referenced circumferential speed of the dispersion disc. Paint coatings were applied by immersion (one coat) of 120×40×2 mm^3 steel panels, which were previously degreased with acetone and polished with zirconium balls (*UNE-EN-ISO 8504: Preparation of steel substrates before application of paints and related products - Surface preparation methods*), in the paint formulations. The paints were dried on air for one week before corrosion tests. The dry film thickness (DFT) was 50-70±10 μm, measured with a machine model Uno-Check Fe from Neurtek S.A. company.

6.2.3. Characterization of alkyd paints

Structural characterization of the coating films was performed using a Jasco 4100 FTIR spectrometer with a resolution of 4 cm^{-1} in a wavenumber range of 4000-600 cm^{-1}. Samples were placed in an attenuated total reflection accessory with thermal control and a diamond

crystal (Golden Gate Heated Single Reflection Diamond ATR, Specac-Teknokroma). On the other hand, thermogravimetric analyses were carried out with a Perkin-Elmer TGA-6 thermobalance at a heating rate of 10 °C/min under nitrogen atmosphere and a temperature range from 30 to 800 °C. Finally, properties typically used to determine the mechanical characteristics of paints (*i.e.* Young´s modulus, tensile strength and elongation at break) were evaluated using stress-strain assays with a Zwick Z2.5/TN1S testing machine. Regular films were prepared by evaporation at room temperature of the volatile organic solvent of the paint formulation. Plate samples with a length of 30 mm, a width of 3 mm and a thickness of 100-250 μm were cut out from the films for stress-strain experiments. The deformation rate was 10 mm/min. All the mechanical parameters reported in this work were averaged over a total of ten measurements for each paint.

6.2.4. Accelerated corrosion tests

Corrosion studies were carried out using a home-made equipment developed and patented in our laboratory[37] that allows accelerated immersion assays in an aggressive solution medium. This medium was an aqueous solution of NaCl (3.5 wt.%, pH=6.6) or an aqueous solution of $NaHSO_3$ (3 wt.%, pH=3.5) stored in a glass container. The operating controlled program conditions for one cycle were: immersion of coated steel sheets (15 min), wring out (30 min), drying stage with bulbs (230 V-100 W, 10 min) and cooling time at room temperature (5 min). Painted panels were sealed at the edges and around the hole used for securing the pieces. Tests were performed for a total time of 480 h, which corresponds to 480 cycles. Samples were continually evaluated at regular time intervals according to *ASTM D714 (Standard Test Method for Evaluating Degree of Blistering of Paints)*, *ASTM D1654 (Standard Test Method for Evaluation of Painted or Coated Specimens)* and *UNE-EN-ISO 4624 (Paints and varnishes: Pull-off Test for Adhesion, ISO 4624:2002)*.

6.2.5. Scanning electron microscopy and energy dispersive X-ray spectroscopy

SEM and energy dispersive EDX spectroscopy studies were performed using a Focussed Ion Beam Zeiss Neon 40 scanning electron microscope, equipped with an EDX system.

6.2.6. Electrochemical impedance spectroscopy

EIS was performed as a function of time in aqueous 3.5 wt.% NaCl solution at open circuit potential (E_{OCP}). The dry film thickness (DFT) was 80 ± 3 μm. Although the four paints prepared in this work were preliminary studied by EIS, Alkyd-Zinc/10 and Alkyd-PTE/1 coatings were studied in more detail since the anticorrosive properties of the latter were significantly better than those of Alkyd-PAniES/1 and Alkyd-PAniEB/0.3. Three different samples, which were not scribed before assays, were considered in each case. The working electrode area was 4.9 cm^2. Stainless steel and silver|silver chloride (Ag|AgCl) electrodes were used as counter and reference electrodes, respectively. All potentials are referenced to Ag|AgCl. EIS measurements were performed in potentiostatic mode at the E_{OCP}. The amplitude of the EIS perturbation signal was 10 mV, the frequency ranged from 10^5 to 10^{-2} Hz taking 70 frequencies per decade with a potentiostat Autolab PGSTAT 302N.

6.3. Results and Discussion

6.3.1. Paint formulation and characterization

When the white alkyd paint (Alkyd-Zinc/10) is modified with CPs its color changes and the final aspect depends on the CP used. More specifically, the coating becomes blue upon the addition of PAni-EB, whereas PAni-ES and PTE promotes green and yellow colors, respectively. It is well know that CPs act as pigments and their colors depend on their redox

properties. In all cases, the anticorrosive CPs pigments provided very homogeneous dispersions when added to the paint, which is extremely important for the barrier property.[25]

PAni-EB has been extensively employed as anticorrosive additive due to its very high stability and good redox properties, which are able to passivate the metal surface through an anodic protection mechanism. However, this CP is extremely insoluble, forming agglomerates when it is in contact with solvents. The key for the good miscibility with our paint formulation was achieved by reducing the PAni powder size, which was subsequently mixed with chloroform to form a very fine colloidal dispersions, as suggested by B. Wessling in reference [25]. Another important requirement for the use of PAni-EB in paint formulations is the addition of a very low concentration. We found that 0.3 wt.% is better than 1.0 or 1.5 wt.%. Thus, concentrations higher than 0.3 wt.% provoke the formation of polymer agglomerates in the film surface giving worse adherence and high permeability to the coating (this observation is detailed in section 6.3.2). In contrast, PAni-ES has excellent miscibility with solvent-based alkyd paints due to its good dispersion properties in xylene solutions. We did not observe the formation of agglomerates in the coating surface when PAni-ES 1.0 wt.% was employed. However, the best miscibility was obtained when we applied the partially oxidized PTE as additive. The PTh derivative synthesized in our laboratory showed a very high compatibility with the alkyd paint formulation, giving very smooth coating surfaces for concentrations ranging between 0.3 to 1.5 wt.%. This high compatibility should be attributed to the fact that PTE is soluble in the paint solvents (*i.e.* alcoholic solvents and aromatic hydrocarbons).

Due to the very low concentration of the CPs in the alkyd formulations (0.3-1.0 wt.%), the vibration bands associated to their molecular groups are not observed in the FTIR spectra of the paints, as reported in our previous works.[17-23] Figure 6.1 shows the main absorption bands for the phenolic alkyd coating with zinc phosphate as anticorrosive additive. The FTIR spectrum shows a broad band in the 3500–3200 cm^{-1} corresponding to OH stretching, the broadness of the signal being consequence of a distribution of OH groups associated by hydrogen bonds. Other characteristic bands are observed for C-H aliphatic (2850 and 2920 cm^{-1}) and aromatic (3025 cm^{-1}) stretching, and for the bending

mode of C-H groups in *ortho*-substituted benzene. Moreover, identification of some bands arising from rheological additives, as carbonates at 1400 cm^{-1} (strong band due to the CO_3^{2-} bonds), silicates at ~1000 cm^{-1} (SiO_4^{2-}) and zinc phosphate (PO_4^{2-}), is also possible. Unfortunately, the signals of titanium dioxide, used as white pigment, are out of range of the apparatus scale.[17]

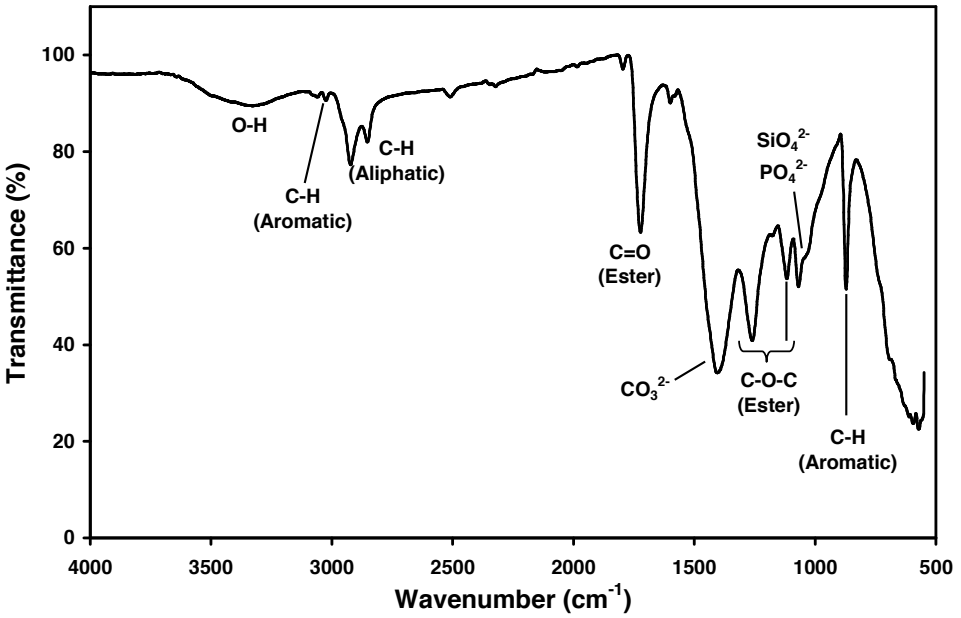

Figure 6.1. FTIR spectrum of the phenolic alkyd resin (Alkyd-Zinc/10).

The thermogravimetric analysis (Figure 6.2) shows that the decomposition process of the film starts at 300 °C ($T_{d,0}$). Three consecutive decomposition decays are observed at 390, 492 and 754 °C. The first decomposition, which corresponds to a 15% weight loss, is due to the polymer base. The second decomposition, with a very low mass loss (~2 %), has been attributed to cross-linked polymeric fractions in the alkyd film. The thermal transition detected between 650 to 754 °C is related with the chemical reaction of calcium carbonate, generating calcium oxide and carbon dioxide. Finally, a remained weight of 52 %, which corresponds to the weight percentage of inorganic pigments in the char-yield, is obtained at 800 °C. Thermogravimetric curves of the alkyd films with CPs are not displayed because,

as evidenced in our previous work,[18-23] the thermal stability of the films is not affected by the addition of 0.3-1.0 wt.% concentration of these organic compounds.

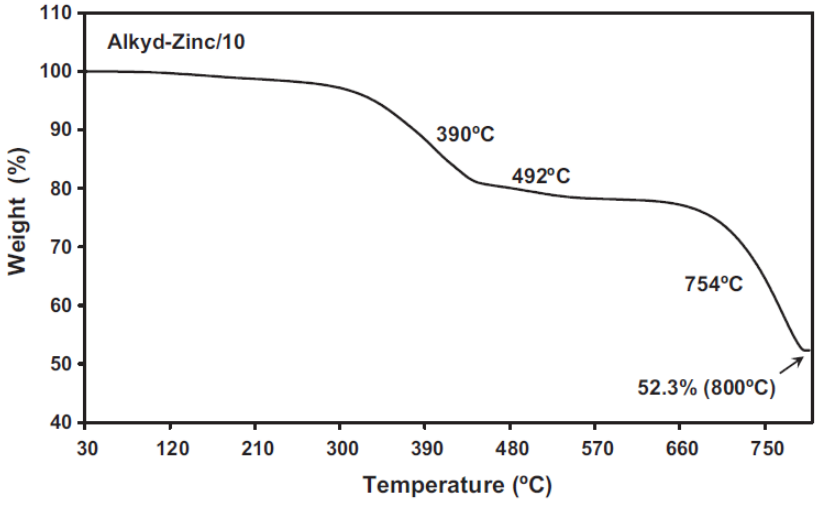

Figure 6.2. Thermogravimetric curve of the alkyd resin (Alkyd-Zinc/10) with scan rate of 10 °C/min.

The alkyd resin showed very low elongation at break (ε_b=6.5 %), elastic modulus (*E*=365 MPa) and tensile strength (σ_{max}=12 MPa). The films are very brittle and the energy required to deform the sample to the point of failure is small with respect to other coatings.[19] Such brittle behavior is due to the characteristics of this particular formulation: low concentration of the phenolic resin (29 wt.%) combined with the high concentration of inorganic additives and pigments (39.3 wt.%). Thus, alkyd paints with higher resin content (~50 wt.%) typically show better mechanical properties than this coating. However, it should be mentioned that the alkyd formulation used in this work is recommended for industrial environments, which require paints with higher Young's modulus and impact resistance. Moreover, this formulation is intended for priming uses only, an intermediate paint and/or a top coat being needed before final application. On the other hand, the influence of the low concentration of CP in the mechanical properties of the paint (data not shown) was found to be practically negligible, which is in excellent agreement with findings reported in our previous studies.[18-23]

6.3.2. Accelerated corrosion assays

As mentioned above, the main aim of this work is the identification of an efficient substitute for zinc phosphate additives typically employed as anticorrosive additive in alkyd paint formulations. Accordingly, accelerated corrosion tests using two aggressive media, NaCl 3.5 wt.% and $NaHSO_3$ 3.0 wt.%, were performed. Table 6.1 summarizes the main results obtained after 480 h of exposure, while Figure 6.3 displays the temporal evolution of the corrosion area failed in the alkyd panels according to the ASTM Standard Method D-1654. This procedure is based on the use of scrapped panels to evaluate the corrosion resistance through the progress of the rust, which is determined by the loss of adherence near to the scribe mark and the area corroded under the film.

As it can be seen, the corrosion protection imparted by the coating was excellent when PAni-ES and PTE were incorporated to the paint formulation with a concentration of 1.0 wt.% (Figure 6.3a). However, PAni-EB showed the worst result in NaCl. This poor protection has been attributed to both the low adherence of PAni-EB and the limited miscibility of this material with solvent-based paints, both provoking high permeability in the Alkyd-PAniEB/0.3 coating. In contrast, the corrosion inhibition of the alkyd primer improves substantially when PTE was used as anticorrosive additive, the protection against corrosion provided by this CP being excellent until 480 h of exposure in the saline solution. This high protection performance is due to the excellent miscibility of such PTh derivative with organic solvents like xylene, chloroform, and others. Similar conclusions can be reached from PAni-ES results. This CP, which has been used as a well dispersed powder in xylene solution, shows good miscibility with the alkyd formulation. Therefore, the adherence to the metal substrate is significantly better for the Alkyd-PAniES/1 paint than for the Alkyd-PAniEB/0.3, which contributes to the excellent corrosion resistance of the former coating. Similar trends were observed in $NaHSO_3$ aqueous solutions, as is evidenced in Figure 6.3b and Table 6.1. However, after 480 h, immersion tests showed that the percentage of corrosion area failed is lower than obtained in NaCl solution since the chloride anions of the latter medium are more aggressive. This must be attributed to the higher mobility and penetration power of chloride ions, which in addition show an exceptional high

surface activity that affect the surface tension on the metal. The coating failed area in $NaHSO_3$ for the Alkyd-PTE/1 is almost zero during the first ten days of exposure, and only 3 % after 480 h of exposure. The corrosion area failed in NaCl solution increases to only 7-8 % between ten and twenty days. In contrast, the corrosion area failed in $NaHSO_3$ and NaCl for the Alkyd-Zinc/10 is 22 % and 42 %, respectively. Moreover, after 20 days the paint is not well adhered and the amount of rust under the coatings is important. These results clearly indicate that the PTE eco-friendly additive, which shows better miscibility properties than PAni, is an excellent alternative to zinc phosphates.

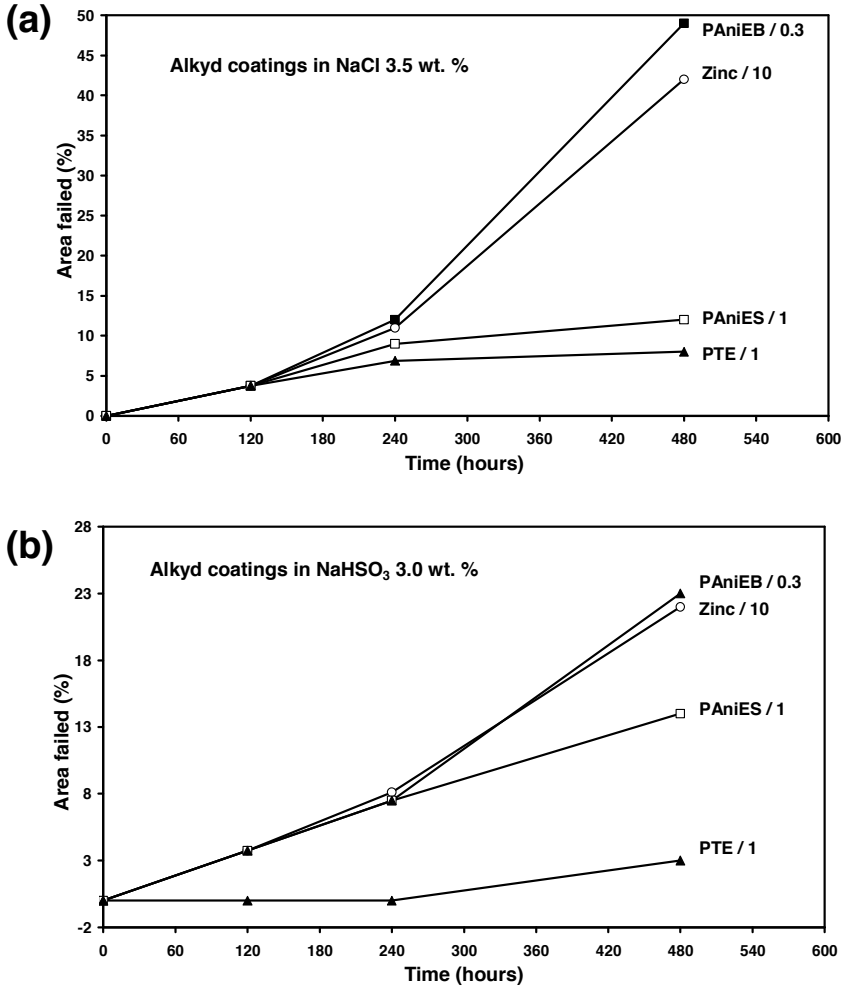

Figure 6.3. Progression of corrosion area failed v.s. time in the alkyd panels immersed in (a) NaCl 3.5 wt.% and (b) $NaHSO_3$ 3.0 wt.% solutions.

Sample		Alkyd-Zinc/10		Alkyd-PTE/1		Alkyd-PAniES/0.3		Alkyd-PAniES/1	
Corrosive Medium		NaCl	$NaHSO_3$	NaCl	$NaHSO_3$	NaCl	$NaHSO_3$	NaCl	$NaHSO_3$
Adherence	D1654 [a]	5-6	6	8-9	10	4-5	5	7-8	6-7
	ISO 4624 [b]	32 % B 68 % B/C		25 % B 75 % B/C		NA		NA	
Corrosion [c]	Scratch (mm)	3	2.5	0.5	0	5	4	1	2
	Area failed (%)	42	22	8	0	49	23	12	14
Blistering [d]	Scratch	4 MD	2MD	8 F	10	2D	6 M	10	10
	Surface	4 MD	10	10	10	2 D	10	10	10

[a] ASTM D1654: Procedure A, rating number from 0 to 10, where 10 indicates no creepage from scribe and 0 indicates more than 16 millimeters of creepage from scribe. [b] UNE-EN-ISO 4624: B indicates cohesive break of the first layer of the coating, B/C indicates adhesive break between the epoxy adhesive employed to join the dolly and the coating. NA: data not available. The percentages refer to the failed area. [c] ASTM D1654: Procedure A, representative mean creepage from scribe in mm; Procedure B, area failed referred to the corrosion on areas removed from scribe in percentage. [d] ASTM D714: numbers are associated to the size of blistering where 6, 4 and 2 represents a progressive increase of blistering size and 10 represents no blistering; whereas letters are referred to the blistering density or frequency of blistering in the coating surface: D, dense; MD, medium dense; M, medium; F, few.

Table 6.1. Rating failure at scribed and unscribed area, adherence properties and blistering degree of the alkyd coatings after 480 h of immersion in NaCl (3.5 wt.%) and $NaHSO_3$ (3.0 wt.%) corrosion solutions.

Digital photographs of the panels after 120, 240 and 480 corrosion cycles, which corroborate the previous discussion, are displayed in Figure 6.4. Moreover, comparison of the Alkyd-Zinc/10 and Alkyd-PTE/1 adherence properties using the UNE-EN-ISO 4624 standard shows similar stress to break, 0.351 MPa and 0.409 MPa, respectively, which correspond to the B/C type (Table 6.1). This result also is fully consistent with our observations that PTE promotes the adhesion between the coating and the metal substrate.

The overall of the results presented in this section allows us to conclude that CPs miscible with the paint formulation promote the adherence and reduce the permeability of the alkyd modified primer. After pull-off adhesion tests we also observed that PTE induces the formation of very thin white spots dispersed on the surface of the metal, which appears after 72 h of immersion in NaCl solution. Analysis of these spots by EDX (not shown) revealed the presence of sulfur, carbon, oxygen and calcium. This suggests the favorable interaction between PTE and calcium carbonate ($CaCO_3$) molecules from the paint formulation, which may induce the formation of complexes in a well adhered passivating layer. This phenomenon was not detected in the Alkyd-Zinc/10, Alkyd-PAniEB/0.3 and Alkyd-PAniES/1 coatings. Figure 6.5 shows both the optical micrograph of the metal surface with the white spots and the SEM micrographs evidencing the homogeneous distribution of globular $CaCO_3$ particles in the metal surface. Therefore, we assumed that calcium carbonate was, in part, responsible of the adhesion promoted by PTE. Thus, the interaction between PTE and $CaCO_3$ molecules may induce the formation of a passivating and well-adhered layer between the coating and the metal surface, preventing the access of the chloride anions and oxygen to the substrate. Additional experiments were performed to check this hypothesis. Specifically, EIS measurements showed the coating resistance of Alkyd-PTE/1 is higher than that of Alkyd-Zinc/10 after 72 h of exposure in NaCl solution (see next subsection), confirming the validity of the previous assumption.

Regarding to the blistering evaluation, Table 6.1 indicates that Alkyd-PTE/1 and Alkyd-PAniES/1 compositions present the higher resistance to blistering formation. This behavior is fully consistent with the good adhesion and barrier properties found for both formulations.

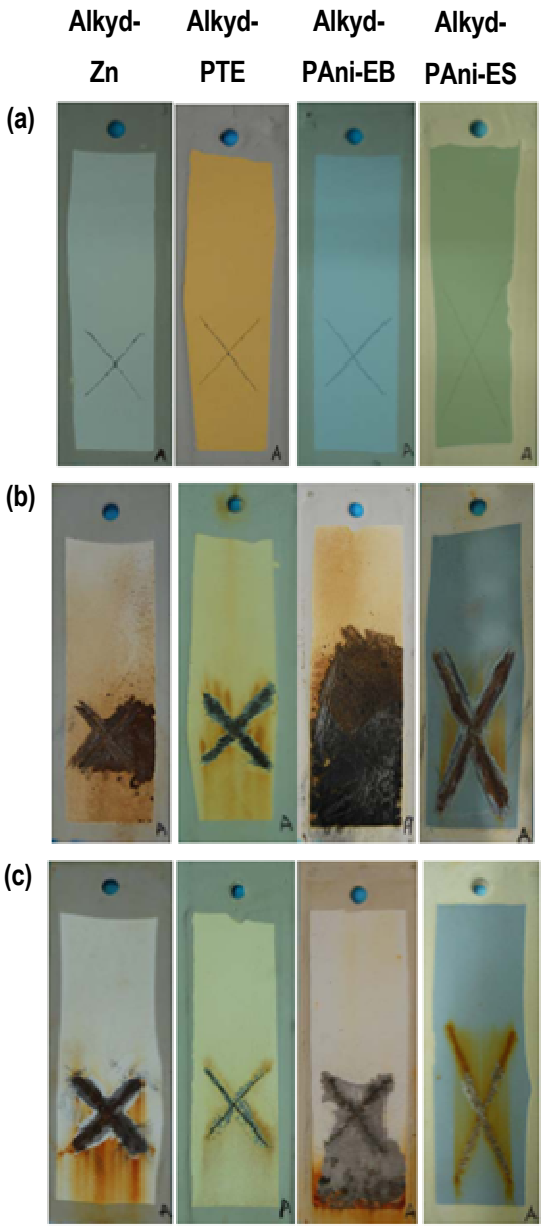

Figure 6.4. Scrapped test panels of the alkyd panels after (a) 120, (b) 240 and (c) 480 corrosion cycles in $NaHSO_3$ aqueous solution.

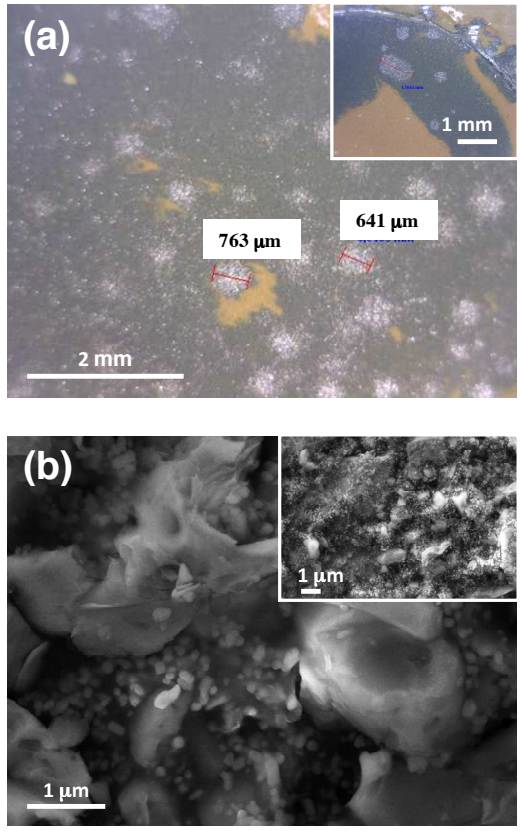

Figure 6.5. (a) Optical and (b) SEM micrographs of Alkyd-PTE/1 after pull-off test and 20 days of exposure in NaCl solution. Scale bars are indicated.

6.3.3. EIS measurements

The effect of the metal surface treatments was evaluated by EIS considering samples with various immersion times. Preliminary EIS results indicated that the protection imparted by Alkyd-PAniES/1 and Alkyd-PAniEB/0.3 was clearly smaller than that offered by Alkyd-PTE/1. Therefore, this section has been focused on the comparison between Alkyd-Zinc/10 and Alkyd-PTE/1. Figure 6.6 shows the Nyquist plots of the steel coated with the Alkyd-Zinc/10 and Alkyd-PTE/1 coatings after 1, 3 and 72 h of immersion in 3.5 % NaCl solution. These diagrams are characterized by one time constant, high values for the overall impedance (>10^9 $\Omega \cdot cm^2$) being observed for immersion times up to 3 h. When the

immersion time increases to 72 h, samples with the Alkyd-Zinc/10 coating display a deep decrease of the overall impedance. This should be attributed to the beginning of the paint degradation process, which facilitates the electrolyte penetration. In contrast, the impedance modulus at the low frequency limit remains high for the Alkyd-PTE/1 samples, due to the good barrier properties of this coating.

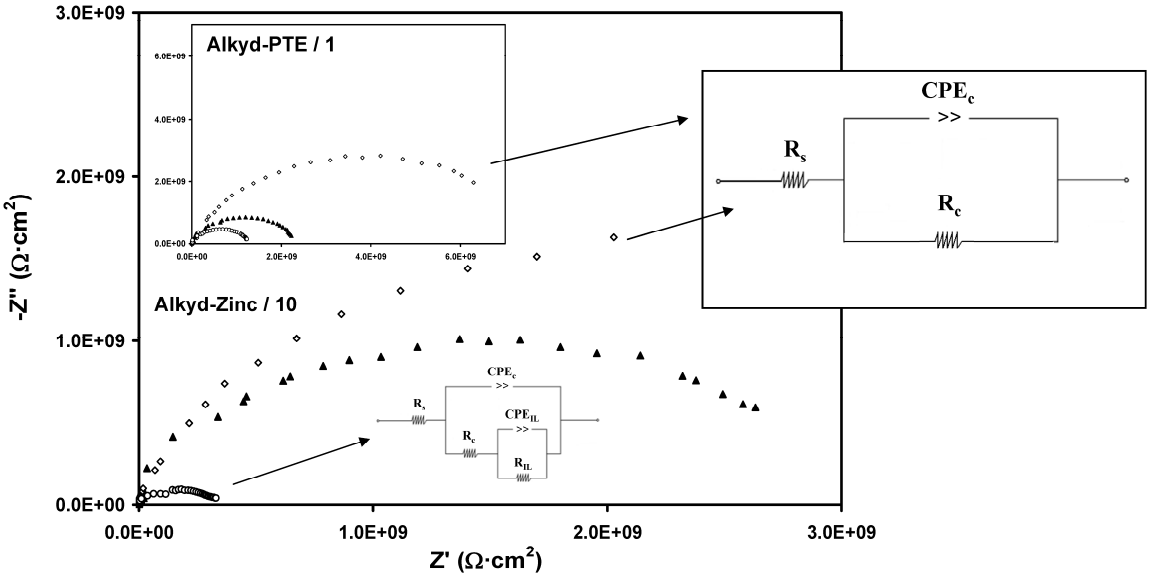

Figure 6.6. Nyquist diagrams of Alkyd-Zinc/10 and Alkyd-PTE/1after 1 h (empty diamonds), 3 h (filled triangles) and 72 h (empty circles) of immersion in NaCl solution. The insets represent the equivalent circuits used for modelling the experimental data.

EIS spectra depicted in Figure 6.6 were fitted using an equivalent circuit (EC) composed by one time constant $R_s(R_pC_s)$, where R_s represents the ohmic resistance between the working and the reference electrodes, R_p is the polarisation resistance and C_s corresponds to the system capacitance. The capacitance was replaced by a constant phase element (CPE) which describes the non-ideal capacitor when the phase angle is not -90°.

The CPE impedance is generally attributed to the surface reactivity, surface heterogeneity, and roughness regarding to current and potential distribution, which in turn are related with the electrode geometry and electrode porosity.[38] The CPE impedance has been expressed as:

$$Z_{CPE} = [Q(j\omega)^n]^{-1} \quad (6.1)$$

The CPE represents a capacitor and a resistor for n=1 and n=0, respectively, while it is associated with a diffusion process when n=0.5. Table 6.2 shows the R_s, R_p and CPE values derived from the fitting of the EIS plots displayed in Figure 6.6 to the EC. The aim of the choice of the EC was to obtain a satisfactory fitting of the experimental data, where the circuit elements can be associated with the physical phenomena that are probably taking place at the electrode surface. The quality of fitting was evaluated using the error percentage associated to each circuit component, errors smaller than 5 % being obtained in all cases.

As the time elapsed, the EIS plots change. Figure 6.7 shows the Nyquist plots after 7 days of immersion in 3.5 % NaCl solution. The diagram of the Alkyd-Zinc/10 shows two time constants. The one at high frequency was attributed to the coating layer properties, while that at low frequencies was related to interfacial phenomena. The latter is affected by the presence of pores and defects on the film layer, which allows the solution to reach the metal surface. The proposed EC is given by $R_s(R_c \cdot CPE_c) \cdot (CPE_{IL} \cdot R_{IL})$, where the CPE_c and R_c represent the capacitance and resistance of the coating, respectively, and CPE_{IL} and R_{IL} correspond to the capacitance and resistance of the metal/coating interface. The Alkyd-PTE/1 diagram presents one time constant with a polarisation resistance of around 520 $M\Omega \cdot cm^2$ and a capacitance of $6.37 \cdot 10^{-11}$ $F \cdot cm^2$ with n=0.91 (*i.e.* capacitor behavior), evidencing an improvement of the protective properties with respect the Alkyd-Zn/10 coating. Thus, the electrolyte penetration and the first signs of corrosion activity of the latter paint indicate that the barrier properties are considerably worse in absence of PTE. The Alkyd-Zn/10 time constant at lower frequencies presents R_{IL}=66 $M\Omega \cdot cm^2$ and CPE_{IL}=$2.98 \cdot 10^{-10}$ $F \cdot cm^{-2}$.

Immersion time	1 hour		3 hours		72 hours	
Sample	Alkyd-Zinc	Alkyd-PTE	Alkyd-Zinc	Alkyd-PTE	Alkyd-Zinc	Alkyd-PTE
R_s ($\Omega \cdot cm^2$)	150.6	156.4	155.7	163.3	161.9	164.2
R_c ($\Omega \cdot cm^2$)	3.20 G	6.34 G	2.47 G	2.13 G	271 M	1.16 G
CPE_c ($F \cdot cm^{-2} \cdot s^{n-1}$)	$3.61 \cdot 10^{-11}$	$2.54 \cdot 10^{-11}$	$2.29 \cdot 10^{-11}$	$2.63 \cdot 10^{-11}$	$3.11 \cdot 10^{-11}$	$4.01 \cdot 10^{-11}$
n	0.90	0.90	0.88	0.89	0.87	0.89

Immersion time	7 days		30 days	
Sample	Alkyd-Zinc	Alkyd-PTE	Alkyd-Zinc	Alkyd-PTE
R_s ($\Omega \cdot cm^2$)	161.6	166.4	177.9	175.2
R_p ($\Omega \cdot cm^2$)	15.3 M	514 M	3.67 k	238 k
CPE_c($F \cdot cm^{-2} \cdot s^{n-1}$)	$7.39 \cdot 10^{-11}$	$6.37 \cdot 10^{-11}$	$3.11 \cdot 10^{-7}$	$6.38 \cdot 10^{-10}$
n	0.90	0.91	0.57	0.88
R_{IL} ($\Omega \cdot cm^2$)	66 M		4.56 k	344 k
CPE_{IL} ($F \cdot cm^{-2} \cdot s^{n-1}$)	$2.98 \cdot 10^{-10}$		$1.47 \cdot 10^{-6}$	$2.06 \cdot 10^{-6}$
n	0.76		0.79	0.49
R_{ct} ($\Omega \cdot cm^2$)			8.2 k	
CPE_{dl} ($F \cdot cm^{-2} \cdot s^{n-1}$)			$1.87 \cdot 10^{-4}$	
n			0.61	

Table 6.2. Data of EIS results obtained from the equivalent circuit for Alkyd-Zinc/10 and Alkyd-PTE/1 coatings after exposure to NaCl 3.5 wt.% aqueous solution.

The Nyquist plots obtained after 30 days of immersion are provided in Figure 6.8. The coating degradation, which is due to the accumulation of chloride ions at the substrate/paint interface, leads to corrosion development in the Alkyd-Zn/10 sample. This process is characterized by the presence of a new time constant (R_{ct})/(CPE_{dl}) at lower frequencies, which accounts for the charge transfer and the double layer capacitance in the metal surface. The EIS response of the Alkyd-PTE/1 sample corresponds to a two time constant behavior indicating an improved corrosion performance when compared to that of the Alkyd-Zn/1 sample. As it can be seen, both the shape of the depressed capacitive loops and the values from the analysis of the simulated parameter (Table 6.2) indicate that the corrosion process is dominated by the mass transport of oxides from rust. However, the EIS plot of the Alkyd-PTE/1 sample shows only two time constants, which evidences a delay in the electrolyte penetration. Thus, PTE plays a crucial role sealing the pores and/or defects

of the coating. In summary, although the coating resistance of the alkyd primer used in this work is excellent (corrosion resistance 5-8 GΩ·cm^2 for the Alkyd-Zinc/10 before immersion in chloride solution), its corrosion resistance improves considerably upon the addition of PTE 1.0 wt.% (corrosion resistance 10-12 GΩ·cm^2 for the Alkyd-PTE/1). This CP enhances the adhesion and barrier properties of the primer increasing the resistance against corrosion by around thirty times.

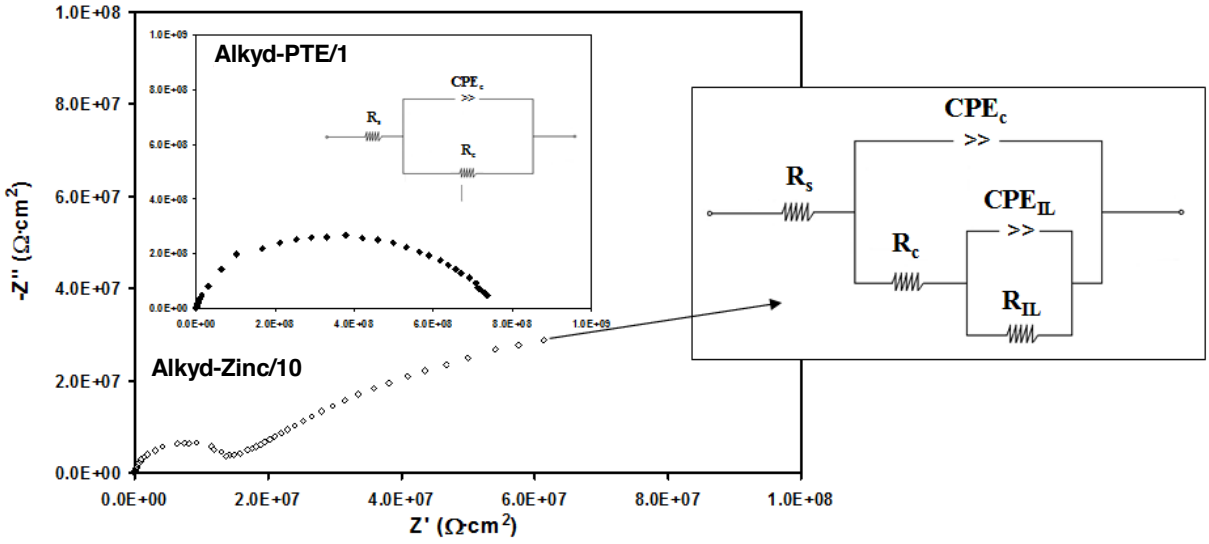

Figure 6.7. Nyquist diagrams of Alkyd-Zinc/10 and Alkyd-PTE/1 after 7 days of immersion in NaCl solution. The insets represent the equivalent circuit used for modelling the experimental data.

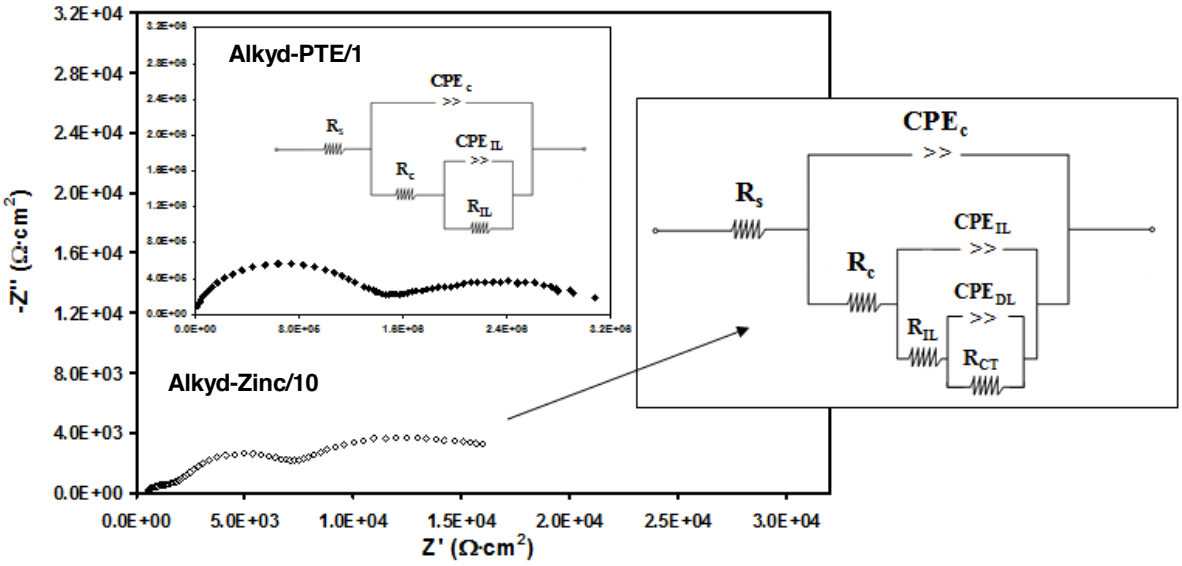

Figure 6.8. Nyquist diagrams of Alkyd-Zinc/10 and Alkyd-PTE/1 after 30 days of immersion in NaCl solution. The insets represent the equivalent circuit used for modelling the experimental data.

Defect areas formed in the Alkyd-Zinc/10 coating were also evidenced by the evolution of the coating resistance (Log R_p) against the immersion time, which is represented in Figure 6.9a. This parameter, which is very useful to understand the corrosion protection imparted by the coating, is inversely proportional to the corrosion rate and to the surface area under corrosion. According to our results, the reduction of Log R_p is lower for the alkyd primer modified with 1.0 wt.% of PTE than for Alkyd-Zinc/10, indicating that the corrosion rate and defect areas until 30 days are lower for the former coating. Thus, the resistance of the Alkyd-PTE/1 primer ($R_p \sim 10^6$ MΩ·cm^2) is several orders of magnitude higher than that of Alkyd-Zinc/10 one ($R_p \sim 10^3$Ω·cm^2).

Figure 6.9b represents the water uptake against the immersion time for the two investigated coatings. The water uptake reaches an approximately constant value in only 3 h of immersion. However, the evolution of rust or pitting formation under the Alkyd-Zinc/10 coating caused the loss of adhesion of the coating and a quickly increase of water uptake in only 30 days of immersion. In contrast, water uptake remained constant for the Alkyd-PTE/1

formulation. On the other hand, the open circuit potential (E_{OCP}) was more positive for the Alkyd-Zinc/10 paint (*i.e.* the E_{OCP} increased from 35 to 50 mV after the first 360 h) than for the Alkyd-PTE/1 one (*i.e.* E_{OCP} changed from 0 to -49 mV after the first 360 h), indicating a more anodic behavior of the former. It should be noted that oxidation at the working electrode is faster for more anodic potentials. Conversely, a negative potential accelerates reduction at the working electrode, as observed for the Alkyd-PTE/1 primer. After 15 days the E_{OCP} of the two paints fastly dropped to negative values, indicating the lost of the anticorrosive protection. Thus, the E_{OCP} of the Alkyd-Zinc/10 and Alkyd-PTE/1 paints was -557 and -447 mV, respectively, after 30 days of immersion in the NaCl solution.

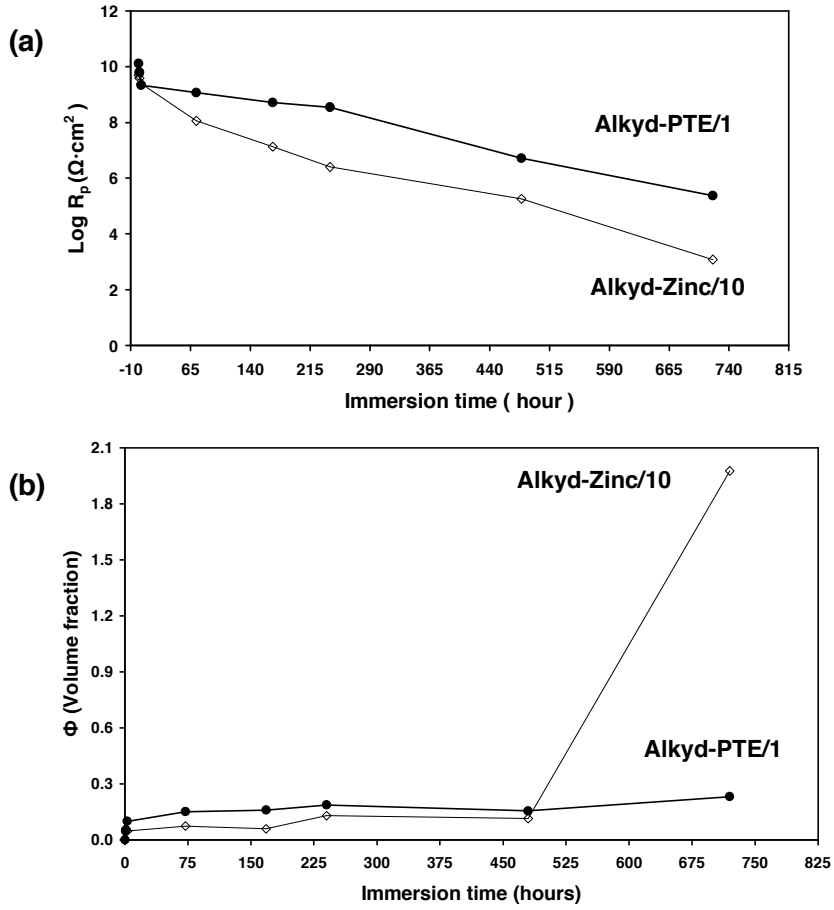

Figure 6.9. Temporal evolution of (a) the logarithm of the coating resistance (R_p) and (b) the water uptake (Φ) for Alkyd-Zinc/10 and Alkyd-PTE/1 primers immersed in NaCl solution.

6.4. Conclusions

Four different formulations of an alkyd primer, which only differ in the corrosion inhibitor have been prepared and compared. Specifically, the four corrosion inhibitors used in this work were: zinc phosphate (10 wt.%), PAni-EB (0.3 wt.%), PAni-ES (1.0 wt.%) or PTE (1.0 wt.%). Among the three CP-containing formulations, the Alkyd-PET/1 was found to impart the highest protection against corrosion. This has been attributed to the fact that the PTE eco-friendly additive shows better miscibility properties with the alkyd formation than PAni-ES and PAni-EB.

Results allow us to conclude that both the high adherence and low permeability of the Alkyd-PTE/1 primer, as compared to the Alkyd-Zinc/10 one, are promoted by the very low concentration of CP added to the paint formulation. Accelerated corrosion assays showed that PTE induces the formation of very thin white spots dispersed on the surface of the metal after 72 h of immersion test. Analyses of these spots proved that they are well adhered calcium carbonate particles released from the paint formulation modified with PTE. This phenomenon has not been observed in the alkyd formulations containing zinc, PAni-EB and PAni-ES.

The Alkyd-Zinc/10 coating allows the electrolytes to reach the working electrode surface in only 7 days of immersion in NaCl 3.5 %. This was demonstrated by EIS measurements, which showed a decrease of the overall impedance. In contrast, the Alkyd-PTE/1 primer evidenced a higher corrosion resistance, retaining the barrier properties until 20 days of immersion in the aggressive solution.

In summary, this study presents an alkyd formulation modified with a very low concentration of PTE, which acts as a powerful corrosion inhibitor. This paint is able to retain the adherence and barrier properties for at least 20 days of immersion in an aggressive NaCl 3.5 % solution, which represents an improvement in the corrosion protection of at least 13 days with respect to the same alkyd primer formulated using zinc phosphate as anticorrosive additive.

6.5. References

[1] F. Fragata, R.P. Salai, C. Amorimc and E. Almeida, “Compatibility and incompatibility in anticorrosive painting: The particular case of maintenance painting”, *Prog. Org. Coat.*, 2006, **56**, 257-268.

[2] Y. González-García, S. González and R.M. Souto, “Electrochemical and structural properties of a polyurethane coating on steel substrates for corrosion protection”, *Corr. Sci.*, 2007, **49**, 3514-3526.

[3] M. Hernandez, J. Genescá, J. Uruchurtu, F. Galliano and D. Landolt, “Effect of an inhibitive pigment zinc-aluminum-phosphate (ZAP) on the corrosion mechanisms of steel in waterborne coatings”, *Prog. Org. Coat.*, 2006, **56**, 199-206.

[4] R. Romagnoli and V. Vetere, “Non-pollutant corrosion inhibitive pigments: Zinc phosphate, a review”, *Corros. Rev.*, 1995, **13**, 45-64.

[5] M. Bethencourt, F.J. Botana, M. Marcos, R.M. Osuna and J.M. Sánchex-Amaya, “Inhibitor properties of “green” pigments for paints”, *Prog. Org. Coat.*, 2003, **46**, 280-287.

[6] P. Sorensen, S. Kiil, K. Dam-Johansen and C. Weinell, “Anticorrosive coatings: A review”, *J. Coat. Tech. Res.*, 2009, **6**, 135-176.

[7] J. A. Burkill and J. E. O. Mayne, “The limitations of zinc phosphate as an inhibitive pigment”, *J. Oil & Colour Chem. Assoc.*, 1988, **9**, 273-285.

[8] P. Lima-Neto, A. P. Araújo, W. S. Araújo and A. N. Correia, “Study of the anticorrosive behavior of epoxy binders containing non-toxic inorganic corrosion inhibitor pigments”, *Prog. Org. Coat.*, 2008, **62**, 344-350.

[9] A. Sakhri, F.X. Perrin, E. Aragon, S. Lamouric and A. Benaboura, “Chlorinated rubber paints for corrosion prevention of mild steel: A comparison between zinc phosphate and polyaniline pigments”, *Corr. Sci.*, 2010, **52**, 901-909.

[10] C. D. Klassen in “Casarett and Doull’s, toxicology: The basic science of Poisons”, fifth edition, (1996), 702–709.

[11] EU Regulations, Directive 2006/11/EC of the European Parliament and of the Council of 15 February 2006 on pollution caused by certain dangerous substances

discharged into the aquatic environment of the Community. Official Journal of the European Union, DO L64/52-59, 4.3.2006.

[12] B. Wessling and J. Posdorfer, "Nanostructures of the dispersed organic metal polyaniline responsible for macroscopic effects in corrosion protection", *Synth. Met.*, 1999, **102**, 1400-1401.

[13] G. Spinks, A. Dominis, G .G. Wallace and D.E. Tallman, "Electroactive conducting polymers for corrosion control: part 2. Ferrous metals", *J. Solid State Electrochem.*, 2002, **6**, 85-100.

[14] D.E. Dennis, G. Spinks, A. Dominis and G. G. Wallace, "Electroactive conducting polymers for corrosion control: Part 1. General introduction and a review of non-ferrous metals", *J. Solid State Electrochem.*, 2002, **6**, 73-84.

[15] P. Zarras, J.D. Stenger-Smith and Y. Wei (Eds.) Electroactive polymers for corrosion control, ACS Symposium Series, vol. 843, ACS, Washington DC., 2003.

[16] R.S. Patil and S. Radhakrishnan, "Conducting polymer based hybrid nanocomposites for enhanced corrosion protective coatings", *Prog. Org. Coat.*, 2006, **57**, 332-336.

[17] J.I. Iribarren, F. Cadena and F. Liesa, "Corrosion protection of carbon steel with thermoplastic coatings and alkyd resins containing polyaniline as conductive polymer", *Prog. Org. Coat.*, 2005, **52**, 151-160.

[18] J.I. Iribarren, E. Armelin, F. Liesa, J. Casanovas and C. Alemán, "On the use of conducting polymers to improve the resistance against corrosion of paints based on polyurethane resins", *Mater. Corros.*, 2006, **57**, 683-688.

[19] E. Armelin, C. Ocampo, F. Liesa, J.I. Iribarren, X. Ramis and C. Alemán, "Study of epoxy and alkyd coatings modified with emeraldine base form of polyaniline", *Prog. Org. Coat.*, 2007, **58**, 316-322.

[20] E. Armelin, R. Pla, F. Liesa, X. Ramis, J.I. Iribarren and C. Alemán, "Corrosion protection with polyaniline and polypyrrole as anticorrosive additives for epoxy paint", *Corros. Sci.*, 2008, **50**, 721-728.

[21] E. Armelin, C. Alemán and J.I. Iribarren, “Anticorrosion performances of epoxy coatings modified with polyaniline: A comparison between the emeraldine base and salt forms”, *Prog. Org. Coat.*, 2009, **65**, 88-93.

[22] E. Armelin, A. Meneguzzi, C.A. Ferreira and C. Alemán, “Polyaniline, polypyrrole and poly(3,4-ethylenedioxythiophene) as additives of organic coatings to prevent corrosion”, *Surf. Coat. Technol.*, 2009, **203**, 3763-3769.

[23] E. Armelin, M. Martí, F. Liesa, J.I. Iribarren and C. Alemán, “Partial replacement of metallic zinc dust in heavy duty protective coatings by conducting polymer”, *Prog. Org. Coat.*, 2010, **69**, 26-30.

[24] G. Mengoli, M. Munari, P. Bianco and M. Musiani, “Anodic synthesis of polyaniline coatings onto Fe sheets”, *J. Appl. Polym. Sci.*, 1981, **26**, 4247-4257.

[25] A.J. Epstein in: T.A. Skotheim and J.R. Reynolds. Handbook of conducting polymers, 3nd. Edition, New York, CRC Press, 2007, Capther 15.

[26] M Tiitu, A. Talo, O. Forsén and O. Ikkala, “Aminic epoxy resin hardeners as reactive solvents for conjugated polymers: polyaniline base/epoxy composites for anticorrosion coatings”, *Polymer*, 2005, **46**, 6855-6861.

[27] C. Ocampo, E. Armelin, F. Liesa, C. Alemán, X. Ramis and J.I. Iribarren, ”Application of a polythiophene derivative as anticorrosive additive for paints”, *Prog. Org. Coat.*, 2005, **53**, 217-224.

[28] F. Liesa,1 C. Ocampo, C. Alemán, E. Armelin, R. Oliver and F. Estrany, “Application of electrochemically produced and oxidized poly(3,4-ethylenedioxythiophene) as anticorrosive additive for paints: Influence of the doping level”**,** *J. Appl. Polym. Sci.*, 2006, **102**, 1592-1599.

[29] E. Armelin, R. Oliver, F. Liesa, J. I. Iribarren, F. Estrany and C. Alemán, “Marine paint fomulations: Conducting polymers as anticorrosive additives”, *Prog. Org. Coat.*, 2007, **59**, 46-52.

[30] D. Aradilla, C. Ocampo, E. Armelin, C. Alemán, R. Oliver and F. Estrany, “Application of multilayered particles formed by poly(3,4-ethylenedioxythiophene) and poly(N-methylpyrrole) as anti-corrosive additives of conventional organic coatings”, *Mat. Corr.*, 2007, **58**, 867-872.

[31] J. Iribarren, C. Ocampo, E. Armelin, F. Liesa and C. Alemán, "Poly(3-alkylthiophene)s as anticorrosive additive for paints: Influence of the main chain stereoregularity", *J. Appl. Polym. Sci.*, 2008, **108**, 3291-3297.

[32] E. Armelin, C. Alemán, J.I. Iribarren, F. Liesa and F. Estrany, Patent Cooperation Treaty PCT/ES2010070820, 2010.

[33] L. J. del Valle, D. Aradilla, R. Oliver, F. Sepulcre, A. Gamez, E. Armelin, C. Alemán and F. Estrany, "Cellular adhesion and proliferation on poly(3,4-ethylenedioxythiophene): Benefits in the electroactivity of the conducting polymer", *Eur. Polym. J.*, 2007, **43**, 2342-2349.

[34] L. J. del Valle, F. Estrany, E. Armelin, R. Oliver and C. Alemán, "Cellular adhesion, proliferation and viability on conducting polymer substrates", *Macromol. Biosci.*, 2008, **8**, 1144-1151.

[35] R. A. Green, N. H. Lovell and L. A. Poole-Warren, "Cell attachment functionality of bioactive conducting polymers for neural interfaces", *Biomaterials*, 2009, **30** 3637-3644.

[36] B. Kim, L. Chen, J. Gong and Y. Osada, "Titration behavior and spectral transitions of water-soluble polythiophene carboxylic acids", *Macromolecules*, 1999, **32**, 3964-3969.

[37] C. Alemán, E. Armelin and F. Liesa, ES Patent Nº P200502713, 2005.

[38] J. B. Jorcin, M. E. Orazem, N. Pébere and B. Tribollet, "CPE analysis by local electrochemical impedance spectroscopy", *Electrochim. Acta*, 2006, **51**, 1473-1479.

7

SOLUBLE POLYTHIOPHENES AS ANTICORROSIVE ADDITIVES FOR MARINE EPOXY PAINTS

The work described in this chapter has been submitted for publication

This study compares the resistance against corrosion of a marine epoxy primer modified with $Zn_3(PO4)_2$ (10 wt.%) or a small concentration (0.3 wt.%) of conducting polymer as inorganic or organic anticorrosive pigment, respectively. More specifically, the behavior of three different conducting polymers has been evaluated: polyaniline emeraldine base, poly(3-thiophen-3-yl-acrylic acid methyl ester) and poly(2-thiophen-3-yl-malonic acid dimethyl ester), the latter two being soluble polythiophene derivatives bearing carboxylate side groups. In a first stage, the structural, thermal and mechanical properties of all the modified epoxy coatings were characterized using infrared spectroscopy, thermogravimetric analyses and stress-strain assays, respectively. After this, accelerated corrosion assays have evidenced that the degree of protection imparted by a small concentration of polyaniline is higher than that obtained using 10 wt.% of $Zn_3(PO_4)_2$. Indeed, polyaniline has been found to be more effective as anticorrosive additive than the two polythiophene derivatives. This fact has been attributed to the electroactivity of the former, which is higher than that of the latter. Thus, the ability to store charge has been proposed to be also responsible of protection against corrosion imparted by organic additives, based on conducting polymers.

7.1. Introduction

Marine corrosion is a topic of great interest based in the electrochemical reaction of steel, active metals and alloys with oxygen in presence of sea water. This type of corrosion depends on the particular conditions of the medium, as temperature, oxygen and salts concentration, and presence of marine organisms, which lead to the well-known bio-fouling phenomenon. Although some ionic compounds are protective in form of calcareous deposits, particularly in immersed structures, the presence of chloride ions inside the sea water and in marine environments is the origin of marine corrosion, giving place to both generalized and pitting corrosion in metallic structures.[1]

Organic coatings and, in particular, paints became an important solution to mitigate the consequences of corrosion during the second half of 20th century. Thermoplastic and thermosetting polymers have been successfully applied in different systems as both

anticorrosive paints and powder coatings for several applications.[2,3] In all cases, the main function of such protective coatings is to avoid the access of pollutants to the surface, being also an important dielectric barrier between the metallic substrate and the environment.[4]

In spite of the prolific characteristics of paints in terms of both composition and applications, alkyd and epoxy resins have been considered for years as the most important primers in the market.[5] These conventional anticorrosive primers usually contain inhibitors based on hexavalent chromium, lead compounds and zinc phosphate derivatives,[6-8] the latter being the most widespread at present time due to its ability for steel passivation in acidic media.[7-9] Although zinc phosphate derivatives provide good results, in some cases their anticorrosive performance is lower than that of chromates.[10] On the other hand, in recent years we reported that conducting polymers (CPs) can be successfully used as anticorrosive additives to modify the formulation of conventional organic coatings,[11] the most important benefit of this technology being that a very low concentration of CP is needed. Interestingly, we found that, in principle, the chemical nature of the anticorrosive additive can extend from polythiophene (PTh)[12-16] or polypyrrole (PPy)[13,16,17] derivatives to polyaniline (PAni),[17-19] even though the corrosion protection imparted by each CP may be limited by its compatibility with the paint formulation (*i.e.* the achievement of good and homogeneous dispersions on the resin formulation is essential). Many efforts have been focused on solve the high insolubility of CPs in coatings formulations, in order to improve the dispersion and efficiency of CPs as anticorrosive additive. As an example, Gergely *et. al.* have recently studied the corrosion protection of zinc-rich epoxy paint coatings with highly dispersed polypyrrole-deposited alumina monohydrate particles,[20] achieving a well-balanced active/passive function in the hybrid coating containing zinc and PPy.

In a recent study we investigated the efficacy of the conducting emeraldine salt form of PAni (PAni-ES) as anticorrosive additive for an epoxy paint based on diglycidyl ether of bisphenol A and polyamide.[17] The concentration of the CP in the paint formulation was varied from 0.3 to 1.5 wt.%. Interestingly, accelerated corrosion assays showed that the addition of PAni-ES improves the resistance of the paint, the highest inhibition of corrosion being obtained for the lowest CP concentration (*i.e.* 0.3 wt.%). Furthermore, this CP polymer

was found to act as adhesion promoter, this behavior being fully consistent with that found for PAni coatings.[21-24]

More recently, an alkyd formulation containing zinc phosphate (10 wt.%) was prepared and subsequently modified replacing the latter anticorrosive additive by a very low concentration of CP.[25] Specifically, three modified paints were formulated, which contained polyaniline emeraldine base (PAni-EB), PAni-ES and a partially oxidized PTh derivative. The properties and corrosion resistance of the four alkyd coatings were characterized. Among the three modified paints, the one containing PTh showed the best adherence and the highest corrosion resistance. This was attributed to the fact that the miscibility of the PTh derivative with the alkyd formulation is better than that of PAni. Furthermore, accelerated corrosion assays revealed that the corrosion resistance of the paint with PTh is several orders of magnitude higher than that with zinc phosphate. The PTh derivative was found to induce the formation of a passivating and well-adhered layer between the coating and the surface, preventing the access of chloride anions and oxygen to the substrate.

As a continuation of our recent study on alkyd primers,[25] in this work we compare the performance as anticorrosive pigments of three CPs and zinc phosphate when they are used in a commercial epoxy primer recommended for the protection of steels surfaces in contact with marine environments. Specifically, very small weight percentages of two recently described PTh derivatives,[26,27] which show good solubility in organic solvents, and PAni-EB have been employed. The two main objectives of this study are: (i) to examine the performance as corrosion inhibitors of these two PTh derivatives, comparing them with zinc phosphate, a conventional inorganic pigment; and (ii) to compare the efficacy as anticorrosive additive of the two soluble PTh derivatives with that of the less soluble PAni-EB when used in epoxy primers. Accordingly, our final aim is to find a soluble CP for the satisfactory substitution of classical zinc-containing corrosion inhibitors used in marine epoxy primers, as we recently did for industrial alkyd primers.[25]

7.2. Methods

7.2.1. Materials

The epoxy primer used in this work was kindly supplied by Pinturas Hempel S.A. This primer was prepared by mixing a stoichiometric amount of Epikote 3011 (Hexion) and Crayamid 115 (Cray Valley), a mixture of inert pigments (PVC=27 %), and a mixture of alcoholic solvents and aromatic hydrocarbons (15 % w/w). This composition was free of anticorrosive pigments and additives.

The chemical formulas of the three CPs used in this work, PAni-EB, poly(3-thiophen-3-yl-acrylic acid methyl ester) (PT3AME) and poly(2-thiophen-3-yl-malonic acid dimethyl ester) (PT3MDE), are displayed in Scheme 7.1. PAni-EB is the undoped form of PAni (Scheme 7.1a). PT3AME is a PTh derivative with a conjugated substituent in which the polymer backbone and the electron-withdrawing carboxylate group are separated by a double bond (Scheme 7.1b).[26] Thus, the aim of the acrylate substituent in PT3AME is not only to improve the solubility and dispersion of the PTh chains but also to enlarge the conjugated system from the backbone to the side chain, which results in an improvement of the electronic properties with respect to unsubstituted PTh.[26] PT3MDE is a PTh derivative bearing a substituent with two carboxylate groups per structural unit (Scheme 7.1c).[27] This CP is soluble in a number of solvents such as chloroform, tetrahydrofuran, dimethyl sulfoxide, acetone and dichloroacetic acid. PAni-EB was purchase from Aldrich (catalog number: 476706) whereas both PT3AME and PT3MDE were synthetized in our laboratory by chemical oxidative coupling polymerisation using the experimental procedures recently described.[26,27] Zinc phosphate, $Zn_3(PO_4)_2$, an inorganic additive commonly used with both aqueous and organic primers, was purchased from Europigments S.A.

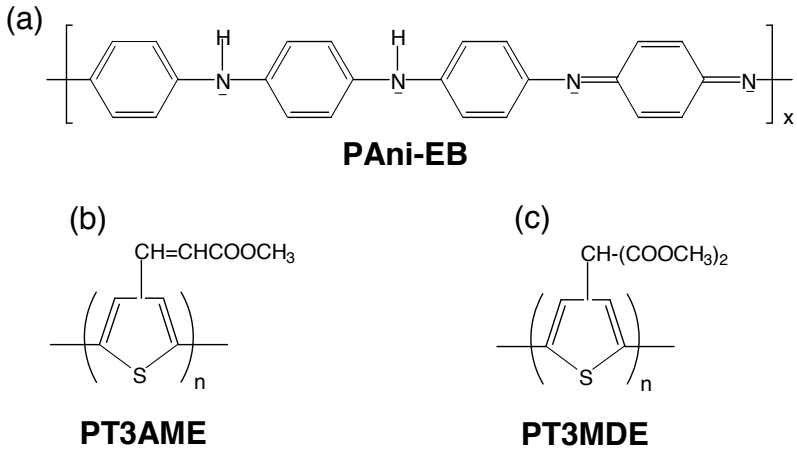

Scheme 7.1. Structures of PAni-EB, PT3AME and PT3MDE.

Corrosion experiments were performed using a naval steel (St F111) as metallic substrate. The elemental composition of this steel is: C=0.20 %, Mn=1.40 %, S=0.045 %, and N=0.009 %, the density being 7.90×10^3 kg/m^3. Rectangular test pieces of 40×50×1 mm^3 with a diameter hole of 6.5 mm were previously degreased with acetone and stored in dried atmosphere until the coating application, using calcium chloride as dryer in a recipient connected to the vacuum.

7.2.2. Preparation and application of the paints

The epoxy paints without corrosion inhibitor and with $Zn_3(PO_4)_2$ (10 wt.%), PT3AME (0.3 wt.%), PT3MDE (0.3 wt.%) and PAni-EB (0.3 wt.%) have been denoted EP-0, EP/$Zn_3(PO_4)_2$-10, EP/PT3AME-0.3, EP/PT3MDE-0.3 and EP/PAniEB-0.3, respectively. Paints were applied by immersion (one coat) of the metallic substrate in a base/solvent/hardener composition with the mixing ratio recommended by the manufacturer. These compositions are detailed in Table 7.1. In the case of EP/$Zn_3(PO_4)_2$-10, small quantities of BYK 500 (0.0809 g) and BYK 525 (0.0457 g), from BYK Chemie, were required to aid the pigment dispersion. Initially, PAni-EB was dissolved in a small volume of xylene (3-5 mL) while both PT3AME and PT3MDE were dissolved in trichloromethane (3-5 mL), before the addition to the paint formulation. It should be

remarked that a good dispersion of the CP is necessary to allow a suitable application of the paint on the metallic substrate and to obtain a covering power able to guarantee the desired protective characteristics. The thickness of the films obtained using this procedure was determined for ten samples of each class using a machine model Uno-Check Fe from Neurtek S.A., the resulting average thickness values being displayed in Table 7.1.

Paint	Base	Hardener	Corrosion inhibitor	Xylene	Thick (μm)	Adherence [a)]
EP-0	41.37	8.62	-	12.50	138	++
EP/$Zn_3(PO4)_2$-10	74.79	15.32	10.09	16.13	113	++++
EP/PT3AME-0.3	81.53	18.64	0.30	10.36	123	++
EP/PT3MDE-0.3	81.53	18.64	0.30	10.36	128	+++
EP/PAniEB-0.3	82.47	17.17	0.30	10.63	125	++++

[a)] The code used to indicate the adherence is: + bad; ++ medium; +++ good; ++++ excellent

Table 7.1. Composition (in g) of the epoxy formulations used in this work, thickness of the films after drying obtained by immersion of the steel substrate in the composition (one coat), and adherence of the film to the substrate.

7.2.3. Characterization

A Jasco 4100 FTIR spectrophotometer with a resolution of 4 cm^{-1} in the absorbance mode was used for the structural characterization of the coatings. Samples were placed in an attenuated total reflection accessory with thermal control and a diamond crystal (Mk II Golden Gate Heated Single Reflection Diamond ATR, Specac-Teknokroma).

Thermogravimetric analyses were carried out with a Perkin-Elmer thermogravimetric analyzer TGA-6 at a heating rate of 10 °C/min under nitrogen atmosphere and a temperature range from 30 to 850 °C.

The mechanical properties of the paints were evaluated through stress-strain assays with a Zwick Z2.5/TN1S testing machine. Regular films were prepared by evaporation of the volatile organic solvent of the paint formulation at room temperature. Plate samples with a length of 30 mm, a width of 3 mm and thickness varying from 200 to 300 μm, measured with Uno-Check Fe machine, were cut out from the films and used for the assays. The

deformation rate was 10 mm/min. Mechanical parameters (*i.e.* Young´s modulus, the tensile strength and the elongation at break) for each coating were averaged considering ten independent measurements.

7.2.4. Corrosion assays

Corrosion tests were performed using a home-made equipment developed in our laboratory.[28] This device was designed to perform accelerated immersion assays in an aggressive solution medium through controlled cycles. The solution medium consists of an aqueous solution of NaCl (3.5 wt.%, pH=6.6) stored in a polypropylene container. The operating conditions programmed for each cycle were: (i) immersion of coated steel sheets (15 min); (ii) wring out (30 min); (iii) drying stage with bulbs (230 V-100 W, 10 min, ~40 °C); and (iv) cooling time at room temperature (5 min). Painted panels were sealed on the edges and around the hole used for securing the pieces. The samples were tested in the solution medium during 30 days (*i.e.* 720 cycles). Laboratory conditions were 20 °C and relative humidity of 50 %. After the beginning of the test, the samples were removed at 120, 240, 480 and 720 hours. The corrosion of steel was monitored by visual and microscopy inspections, as described on the standard method ASTM D-1654.

Scanning electron microscopy (SEM) studies of the coating surfaces were performed using a Focussed Ion Beam Zeiss Neon 40 scanning electron microscope, equipped with an EDX system. Photographs and micrographs of the samples were taken before exposure to the aggressive solution.

7.3. Results and Discussion

7.3.1. Characterization of the formulations

The structural, thermal and mechanical characterization of EP-0 was described in a previous work.[17] Accordingly, in this section we focused in the formulations modified by the addition of $Zn_3(PO_4)_2$, PT3AME, PT3MDE and PAni-EB to the epoxy paint. Figure 7.1

compares the absorption spectrum of EP-0 with those of the four modified formulations. It is worth noting that the addition of the inorganic and organic corrosion inhibitors does not produce any structural change, the absorption bands remaining practically unaltered. No absorption band is detected at 917 cm^{-1}, which is consistent with the absence of terminal epoxy groups and corroborates with the fact that coatings are completely cured. The presence of strong bands in the 1249-1041 cm^{-1} region has been identified as C(Ar)–O–C(alkyl) ether group of bisphenol A, a thermoplastic polymer typically found in epoxy resins and characterized in previous works.[12,29] Furthermore, the presence of aromatic C(Ar)–C has been determined through the characteristic stretching absorption bands at around 1508 and 1608 cm^{-1}. Another interesting band corresponds to the broad and strong absorption at 1100-900 cm^{-1}, which reveals the presence of silicates (O-S-O) and phosphates (O-P-O) groups. The former is frequently employed in paint formulations as inert additives to improve the rheological properties of the emulsion and the late was employed as anticorrosive additive in the case of paint EP/$Zn_3(PO_4)_2$-10. Both polar groups, silicates and phosphates, have absorption bands in the same position due to the similarity of bond stretching or vibration mode in the IR fingerprint region.

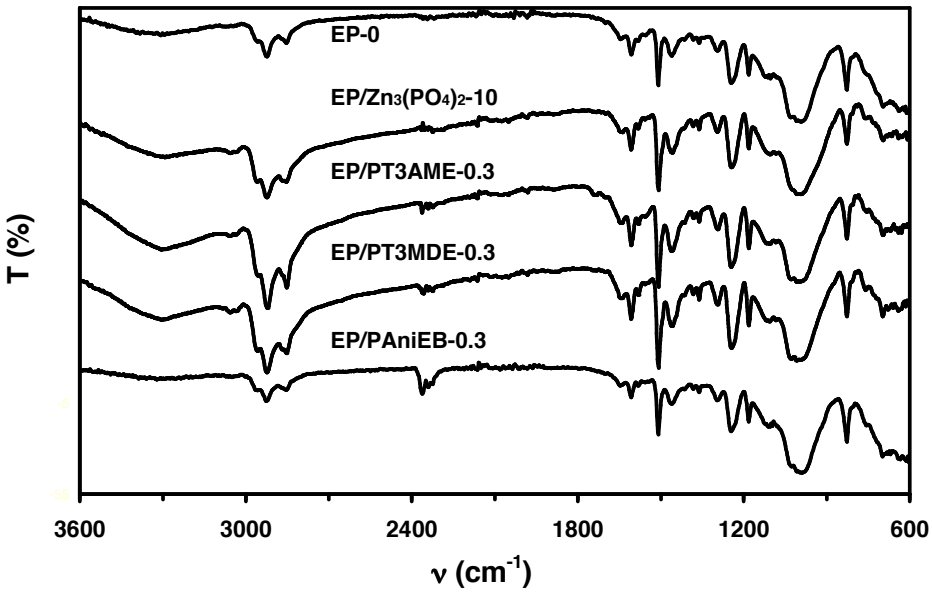

Figure 7.1. Infrared absorption spectra of the epoxy formulations studied in this work: EP-0, EP/$Zn_3(PO_4)_2$-10, EP/PT3AME-0.3, EP/PT3MDE-0.3 and EP/PAniEB-0.3.

The thermal stability of the five coatings was studied by thermogravimetry, the resulting curves being compared in Figure 7.2. The thermal behavior is not influenced by the addition of corrosion inhibitors. Thus, all the paints undergo a weight loss of 10-15 % when the temperature increases from 60 to 330 °C, which has been attributed to the evaporation of solvents trapped in crosslinked polymer chains as well as to the decomposition of low-molecular weight polymer fractions. With increase temperature, the weight loss increases, reaching values of 45-50 % at 500 °C. This pronounced fall corresponds to the degradation of the cured epoxy resin. Finally, the degradation of some inorganic components is observed at higher temperatures. The latter process is particularly relevant for the EP/$Zn_3(PO_4)_2$-10 paint, which shows a curve with a pronounced and progressive fall among 500-850 °C. Moreover, the profile obtained for the EP/$Zn_3(PO_4)_2$-10 paint shows a discontinuity between 500-550 °C with a weight loss of about 10-12 %, which corresponds to the decomposition of the zinc phosphate inorganic additive. The percentage of inorganic pigments and/or additives contained in the paints is reflected by the char-yielded at 850 °C: 45 %, 23 %, 40 %, 39 % and 39 % for EP-0, EP/$Zn_3(PO_4)_2$-10, EP/PT3AME-0.3, EP/PT3MDE-0.3 and EP/PAniEB-0.3, respectively. On the other hand, Figure 7.2 evidences that the thermal stability of EP-0 decreases upon the addition of corrosion inhibitors (*i.e.* modified paints starts the decomposition of the resin at a lower temperature). This effect is very similar for all the corrosion inhibitors, which allows us to conclude that the thermal stabilities of the epoxy paints modified with CPs and with $Zn_3(PO_4)_2$ are practically identical.

The mechanical properties of the epoxy coatings studied in this work are listed in Table 7.2 whereas the strain-stress curves are displayed in Figure 7.3. As it can be seen, all the paints are brittle materials with moderate Young's modulus (*E*) and low elongation at break (ε_b). The Young's modulus varied between 462 (EP/PT3MDE-0.3) and 1562 MPa (EP/$Zn_3(PO_4)_2$-10) while the tensile strengths (σ_{max}) ranged from 17 (EP/PT3MDE-0.3) to 37 MPa (EP-0). Although the elongation at break of EP-0 (ε_b=6.2 %) improves considerably upon the addition of a small concentration of PT3MDE (ε_b=8.7 %) and, especially, PT3AME (ε_b=10.0 %), the Young's modulus and the tensile strength deteriorate. The presence of $Zn_3(PO_4)_2$ in the epoxy composition provokes a

very significant reduction of both the elongation at break (ε_b=2.9 %) and the tensile strength (σ_{max}=20 MPa). On the other hand, the Young's moduli increases (*E*=1562 MPa) and provokes the formation of a very brittle epoxy film. Despite of these limitations, it should be remarked that the mechanical properties listed in Table 7.2 are very similar to those reported for commercial paints that are typically used for corrosion protection in marine environments.[12,17,19] On the other hand, Figure 7.3 shows that the EP-0 formulation presents both plastic and elastic limits. The addition of $Zn_3(PO_4)_2$, PT3AME and PT3MDE preserves this behavior while the formulation with PAni-EB only presents elastic limit. The latter feature has been attributed to the existence of secondary reactions between the amine groups of PAni and some components of the epoxy formulation.

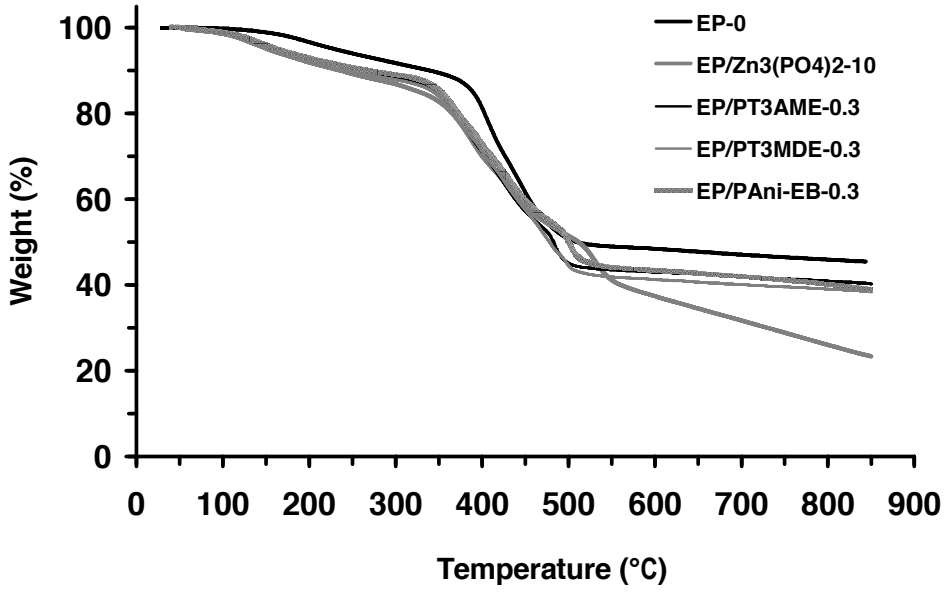

Figure 7.2. Thermogravimetric curves of the epoxy paints studied in this work: EP-0, EP/$Zn_3(PO_4)_2$-10, EP/PT3AME-0.3, EP/PT3MDE-0.3 and EP/PAniEB-1. Scan rate: 10 °C/min.

Sample	*E* (MPa) [a]	σ_{max} (MPa) [b]	ε_b (%) [c]
EP-0	896	37	6.2
EP/$Zn_3(PO_4)_2$-10	1562	20	2.9
EP/PT3AME-0.3	675	19	10.0
EP/PT3MDE-0.3	462	17	8.7
EP/PAniEB-0.3	1063	19	7.4

[a] Young's modulus. [b] Tensile strength. [c] Elongation at break.

Table 7.2. Mechanical properties of the epoxy paints studied in this work: EP-0, EP/$Zn_3(PO_4)_2$-10, EP/PT3AME-0.3, EP/PT3MDE-0.3 and EP/PAniEB-0.3.

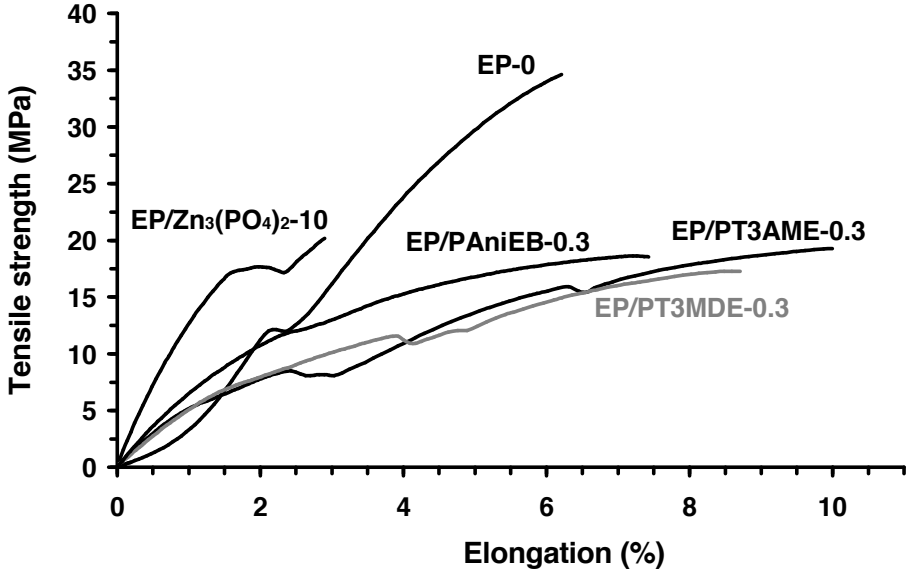

Figure 7.3. Tensile strain-stress curves for the epoxy paints studied in this work: EP-0, EP/$Zn_3(PO_4)_2$-10, EP/PT3AME-0.3, EP/PT3MDE-0.3 and EP/PAniEB-0.3. Deformation rate: 10 mm/min.

7.3.2. Accelerated corrosion assays

Samples coated with the EP-0 epoxy paint and its four modified formulations are displayed in Figure 7.4. All photographs are related to the panels after to rinse with water at a temperature up to 45 °C and before to scrape the specimens in order to evaluate the blistering formation around scribe and rust. In the EP-0 samples, the apparition of areas with blisters and rust under the film were detected after only 240 cycles. The resistance against corrosion of this epoxy coating improves upon the addition of $Zn_3(PO_4)_2$, as expected. Thus, the degree of blistering and rusting after 240 cycles were smaller for EP/$Zn_3(PO_4)_2$-10 than for EP-0. The CP-containing formulations, especially the EP/PAniEB-0.3, showed the higher anticorrosive properties. Thus, the blistering formation after 720 cycles is practically inappreciable for EP/PAniEB-0.3 while it is smaller for EP/PT3AME-0.3 and EP/PT3MDE-0.3 than for EP/$Zn_3(PO_4)_2$-10. On the other hand, we observed that the color of panels painted with EP/PT3AME-0.3 and EP/PT3MDE-0.3 changed with the time of exposure to the corrosive environment, which has been attributed to the variation of the $FeCl_3$ content into the paints and, probably, to the oxidation process suffered by CP after chlorine permeability to the film. EP/PaniEB-0.3 showed better color stability during corrosion assays.

Figure 7.5 represent the progression of rust from scribe against time according to the ASTM standard method D-1654. The progress of rust indicates the loss of adherence near to the scribe mark. After 720 cycles, the sample coated with the EP-0 formulation presented 25 mm of rust compared to the 5 mm of EP/$Zn_3(PO_4)_2$-10 and EP/PAniEB-0.3, evidencing that water, oxygen and chloride ions cannot overcome the protective barriers promoted by $Zn_3(PO_4)_2$ and PAni-EB corrosion inhibitors. The addition of PT3AME and PT3MDE enhances the corrosion protection with respect to the unmodified epoxy formulation, presenting 17 and 8 mm of rust, respectively. Although PT3AME and PT3MDE improve significantly the anticorrosive properties of EP-0, the protection imparted by these two polythiophene derivatives is lower than those obtained with $Zn_3(PO_4)_2$ and PAni-EB. Moreover, this behavior is practically independent of the number of cycles. These results are in agreement with our previous studies,[17] which indicated that PAni-EB promotes significantly the adherence between the coating and the steel. In opposition, in our recent

study with alkyd compositions,[25] the protection performance provided by the PTh ester derivative was found to better than that of PAni-EB. Nevertheless, the anticorrosive behavior of CPs depends on the nature of the polymer resin. In the present study, the adherence of coatings was only qualitatively investigated, *i.e.* with visual inspection after removing the film from the scribe mark, according to the ASTM 1654, and the resultant observation are displayed on Table 7.1. Figure 7.6 shows the panels that were scrapped after 120, 240, 480 and 720 cycles of accelerated corrosion assays.

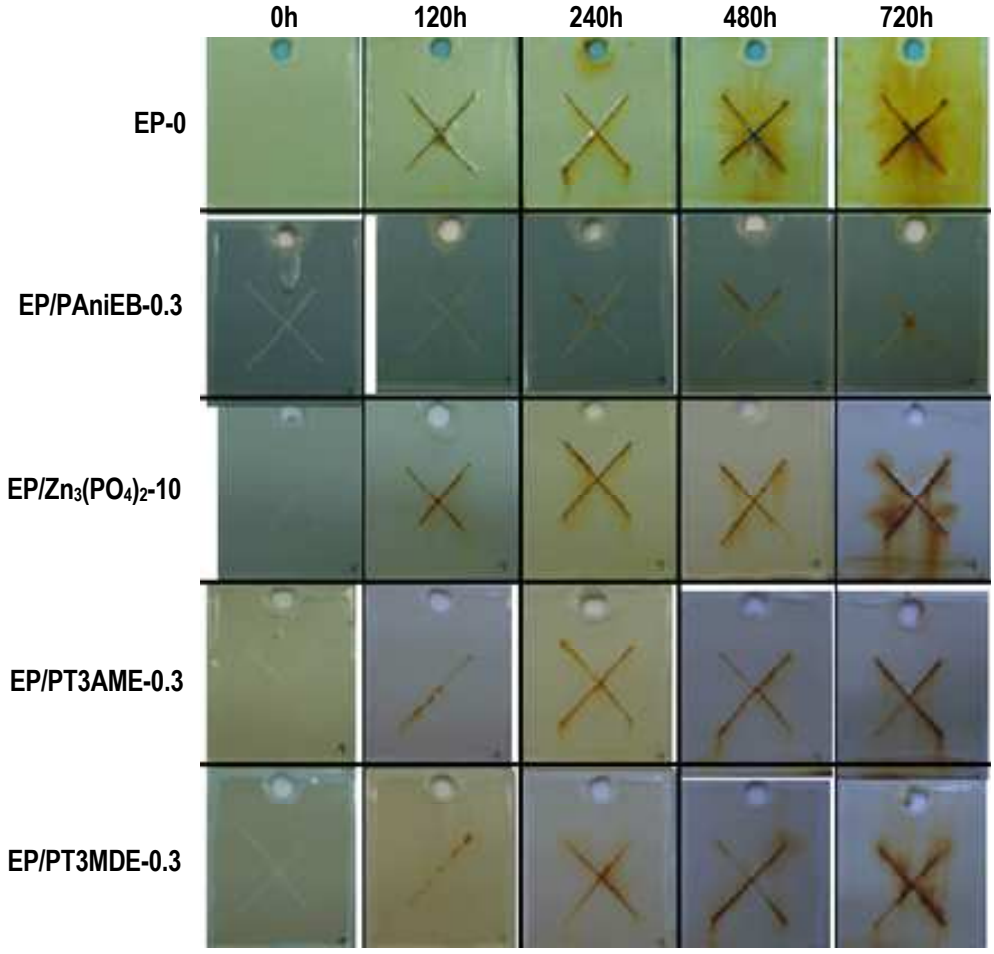

Figure 7.4. Test panels of the epoxy coating without anticorrosive pigment (EP-0) and modified with $Zn_3(PO_4)_2$ (10 wt.%), PAni-EB (0.3 wt.%), PT3AME (0.3 wt.%) and PT3MDE (0.3 wt.%) before and after 120, 240, 480 and 720 accelerated corrosion cycles (see text).

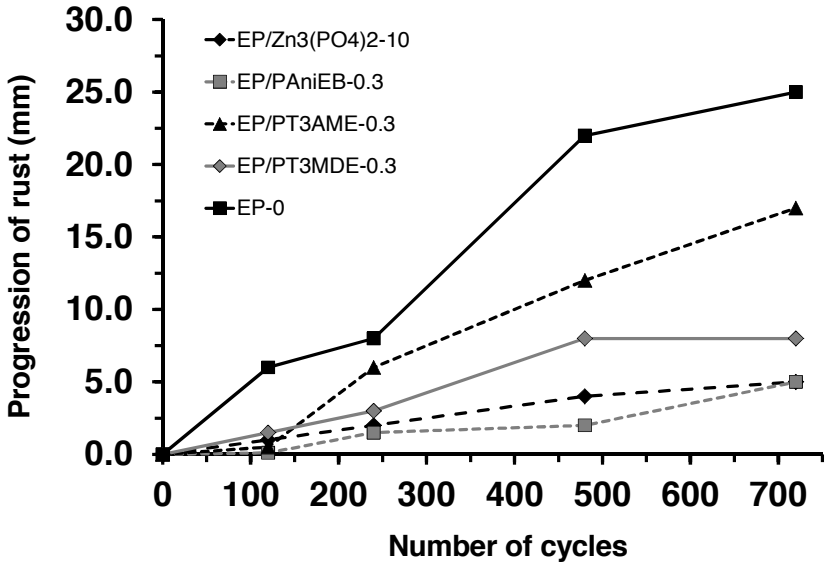

Figure 7.5. Progression of rust from scribe against the number of accelerated corrosion cycles according ASTM standard method D-1654 for the epoxy paints studied in this work: EP-0, EP/$Zn_3(PO_4)_2$-10, EP/PT3AME-0.3, EP/PT3MDE-0.3 and EP/PAniEB-0.3.

SEM micrographs of the coatings surfaces, which are displayed in Figure 7.7, allowed us to reach some conclusions regarding the variability of organic-inorganic anticorrosive protection found in this work. Films without $Zn_3(PO_4)_2$ or CPs show higher particles agglomerates at surface (Figure 7.7a) and, at higher magnification scale (Figure 7.7b), seems more porous than those with such additives. This supports the behavior of EP-0, which was worse than those films with anticorrosive additives (*i.e.* the water uptake should be very fast through coating. On the other hand, micrographs of the surfaces of coatings with $Zn_3(PO_4)_2$ and CPs reveals the presence of an amount of poorly dispersed pigments and additives, as is evidenced by the white particles in the Figures 7.7c-7.7d (EP/$Zn_3(PO_4)_2$-10), 7.7e-7.7f (EP/PAniEB-0.3) and 7.7g-7.7h (EP/PT3AME-0.3). Interestingly, the PT3AME-containg coating shows many spherical holes at surface compared to the EP/PAniEB-0.3 coating. However, these concave shapes are just surface defects that appeared after solvent evaporation. Due to its high solubility, the small CP particles, weakly adhered to the epoxy matrix, can be easily

detached when a high vacuum system, like that of the sample chamber in the SEM microscope, is applied. This kind of concave forms were also observed for the poly[2,2'-(3-methylacetate)thiophene], as was reported in previous works.[25,30] SEM micrographs of EP/PT3MDE-0.3 are not showed because they were very similar to those of EP/PT3AME-0.3.

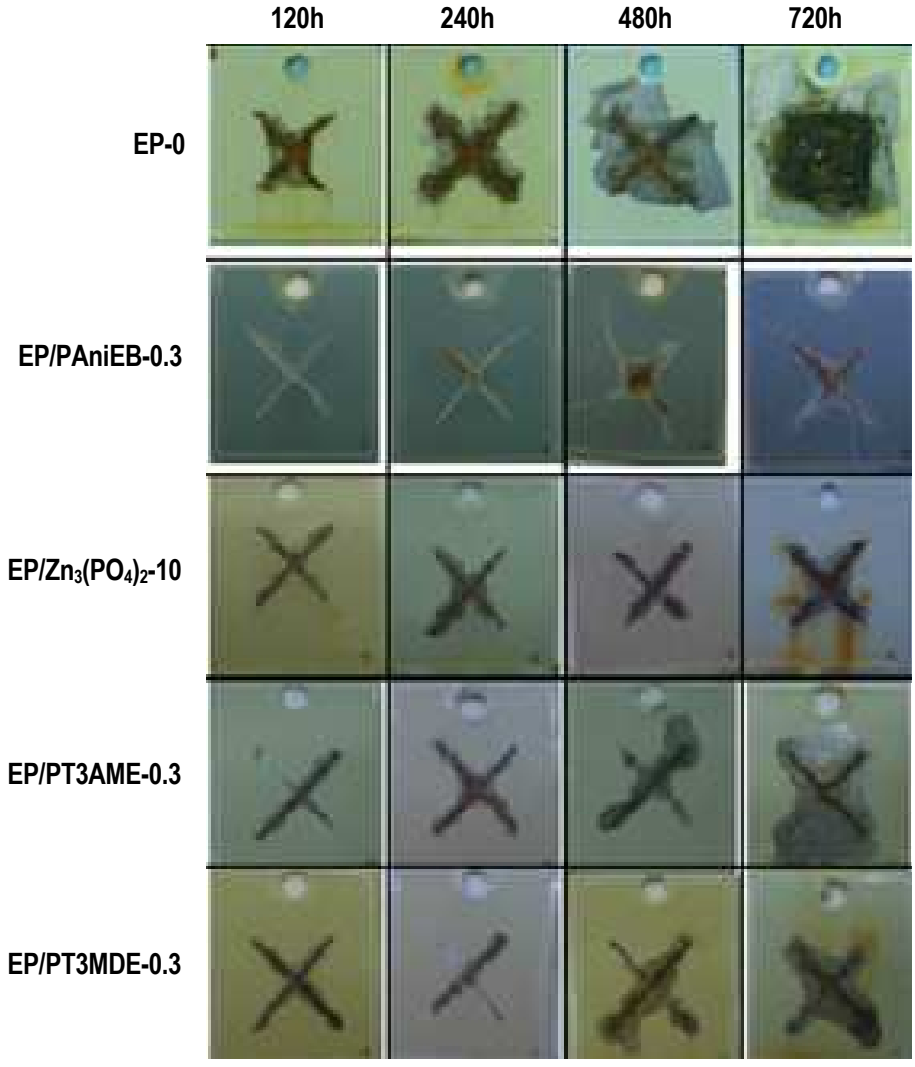

Figure 7.6. Scrapped test panels of the epoxy coating without anticorrosive pigment (EP-0) and modified with $Zn_3(PO_4)_2$ (10 wt.%), PAni-EB (1.0 wt.%), PT3AME (0.3 wt.%) and PT3MDE (0.3 wt.%) after 120, 240, 480 and 720 accelerated corrosion cycles.

Micrographs of EP/PAni-EB-0.3 (Figure 7.7f) show a smooth surface with few white particles inside the epoxy film, which is consistent to a good dispersion of PAni-EB compared to $Zn_3(PO_4)_2$. Figure 7.7h also shows a smooth surface but corrosion results were not the desirable due to different factors, like the high hydrophilicity and, especially, the low electroactivity of the CPs bearing ester groups.

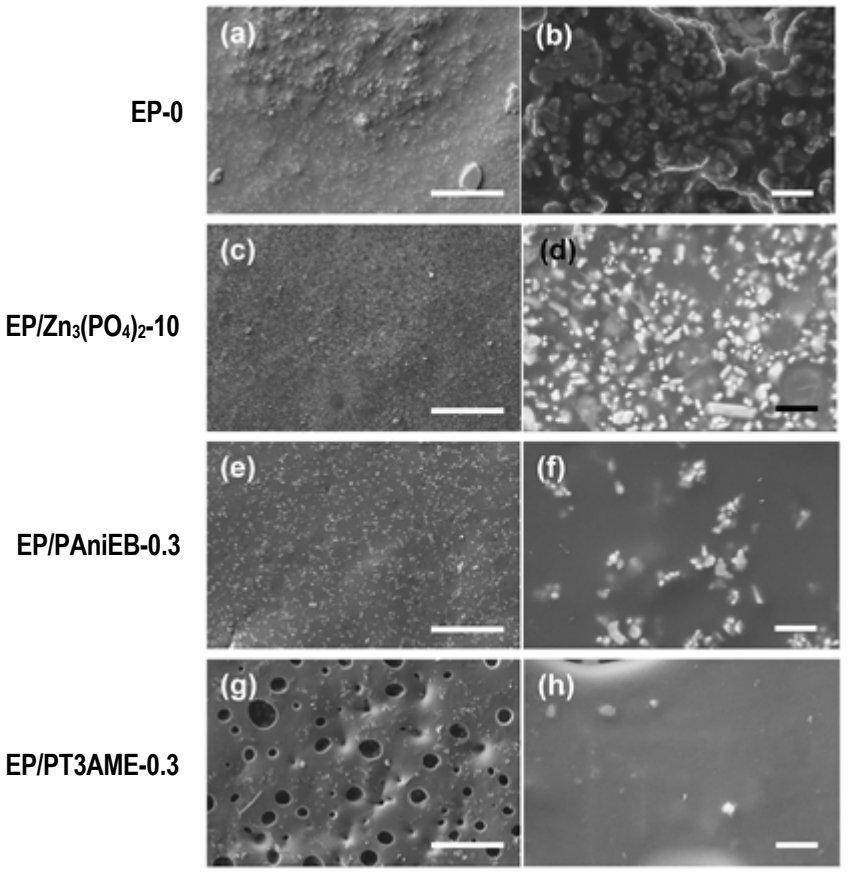

Figure 7.7. SEM micrographs of the surface of films studied in this work before the immersion of the coated panels in the aggressive solution. Scale bar: 20 μm (left) and 1 μm (right).

Summarizing, results reported in Figures 7.4-7.7 show that PAni-EB performs better corrosion protection than PT3AME, PT3MDE and $Zn_3(PO_4)_2$ when used as anticorrosive

additive of epoxy coatings. It is worth nothing that undoped PAni-EB was reported to be more effective as anticorrosive additive than the doped PAni-ES,[31,32] even though it is generally accepted that the ability of CPs to intercept electrons at the metal surface and to transport them in a very effective mechanism to retard corrosion. However, in a recent study we demonstrated that the ability to store charge (*i.e.* the electroactivity) is also responsible of protection against corrosion.[15,16] More specifically, we found that the mechanism based on the ability of organic materials to act as molecular condensers predominate over the mechanism based on the electrical properties. The results obtained in the present work are fully consistent with the previous observation since PAni-EB shows higher ability to store charge but lower electrical conductivity than the PTh derivatives. Thus, the success of PAni-EB as anticorrosive additive should be attributed to the fact that the epoxy formulation used in this work does not alter its intrinsically high redox capacity (*i.e.* ability to oxidize and reduce in a reversible way).[33,34] In contrast, the electroactivity of PT3MDE and, especially, PT3AME is very low because of the intrinsic tendency of PTh and its derivatives to promote crosslinking.[26,27] Accordingly, the protection imparted by EP/PT3MDE-0.3 and EP/PT3AME-0.3 is essentially based on their ability to transport charge, which was found to be only moderate. More specifically, the electrical conductivity of PT3MDE and PT3AME was reported to be 6 S/cm[27] and 15 S/cm,[26] respectively, these values being significantly lower than those reported for other PTh derivatives [*e.g.* 315 S/cm for poly(3,4-ethylenedioxythiophene)].[35].Thus, soluble CPs able to provide good miscibility with the epoxy resin are not enough to produce effective organic anticorrosive additives, fulfillment of other requirements like intrinsically high electroactivity and/or electrical conductivity being necessary. On the other hand, it is worth noting that PAni-EB has many amine groups that are capable of complexing metal ions. In an early study, it was reported that a PAni-EB film led to the extraction of Cu from the top several hundred angstroms of Al 2024-T3,[36] thus removing the Cu/Al galvanic couple that is primarily responsible for the corrosion behavior of this alloy. These complexing abilities of PAni-EB may also play a role in this process.

7.4. Conclusions

A marine epoxy paint has been modified by adding a 10 wt.% of $Zn_3(PO_4)_2$ or a very low concentration of CP (PT3AME, PT3MDE or PAni-EB) as anticorrosive pigment. FTIR spectroscopy studies showed that the structure of the four modified formulations is practically identical to that of unmodified one, epoxy resin being completely cured in all cases. Thermogravimetric analyses indicated the thermal stability of the epoxy primer decreases upon the addition of both organic and inorganic corrosion inhibitors. On the other hand, films prepared using the unmodified epoxy primer and the formulations containing $Zn_3(PO_4)_2$, PT3AME and PT3MDE presented both plastic and elastic yield, whereas the no plastic behavior was found for the formulation with PAni-EB.

As it was expected, the resistance against corrosion of the epoxy primer improved upon the addition of an anticorrosive pigment. The highest corrosion protection was provided by the formulation with 0.3 wt.% of PAni-EB. Although PT3AME and PT3MDE enhanced the corrosion protection imparted by the unmodified epoxy paint, the electroactivity and electrical conductivity of these polythiophene derivatives was not large enough to improve the outcomes obtained with the PAni-EB-containing paint. The overall of the results obtained in this work allows us to conclude that, although the miscibility between the different components is essential to obtain a good paint, CPs used as corrosion inhibitors must satisfy other requirements, such as high electroactivity and/or electrical conductivity.

7.5. References

[1] F. L. LaQue, "Marine corrosion and prevention", John Wiley and Sons, Inc., New York, 1975.

[2] T.A. Misev and R. van der Linde, “Powder coatings technology: new developments at the turn of the century”, *Prog. Org. Coat.*, 1998, **34**, 160-168

[3] E. Lugscheider, S. Bärwulf, C. Barimari, M. Riester and H. Hilgers, “Magnetron-sputtered hard material coatings on thermoplastic polymers for clean room applications”, *Surf. Coat. Technol.*, 1998, **108/109**, 398-402.

[4] C.K. Schoff, "Organic coatings: the paradoxical materials", *Prog. Org. Coat.*, 2005, **52**, 21-27.

[5] T. Schauer, A. Joos, L. Dulog, C.D. Eisenbach, "Protection of iron against corrosion with polyaniline primers", *Prog. Org. Coat*., 1998, **33**, 20-27.

[6] M. Hernandez, J. Genescá, J. Uruchurtu, F. Galliano and D. Landolt, "Effect of an inhibitive pigment zinc-aluminum-phosphate (ZAP) on the corrosion mechanisms of steel in waterborne coatings, *Prog. Org. Coat*., 2006, **56**, 199-206.

[7] R. Romagnoli and V. Vetere, "Non-pollutant corrosion inhibitive pigments: Zinc phosphate, a review", *Corros. Rev*., 1995, **13**, 45-64.

[8] M. Bethencourt, F.J. Botana, M. Marcos, R.M. Osuna and J.M. Sánchex-Amaya, "Inhibitor properties of "green" pigments for paints", *Prog. Org. Coat*., 2003, **46**, 280-287.

[9] P. Sorensen, S. Kiil, K. Dam-Johansen and C. Weinell, "Anticorrosive coatings: A review", *J. Coat. Tech. Res*., 2009, **6**, 135-176.

[10] J. A. Burkill and J. E. O. Mayne, "The limitations of zinc phosphate as an inhibitive pigment", *J. Oil & Colour Chem. Assoc*., 1988, **9**, 273-285.

[11] E. Armelin, R. Oliver, F. Liesa, J. I. Iribarren, F. Estrany and C. Alemán, "Marine paint fomulations: Conducting polymers as anticorrosive additives", *Prog. Org. Coat*., 2007, **59**, 46-52.

[12] C. Ocampo, E. Armelin, F. Liesa, C. Alemán, X. Ramis and J.I. Iribarren, "Application of a polythiophene derivative as anticorrosive additive for paints", *Prog. Org. Coat*., 2005, **53**, 217-224.

[13] J.I. Iribarren, E. Armelin, F. Liesa, J. Casanovas and C. Alemán, "On the use of conducting polymers to improve the resistance against corrosion of paints based on polyurethane resins", *Mat. Corr*., 2006, **57**, 683-688.

[14] C. Alemán, C. Ocampo, E. Armelin, D. Curcó, J. Casanovas and F. Liesa, "Conducting polymers: Influence on the anticorrosive properties of marine paints", *Cien. Mar*., 2006, **32**, 361-368.

[15] F. Liesa, C. Ocampo, C. Alemán, E. Armelin, R. Oliver and F. Estrany, "Application of electrochemically produced and oxidized poly(3,4-ethylenedioxythiophene) as

anticorrosive additive for paints: Influence of the doping level", *J. Appl. Polym. Sci*., 2006, **102**, 1592-1599.

[16] D. Aradilla, C. Ocampo, E. Armelin, C. Alemán, R. Oliver and F. Estrany, "Application of multilayered particles formed by poly(3,4-ethylenedioxythiophene) and poly(N-methylpyrrole) as anti-corrosive additives of conventional organic coatings", *Mat. Corr*., 2007, **58**, 867-872.

[17] E. Armelin, R. Pla, F. Liesa, X. Ramis, J. I. Iribarren and C. Alemán, "Corrosion protection with polyaniline and polypyrroleas anticorrosive additives for epoxy paint", *Corr. Sci*., 2008, **50**, 721-728.

[18] J.I. Iribarren, F. Cadena and F. Liesa, "Corrosion protection of carbon steel with thermoplastic coatings and alkyd resins containing polyaniline as conductive polymer", *Prog. Org. Coat*., 2005, **52**, 151-160.

[19] E. Armelin, C. Ocampo, F. Liesa, J. I. Iribarren, X. Ramis and C. Alemán, "Corrosion protection of carbon steel with thermoplastic coatings and alkyd resins containing polyaniline as conductive polymer", *Prog. Org. Coat*., 2007, **58**, 316-322.

[20] A. Gergely, I. Bertóti, T. Török, E. Pfeifer and E. Kálmán, "Corrosion protection with zinc-rich epoxy paint coatings embedded with various amounts of highly dispersed polypyrrole-deposited alumina monohydrate particles", *Prog. Org. Coat*., 2006, **76**, 17-32.

[21] D.W. DeBerry, "Modification of the electrochemical and corrosion behavior of stainless steels with an electroactive coating", *J. Electrochem. Soc*., 1985, **132**, 1022-1026.

[22] B. Wessling, "Passivation of metals by coating with polyaniline: Corrosion potential shift and morphological changes", *Adv. Mater*., 1994, **6**, 226-228.

[23] B. Wessling, "Scientific and commercial breakthrough for organic metals", *Synth. Met*., 1997, **85**, 1313-1318.

[24] T. Schauer, A. Joos, L. Dulog and C.D. Eisenbach, "Protection of iron against corrosion with polyaniline primers", *Prog. Org. Coat*., 1998, **33**, 20-27.

[25] M. Martí, G. Fabregat, D. S. Azambuja, C. Alemán and E. Armelin, "Evaluation of an environmentally friendly anticorrosive pigment for alkyd primer", *Prog. Org. Coat*., 2012, **73**, 321-329.

[26] O. Bertran, P. Pfeiffer, J. Torras, E. Armelin, F. Estrany and C. Alemán, "On the structural and electronic properties of poly(3-thiophen-3-yl-acrylic acid methyl ester)", *Polymer*, 2007, **48**, 6955-6964.

[27] E. Armelin, O. Bertran, F. Estrany, R. Salvatella and C. Alemán, "Characterization and properties of a polythiophene with a malonic acid dimethyl ester side group", *Eur. Polym. J*., 2009, **45**, 2211–2221.

[28] C. Alemán, E. Armelin, F. Liesa, ES Patent No. P200502713, 2005.

[29] J. I. Iribarren, M. Iriarte, C. Uriarte and J. J. Iruin, "Phenoxy resin: Characterization, solution properties, and inverse gas chromatography investigation of its potential miscibility with other polymers", *J. Appl. Polym. Sci*., 1989, **37**, 3459-3470.

[30] E. Armelin, A. L. Gomes, M. M. Perez-Madrigal, J. Puiggalí, L. Franco, L. J. del Valle, A. Rodríguez-Galán, J. S. C. Campos, N. Ferrer-Anglada and C. Alemán, "Biodegradable free-standing nanomembranes of conducting polymer:polyester blends as bioactive platforms for tissue engineering", *J. Mater. Chem*., 2012, **22**, 585-594.

[31] W.-K. Lu, R.L. Elsenbaumer and B.Wessling, "Corrosion protection of mild steel by coatings containing polyaniline", *Synth. Met*., 1995, **71**, 2163-2166.

[32] M. Fahlman, S. Jasty and A.J. Epstein, "Polyaniline: An X-ray photoelectron spectroscopy study", *Synth. Met*., 1997, **85**, 1323-1326.

[33] D.E. Tallman and G.P. Bierwagen, "Corrosion protection using conducting polymers", in: T.A. Skotheim and J.R. Reynolds (Eds.), Handbook of Conducting Polymers, 3rd ed., CRC Press, Boca Raton, 2007, Chapter 15.

[34] P.A. Kilmartin, L. Triel and G.A.Wright, "Corrosion inhibition of polyaniline and poly(o-methoxyaniline) on stainless steels", *Synth. Met*. 2002, **131**, 99-109.

[35] C. Ocampo, R. Oliver, E. Armelin, C. Alemán and F. Estrany, "Electrochemical synthesis of poly(3,4-ethylenedioxythiophene) on steel electrodes: Properties and characterization", *J. Polym. Res*., 2006, **13**, 193–200.

[36] A.J. Epstein, J.A.O. Smallfield, H. Guan and M. Fahlman, "Corrosion protection of aluminum and aluminum alloys by polyanilines: A potentiodynamic and photoelectron spectroscopy study", *Synth. Met*., 1999, **102**, 1374-1376.

8

NOVEL EPOXY COATINGS BASED ON DMSO AS GREEN SOLVENT AND FREE OF ZINC ANTICORROSIVE PIGMENT

The work described in this chapter has been submitted for publication

This work reports novel anticorrosive epoxy coatings based on environmentally friendly dimethyl sulfoxide (DMSO) solvent and free of metallic compounds as anticorrosive pigment. The latter have been replaced by a small concentration of organic additives based on conducting polymers, as non-toxic anticorrosive pigments. The procedure used for their formulation, spectroscopic characterization as well as their excellent thermal mechanical properties have been discussed and compared with those of conventional epoxy coatings based on xylene and zinc as anticorrosive pigment. Furthermore, accelerated and long-term corrosion assays have evidenced that the new epoxy coatings protect steel from chlorine aggressive medium for 2880 hours (4 months) and for two years in an industrial corrosive zone over an open brine tank for chlorine gas production, respectively. The overall of the results reflect that epoxy coatings based on DMSO as solvent and a conducting polymer as anticorrosive pigments have excellent corrosion resistance properties, excellent application and handling characteristics, and aesthetic appearance.

8.1. Introduction

Epoxy coatings form a class of high-performance material, chemically resistant, used in protective applications and mainly based on solvent-borne systems.[1] However, due to the persistent interest in the development of low or zero volatile organic compounds (VOC) coatings with high performance, in the past few years innovative coatings technology, such as waterborne systems,[2-6] based on new resins and binders has emerged.[7,8] It is well known, however, that waterborne systems involve a greater degree of difficulty for both formulator and applicator alike. Waterborne coatings are less tolerant to temperature changes and humidity, and have less application in many corrosive mediums than solvent-borne systems.

High solids content solvent-borne epoxy coatings are low viscosity systems typically based on liquid diglycidyl ether of bisphenol A (DGEBA) (Scheme 8.1a) and bisphenol F (DGEBF) epoxy resins. Furthermore, they also require the employment of low viscosity amine curing agents, which must be compatible with liquid epoxies. In contrast,

waterborne epoxy coatings are prepared using solid and liquid epoxy resins dispersed in water.

According to VOCs regulations[9] and REACH[10] (Registration, Evaluation, Authorisation and Restriction of Chemical substances), some of the most important solvents and substances used in the formulation of epoxy coatings and classified as toxic will be withdrawn altogether. Some examples are 4,4'-diaminodiphenylmethane and dibutyl phthalate, which are currently under review and will probably be restricted by the REACH process.

Although not specifically excluded by REACH, the standards for toxic compounds have limited the use of many substances depending on the final product application. For example, the concentrations of xylene, butanol, phenol and benzyl alcohol in organic coatings formulations are restricted by the assigned LCI (Lowest Concentration of Interest) values, which express the critical levels of these toxic substances in a given environment (*i.e.* air, water, soil, or food). Thus, a LCI of 440 $\mu g/m^3$ has been assigned to benzyl alcohol for epoxy floor coatings applications, whereas the LCI of xylene and butanol for the same applications increases to 2200 $\mu g/m^3$ and 3100 $\mu g/m^3$, respectively.

Replacement of volatile solvents is not a simple task due to, among other factors, the climatic conditions and pigment or additives formulations for paints. Therefore, a completely VOC-free solvent-based system will never be offered. Nevertheless, the formulation of low emission epoxy coatings based in alternatives and non-toxic solvents is necessary and extremely urgent. In this way, dimethyl sulfoxide (DMSO) is a good candidate to replace toxic solvents[11-14] due to its high boiling point (189 °C at 760 mmHg) and a very low vapour pressure (0.6 mmHg at 25 °C). DMSO offers many benefits to be used in paint formulations. According to US Environmental Protection Agency (EPA), this solvent is classified as non-toxic with no risk for the human health.[15] DMSO is able to solubilise a wide range of polymers, including epoxy resins, at room temperature. Moreover, DMSO is miscible with all common solvents such as aromatics, ketones, acetate, and it is also completely miscible in water, allowing its use in both solvent- and waterborne coatings. Furthermore, this solvent is

often recycled by its users, limiting discharges. DMSO is present in some industrial wastewaters and is readily biodegradable.

Another aspect to be discussed here, which currently represents a handicap of increasing interest, is the replacement of toxic inorganic anticorrosive pigments on protective coatings. In order to provide higher durability and protection to metal structures, protective coatings usually incorporate inorganic anticorrosive pigments based on zinc metallic or zinc phosphate. Nowadays, particular attention has been paid to the use of zinc derivatives in organic coatings. Accordingly, Lima-Neto *et. al*.[16] proposed that zinc phosphate should be classified as "not hazardous" for the human health but "very toxic" for the aquatic environment. Heavy-duty primers to marine, offshore and structural steelwork industries employee almost 80 wt.% of zinc dust in their formulations while light-duty epoxy formulations for industrial environments use 30-40 wt.% of zinc phosphates as anticorrosive pigment. Therefore, cathodic protection of vessels or maritime platforms is an important source of contamination of the aquatic life. The European Community restricted the use of zinc through a regulation (Directive 76/464 EC, codified as 2006/11/EC),[17] giving place to intense research aimed to the look for alternative pigments useful to replace zinc derivatives.

In this work we apply the principles of "green chemistry" and engineering to design a novel epoxy formulation based on DMSO, as non-toxic and environmental friendly solvent, combined with organic additives based on conducting polymers (CPs), as non-toxic anticorrosive pigments. Thus, our aim is essentially focussed on the formulation of solvent-borne epoxies made of bisphenol A epoxy resin and polyamide curing agent with low VOC emission and efficient anticorrosive performance. Structural and morphological characterization of the coating based on DMSO have been carried out, results being compared with those obtained for the same epoxy primer but based on xylene, a common volatile solvent used in commercially available primers. In order to evaluate the protection performance achieved by the novel epoxy coating, both accelerated corrosion assays in the laboratory and long corrosion exposure of steel painted panels in an aggressive industrial medium (*i.e.* field corrosion assays) have been performed. The modifications introduced in

the paint formulation provide important benefits to manufacturers. Among them, the following ones deserve special mention: (i) significant reduction of health hazards (*i.e.* DMSO is considered a "green-solvent"); (ii) CPs are considered non-toxic materials due to their very low concentration in the coating formulation (0.3-1.0 wt.%) compared to zinc compounds; and (iii) reduction of the formulation cost and the coating weight, caused by the substitution of high concentrations of inorganic additives for very low concentrations of organic additives. It should be remarked that the latter provokes a reduction of combustible consumption in naval applications.

8.2. Experimental

8.2.1. Materials

Solid epoxy resin Epikote™ 1001 (M_n ~800, WPE 400-500) and polyaminoamide curing agent Crayamid™ 195X60 (HEW 240) were supplied by Cray Valley Spain. The organic anticorrosive additives used in this work were polyaniline emeraldine base (PAni-EB) and poly[2,2'-(3-methylacetate)thiophene] (PTE). The first was supplied by Sigma-Aldrich and the late was synthesized in our laboratory, accordingly to the experimental procedure described by Osada and co-workers.[18] All pigments and rheological additives were purchased from different suppliers, as detailed in the next section. Main solvents (dimethyl sulfoxide 99.5 % and *m*-xylene) were supplied by Panreac Química S.A. Corrosion experiments were performed using DIN CK15 (AISI/SAE 1015) steel panels with dimensions of 120×40×2 mm^3 as metallic substratum.

8.2.2. Formulation and preparation of the epoxy coating using DMSO as solvent

The chemical structure of the main components of the epoxy coatings prepared in this work is displayed in Scheme 8.1. Three different bicomponent epoxy formulations, which differ in the anticorrosive additive, were prepared. More specifically, these formulations contained 10 wt.% of zinc phosphate (Epoxy-DMSO/Zn), 0.3 wt.% of

PAni-EB (Epoxy-DMSO/PAni) or 1.0 wt.% of PTE (Epoxy-DMSO/PTE) as anticorrosive additive. Thus, the inorganic additive of the former was substituted by a very small concentration of organic CPs in the latter two. The epoxy/amine ratio is 1.4-1.6 and the PVC/CPVC ratio (Pigment volume concentration / Critical pigment volume concentration ratio) was maintained at 0.65-0.70 in all cases.

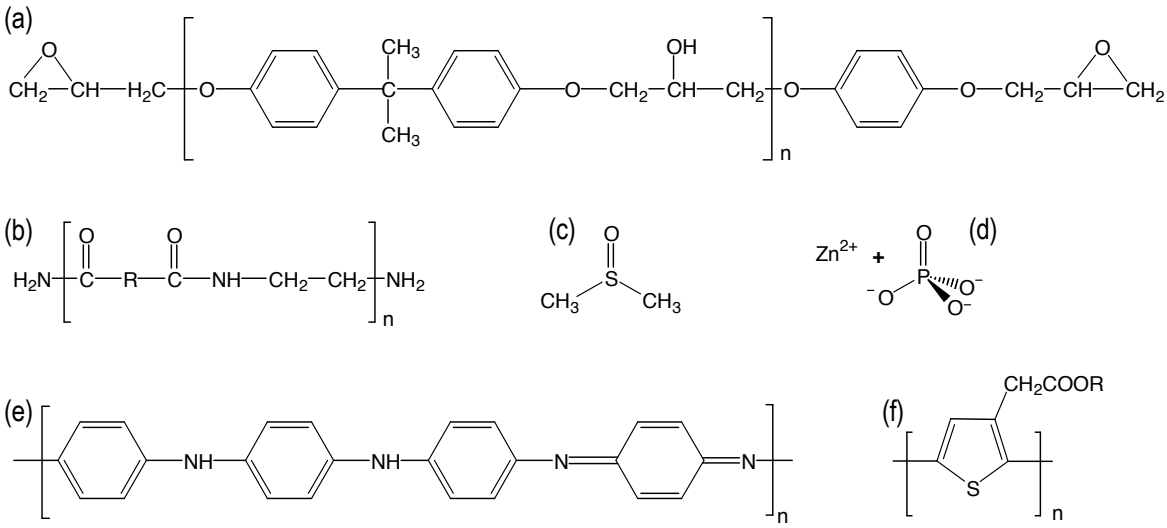

Scheme 8.1. Main components of the epoxy coatings studied in this work: (a) DGEBA epoxy resin; (b) polyaminoamide curing agent; (c) DMSO; (d) zinc phosphate; (e) PAni-EB; and (f) PTE, where R is a methyl group.

For the first formulation, 75 g of epoxy resin (Epikote 1001, Hexion Specialty Chemicals, Inc.) was initially dispersed in 25 mL of DMSO (Panreac Química S.A.). Next, 20 wt.% of such epoxy dispersion, 5 wt.% of titanium dioxide (white oxined, Europigments), 10 wt.% of zinc phosphate (Nubiola), 20 wt.% of barite (Barium sulfate, Viaton Industries Ltd.), 12 wt.% of talc (Industrial Talc FF, T3Química), 0.23 wt.% of Aerosil 200 (Degussa AG), 1 wt.% of Antiterra U (BYK Chemie GmbH), 0.7 wt.% of BYK-500 and BYK-525 (BYK Chemie GmbH), and 19 wt.% of DMSO were mixed and dispersed at 15000 rpm for 20 minutes with a Dispermat disperser model TU. After the mixing and dispersion, the formulation was ground in a batch mill APS 250 provided with

zirconium oxide balls to reduce the particle size below 40 micrometers. After milling at 7000 rpm for 20 minutes, the component A of the epoxy paint was obtained. Then, 12 wt.% of component B, which consisted on a polyaminoamide (Crayamid 195X60, Cray Valley), was added to component A and stirred for 5 minutes with the disperser.

The Epoxy-DMSO/PAni primer was prepared by mixing 19 wt.% of epoxy resin, which was previously dispersed in DMSO, 7 wt.% of titanium dioxide, 24 wt.% of barite, 12 wt.% of talc, 0.27 wt.% of Aerosil 200, 1 wt.% of Antiterra U, 1 wt.% by weight of BYK-500 and BYK-525, and 20 wt.% of DMSO. The dispersion process was identical to that described for the Epoxy-DMSO/Zn formulation. The addition of the organic anticorrosive pigment required special attention, since PAni-EB is a solid with a remarkable tendency to agglomerate when contacted with a liquid medium. In order to incorporate the PAni-EB to the paint formulation (component A), it was necessary to reduce the particle size using an ultrasonic homogenizer. After the particle size reduction and microfiltration, 0.3 wt.% of PAni-EB was added very slowly to the paint formulation. The employment of PAni-EB and PTE as anticorrosive pigments in alkyd and epoxy primers is a new technology recently patented in our laboratory,[19] the complete dispersion procedure being described there. After component A preparation, 12 wt.% of the polyaminoamide (Crayamid 195X60, Cray Valley) used as component B was added and was stirred for 5 minutes with the disperser (Figure 8.1).

The Epoxy-DMSO/PTE paint was prepared by mixing 20 wt.% of epoxy resin, which was previously dispersed in DMSO, 5 wt.% of titanium dioxide, 1 wt.% of PTE, 20 wt.% of barite, 12 wt.% of talc, 0.23 wt.% of Aerosil 200, 1 wt.% of Antiterra U, 0.7 wt.% of BYK-500 and BYK-525, and 19 wt.% by weight of DMSO. The dispersion procedure was identical to that explained for PAni-EB (also detailed on reference 19), the mixing ratio of components A and B being also maintained.

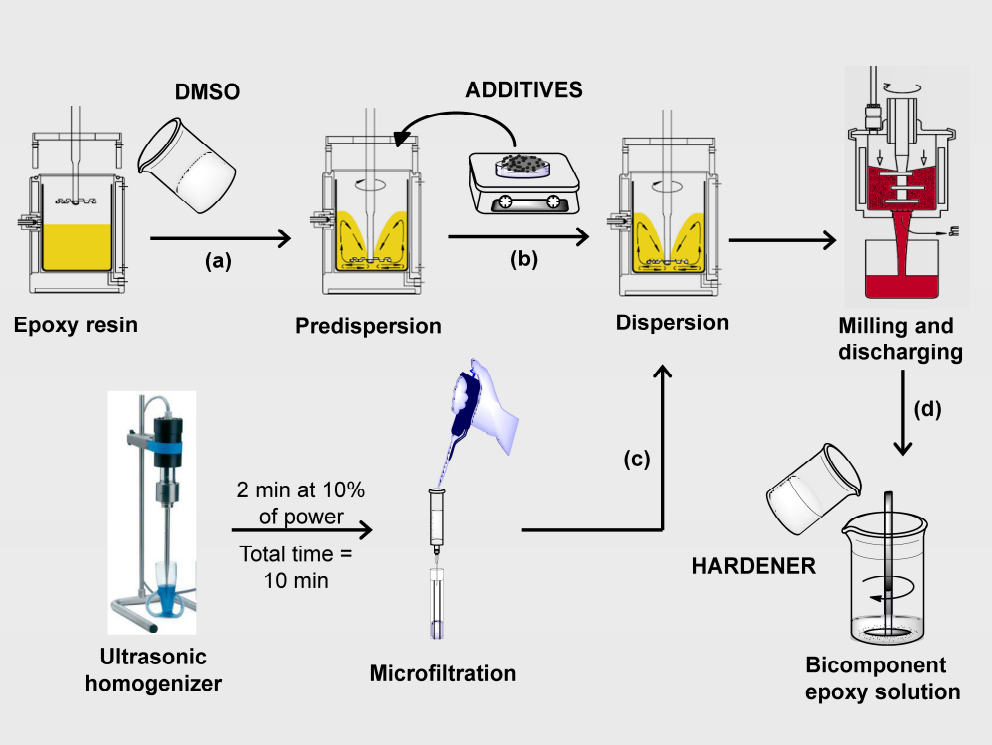

Figure 8.1. Schematic representation of the strategy used in this study for the preparation of the epoxy coatings based on DMSO, as green solvent, and conducting polymers, as non-toxic anticorrosive pigments: (a) predispersion of the epoxy resin in DMSO; (b) addition of pigments and rheological additives; (c) preparation of micrometric particles of conducting polymer in DMSO before its addition to the paint formulation; and (d) addition of polyaminoamide hardener component.

After induction time of 30-40 minutes, the paint coatings were applied by immersion of 120×40×2 mm^3 steel panels, which were previously degreased with acetone and polished with zirconium balls accordingly to standard method UNE-EN-ISO8504,[20] into the formulations. The coatings were dried on air for one week before corrosion tests. The dry film thickness (DFT), which was measured with a machine model Mega-Check pocket NFE from Neurtek S.A. company, was 90±15 μm (one coat).

Preparation of casting films for physical-chemical characterization was carried out using two procedures: (i) drying on air at room temperature for 7 days (RT); and (ii) applying a post-curing treatment at 120 °C for 24 h in an oven (HT).

8.2.3. Characterization methods

Structural characterization of the coating films was performed using a Jasco 4100 FTIR spectrometer with a resolution of 4 cm^{-1} in a wavenumber range of 4000-600 cm^{-1}. Samples were placed in an attenuated total reflection accessory with thermal control and a diamond crystal (Golden Gate Heated Single Reflection Diamond ATR, Specac-Teknokroma). Differential scanning calorimmetry (DSC) was performed using a TA Instruments Q100 series equipped with a refrigerated cooling system (RCS) operating at temperatures from -90 °C to 550 °C and employing a heating rate of 10 °C/min. Experiments were conducted under a flow of dry nitrogen with a sample weight of approximately 5 mg and calibration was performed with indium. On the other hand, thermogravimetric analyses (TGA) were carried out with a Q50 thermogravimetric analyzer of TA Instruments at a heating rate of 20 °C/min under nitrogen atmosphere and a temperature range from 20 to 600 °C. Finally, properties typically used to determine the mechanical characteristics of paints (*i.e.* Young´s modulus, tensile strength and elongation at break) were evaluated using stress-strain assays with a Zwick Z2.5/TN1S testing machine. Regular films were prepared by casting at room temperature (RT) and after post-cured treatment (HT), described on section 8.2.2. Plate samples with a length of 30 mm, a width of 3 mm and a thickness of 250-350 μm were cut out from the films for stress-strain experiments. The deformation rate was 0.8 mm/min. A total of ten independent measurements were performed for each paint film, mechanical parameters reported in this work corresponding to the average of such measurements.

8.2.4. Electrochemical impedance spectroscopy

In order to evaluate the response as anticorrosive coatings of the paints prepared in this work as a function of time, electrochemical impedance spectroscopy (EIS) was performed in aqueous 3.5 % NaCl solution at open circuit potential (E_{OCP}). The DFT is an important parameter in EIS assays and was maintained at 90±15 μm for all coatings. Two different samples were evaluated; Epoxy-DMSO/PTE and Epoxy-xylene/PTE, and two steel painted panels were considered for each one. The working electrode employed was the steel panel (AISI/SAE 1015) used as metallic substratum with an area of 0.7854 cm^2. Platinum and silver|silver chloride (Ag|AgCl) electrodes were used as counter and reference electrodes, respectively. EIS measurements were performed with a potentiostat Autolab PGSTAT 302N. The amplitude of the EIS perturbation signal was 10 mV, the frequency ranged from 10^5 to 10^{-2} Hz taking 70 frequencies per decade.

8.2.5. Field corrosion assays

Test panels of carbon steel (120×40×2 mm^3) were coated with two paint systems: epoxy priming paints prepared with DMSO non-volatile solvent as first coat and commercial epoxy paint (Hempadur epoxy primer 15300 and curing agent 95040) as topcoat. The DFT of first coat varied from 80 ± 10μm to 150 ± 20μm and the topcoat presented a DFT of 190± 20μm after one week of drying at room temperature (higher than 20 °C). All test panels were placed in a stainless steel rack (Figure 8.2a-8.2b), specially designed for the panels dimensions described before, and moved to an industrial corrosive zone over an open brine tank for chlorine gas production (Figure 8.2c). The concentration of the brine tank is about 240 g/L of NaCl and the temperature during the winter months is around 35 °C whereas in the summer months the temperature reach almost 60 °C. Field corrosion assays were performed in Hispavic Ibérica S.L., which is an important company from Solvay S.A. Group and PVC manufacturer. This company is located at Martorell, a Spanish city 30 km far from Barcelona.

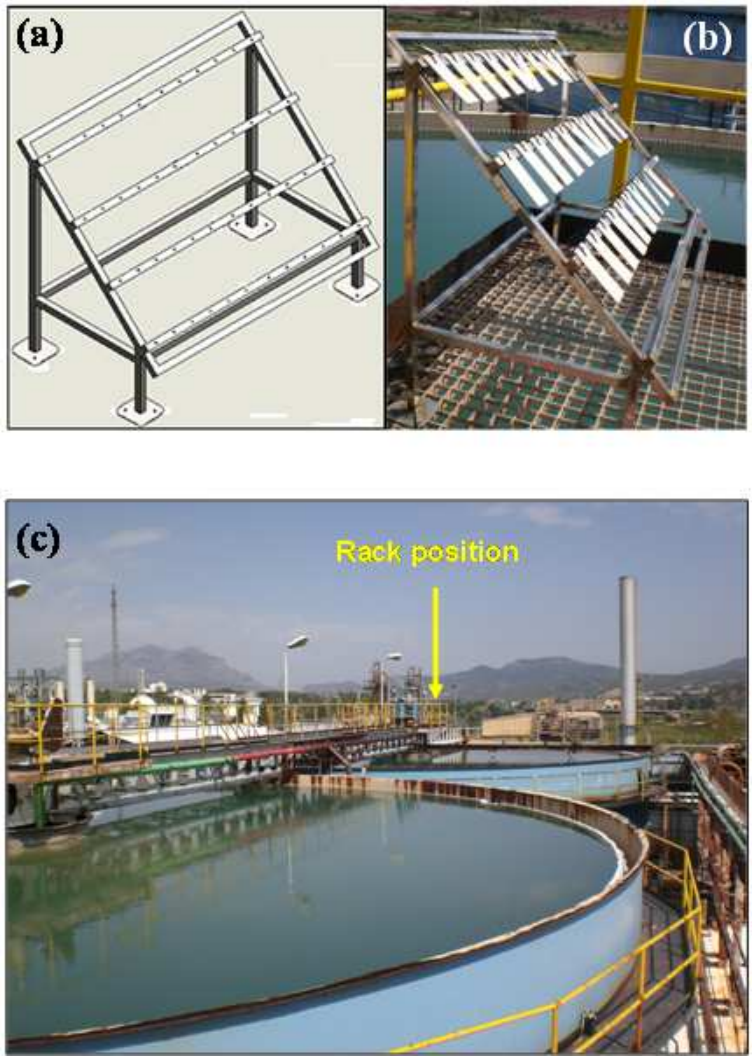

Figure 8.2. (a) Rack prototype with scale dimensions of 1:20. (b) Photography of stainless steel AISI 316L rack constructed as samples holder. (c) Open brine tanks at Hispavic Ibérica S.L., located at Martorell (Spain). Arrow indicates the position of rack for long-term corrosive assays.

8.3. Results and Discussion

8.3.1. Epoxy-DMSO formulation

Organic coatings are a complex mixture of binder, which is the main constituent, pigments, solvents and additives. In order to replace xylene by DMSO as solvent in the two-component epoxy coating (*i.e.* composed by an epoxy resin and a curing agent), the compatibility between the Epikote resin 1001 (solid epoxy resin produced from bisphenol A and epichlorohydrin) and DMSO was evaluated. Accordingly, an epoxy-DMSO solution was prepared using the same conditions that for the commercial available epoxy resin prepared in xylene. Due to the high viscosity of the Epikote 1001, homogenisation of the solid resin with a low concentration of DMSO required 6 hours of magnetic stirring at room temperature (higher than 20 °C).

After this, the solubility in DMSO of the CPs, PAni-EB and PTE, and the zinc phosphate dihydrate used as anticorrosive pigments was examined. As expected, zinc phosphate dehydrate was very easy to disperse in DMSO due to the high miscibility of this solvent in water. On the other hand, the strong aggregation tendency and poor solubility of CPs in common solvents are well-known. However, PAni-EB was ease to dissolve in DMSO, reasonable dispersion being achieved when the PAni-EB powder size was reduced applying 20 minutes of ultrasound stirring. Previous works demonstrated that chloroform,[21] N-methyl pyrrolidone,[22] and xylene[23] are solvents able to disperse various forms of polyaniline. Nevertheless, as they are not green solvents, they have not been considered for the formulation of sustainable paints.

CPs based on PAni and PTh have been previously dispersed in DMSO with ultrasounds before of their incorporation to the paint formulation (Figure 8.1). In opposition to PAni-EB, PTE has no tendency to agglomerate, even though it is very important reduce its particle size to achieve a well dispersed solid in the liquid paint. The particle size of PTE in DMSO after microfiltration is around 141.05 ± 38.88 nm, measured by Static Light Scattering with a Vasco Particle Size Analyzer. PTE and behaves as anticorrosives and as pigments, providing yellow color to the final paint. PAni-EB offers lilac-colored films.

In order to compare with conventional epoxy formulations, epoxy-xylene formulations with the same epoxy/amine and PVC/CPVC ratios were prepared. The volatile and toxic aromatic hydrocarbon solvent content of the latter xylene formulations (260 g/L) drastically decreased to 70 g/L for in epoxy-DMSO based paint. Thus, complete elimination of xylene as solvent, methyl isobutyl ketone (MIBK) or butanol as co-solvents, from epoxy formulation was not possible due to the high insolubility a of the curing agent in DMSO and as well to its high viscosity parameters. New directives related with the VOC content in paints and varnishes were implemented in the last European Council of the Paint, Printing Ink and Artists' Colours Industry (CEPE), the maximum VOC content for chemically curing anticorrosive primers being established to be 290 g/L.[24] Therefore, the formulations described in this work not only use a less toxic solvent with very low releases into the environment but also accomplish with the European Commission regulations. On the other hand, replacement of zinc phosphate anticorrosive additive by a low concentration of CP, either PAni-EB or PTE, results in a decrease of the coating density: from 1370 kg/cm^3 for Epoxy-DMSO/Zn to 1100 kg/cm^3 and 1160 kg/cm^3 for Epoxy-DMSO/PAni and Epoxy-DMSO/PTE coatings, respectively. This represents an important benefit for many applications.

However, formulation of such coatings is not an easy task and some experimental problems must be overcome. When xylene is substituted by DMSO, the coating maintains its low-temperature curing (discussed in section 8.3.2) but the time of dry to touch increases from 6-8 h to 48 h at 20 °C. This drawback can be overcome by applying surface thermal treatment to accelerate the solvent evaporation and curing process. Another handicap is the service temperature, which must be higher than the DMSO melting point of 18.45° C. This limitation affects both the paint frabrication process and the use of the paints. Regarding to the former, problems can be easily avoided if manufacturers use a dissolver system with a double-wall container with slight heating (*i.e.* to minimise the risk of epoxy base resin solidification inside the container). However, the use of these new paints below 19-20 °C is not recommended and customers should avoid their application in winter season or in Nordic countries.

8.3.2. Spectroscopy and thermal characterization

Epoxy systems are preferred materials chosen for application as protective coatings due to their excellent barrier properties, high chemical resistance to common solvents, high thermal stability and good mechanical properties. The properties of these thermosetting polymers are highly dependent on the curing process. For this reason, paint manufacturers always indicate some physical constants and application details related to the curing process, (*i.e.* the mixing ratio between the epoxy base resin and the hardener, the time and temperature for fully cured material, or the dry film thickness). Two component epoxy-xylene primers are usually considered to be fully cured without further thermal treatment after 7 days at 20 °C. We assumed that replacement of xylene by DMSO will affect the curing process of the epoxy system.

Figure 8.3 compares the FTIR spectra obtained for Epoxy-xylene RT and Epoxy-DMSO RT films, which were prepared by solvent casting at room temperature and allowed to dry for 7 days without vacuum, with the Epoxy-DMSO HT films that were prepared by casting and cured at 120 °C for 24 hours. We observed that the polymerisation of epoxy terminal groups from DGEBA and polyaminoamide was complete, independently of both the solvent and application of the thermal treatment at 120 °C. The absence of the absorption of epoxy ring (~915 cm^{-1}) and the presence of OH and C–N groups corroborate the conversion of epoxy group into the corresponding polymer and the crosslinking process.

Another aspect that deserves consideration is the evaporation of DMSO from the polymer matrix in films. Although the DMSO absorption bands are not present in the FTIR spectra in Epoxy-DMSO RT or HT coatings (see Table 8.1), complete evaporation from the polymer films cannot be ensured. Indeed, we assumed that a small amount of solvent remains trapped inside the epoxy polymer chains because of its very high boiling point. Table 8.1 summarizes the main absorption bands obtained for the epoxy coatings studied in this work, comparison with xylene[25] and DMSO[26] pure solvents being also provided. It is well known that the characterization of coatings by FTIR spectroscopy is a difficult task due to the presence of many additives and pigments. Figure 8.3 allows us to distinguish the

presence of silicates and phosphates additives in the complex composition by the presence of Si-O and P-O bands at ~1000 cm^{-1}, whereas the identification of CPs is due to their very low concentration in the paint formulation (0.3 wt.%), as reported in previous works.[27]

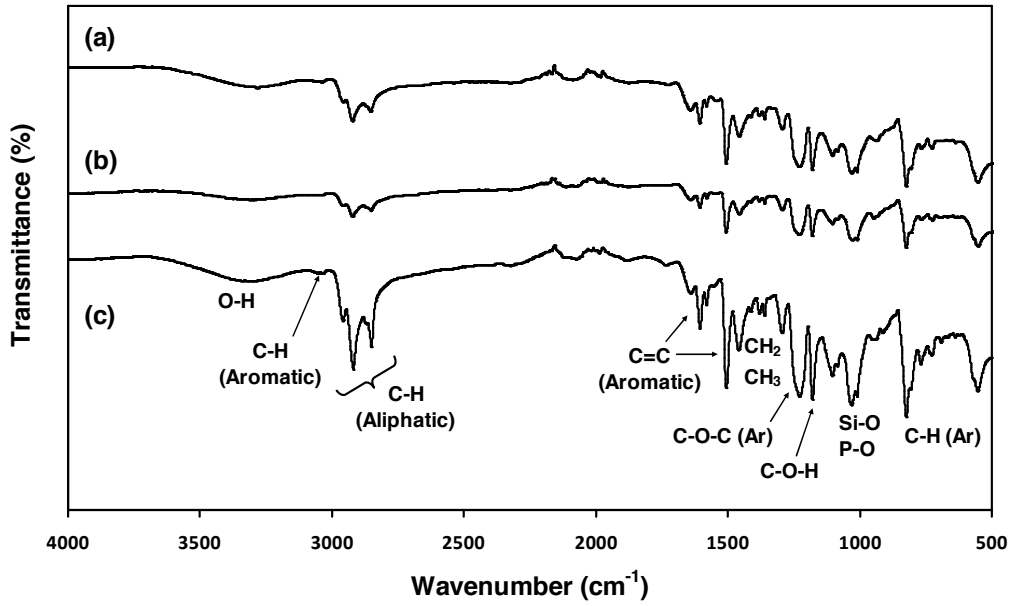

Figure 8.3. FTIR-ATR spectra of the epoxy coatings: (a) Epoxy-DMSO after cured at 120 °C for 24 h; (b) Epoxy-DMSO and (c) Epoxy-xylene both cured at room temperature for 7 days.

Sample	Absorption band [a] (cm^{-1})	Assignments [b]
Epoxy-xylene	3570-3144 (m, bd)	O-H stretch (H-bonded)
	3060 (vw), 3036 (vw)	Aromatic C-H stretch
	2958 (m), 2918 (s), 2850 (m)	Aliphatic C-H stretch
	1644 (w), 1605 (m), 1580 (w), 1545 (w, sh)	Aromatic C=C stretch
	1505 (vs)	Aromatic ring stretch
	1460 (m)	CH_3 bend (asym and sym)
	1384 (vw), 1363 (vw)	*gem*-dimethyl (doublet)
	1412 (vw)	CH_2 bend
	1295 (m)	O-H in-plane bend (secondary alcohol)
	1229 (s, bd)	C-O stretch (Aryl substituted ether)
	1179 (s)	C-O stretch (secondary alcohol)
	1105 (w, bd)	C-N stretch
	1085 (vw, sh)	C-O stretch (Alkyl substituted ether)
	1032 (s, bd), 1009 (m, sh)	Si-O, P-O stretch (silicates and phosphates additives)
	823 (s), 804 (sh), 768 (m), 727 (w)	Aromatic C-H bend (in *para*-substituted benzene)
	570 (m, sh), 553 (s, bd)	C-H, N-H bend
Epoxy-DMSO	3600-3120 (m, bd)	O-H stretch (H-bonded)
	3062 (vw), 3035 (vw)	Aromatic C-H stretch
	2959 (m), 2921 (s), 2854 (m)	Aliphatic C-H stretch
	1644 (w), 1607 (m), 1581 (w), 1542 (w, sh)	Aromatic C=C stretch
	1507 (vs)	Aromatic ring stretch
	1457 (m)	CH_3 bend (asym and sym)
	1384 (vw), 1362 (vw)	*gem*-dimethyl (doublet)
	1414 (vw)	CH_2 bend
	1294 (m)	O-H in-plane bend (secondary alcohol)
	1232 (s, bd)	C-O stretch (Aryl substituted ether)
	1178 (s)	C-O stretch (secondary alcohol)
	1104 (w, bd),	C-N stretch
	1085 (vw, sh)	C-O stretch (Alkyl substituted ether)
	1033 (s, bd), 1010 (m, sh)	Si-O, P-O stretch (silicates and phosphates additives)
	823 (s), 807 (sh), 767 (m), 727 (w)	Aromatic C-H bend (in *para*-substituted benzene)
	554 (s, bd)	C-H, N-H bend
Xylene [c] (mixture of isomers)	3130-3070 (m)	Aromatic C-H stretch
	2950 (m), 2850 (m)	Aliphatic C-H stretch
	1615 (w), 1510-1450 (s)	Aromatic C=C stretch
	1225-950 (m)	Aromatic C-H in-plane bend
	900-670 (several, m, w)	Aromatic C-H out-of-plane bend
	860 (m), 810 (w), 730 (s)	Aromatic C-H bend (in *ortho*-, *meta*- and *para*-substituted benzene)

	3000 (m), 2918 (m)	C-H stretch
	1436 (s), 1416 (m), 1404 (m)	CH_3 asymetric deformation
DMSO [d]	1325 (w, sh), 1306 (m), 1291 (w, sh)	CH_3 symetric deformation
(liquid)	1055 (vs, bd)	S-O stretch
	1012 (s), 946 (s), 921 (m), 887 (w)	CH_3 rocks
	690 (s), 661 (m)	C-S stretch

Note: [a] s = strong, m = medium, w = weak, v = very, sh = shoulder, bd = broad; [b] sym = symmetric, asym = asymmetric, gem = geminal [c] Data from reference [25] and [d] Data from reference [26].

Table 8.1. Infrared absorption bands for the epoxy paint films prepared in this work. Comparison with the bands of the solvents used for the paint formulation is included.

Thermal analyses revealed important differences between the xylene and DMSO compositions. Figure 8.4 displays the calorimetric curves for the Epoxy-xylene RT and Epoxy-DMSO RT after 7 days of evaporation at room temperature, and the Epoxy-DMSO HT with curing treatment at 120 °C for 24 hours. As it can be seen in the first heating, the Epoxy-xylene RT (Figure 8.4a) has a glass transition (T_{g0}, without further thermal treatment) at 52.4 °C and a fusion process between 120 and 160 °C, whereas the Epoxy-DMSO RT (Figure 8.4b) has a T_{g0} at 43.6 °C and many fusion and crystallisation processes at temperatures higher than 67 °C. This phenomenon is associated with our previous assumption that an amount of DMSO remains inside the polymer matrix, the peaks observed being associated to the DMSO evaporation and further polymerisation of the epoxy coating. Both xylene and DMSO, affect the thermal behaviour of epoxy coatings, making difficult the complete polymerisation of the epoxy (*i.e.* they prevent the complete curing of the films). Thus, additional peaks related to fusion process are not expected to appear in completely epoxy resins. Within this context, DMSO behaves worse than xylene because some molecules of the former solvent remains trapped inside the polymer matrix.

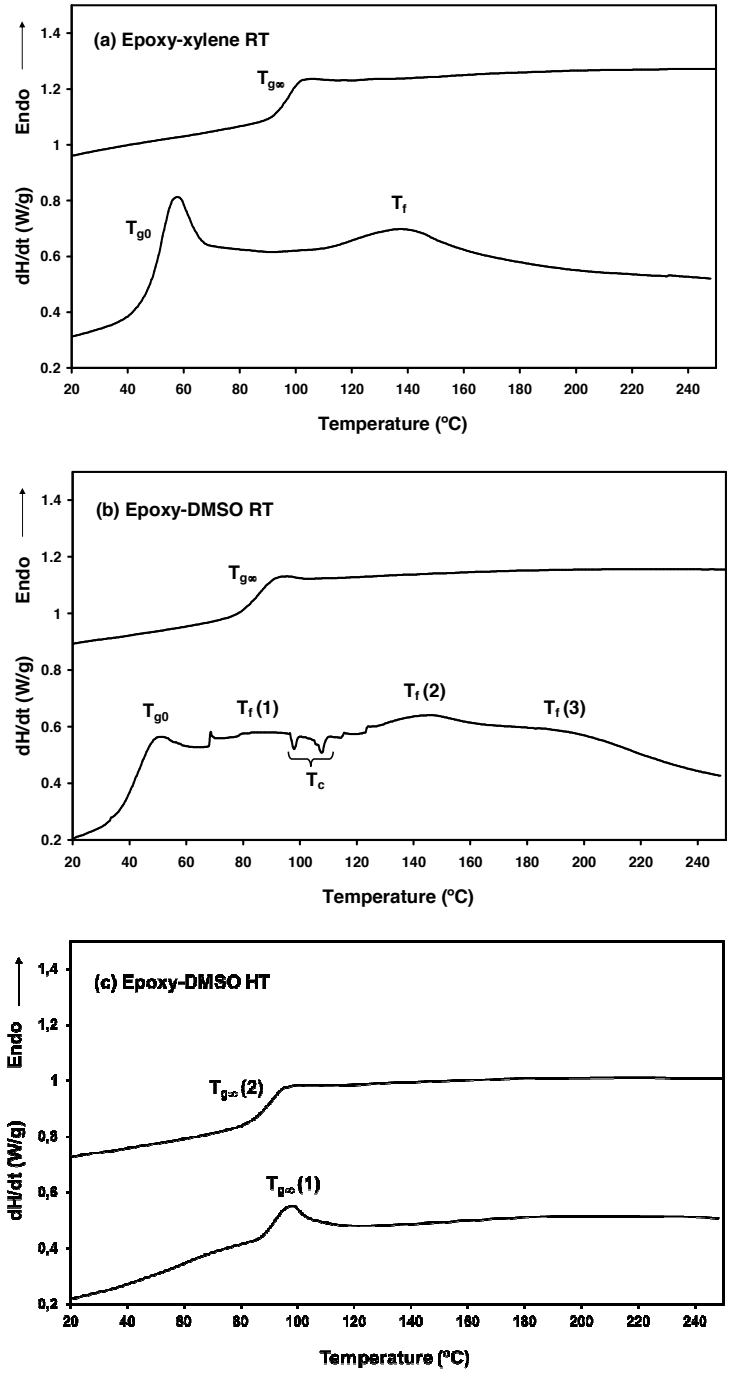

Figure 8.4. DSC curves showing the glass (T_g), crystallisation (T_c) and melting (T_f) transitions associated to: (a) Epoxy-xylene RT, (b) Epoxy-DMSO RT and (c) Epoxy-DMSO HT. Heating rate: 20 °C/min. First heating: down; and second heating: up.

In the second heating process, DMSO induces a lower $T_{g\infty}$ (where $T_{g\infty}$ corresponds to the glass transition of a sample fully cured) for the epoxy system than xylene (*i.e.* 87.0 °C and 91.4 °C, respectively). This behaviour suggests that the solvent participates in the crosslinking of polymer chains, acting as a plasticizer and improving the post-curing process. However, this observation only appears after application of additional isothermic treatment. These results indicate that the thermal treatment at 120 °C is not necessary for the paint application since the T_{g0} of the epoxy system (*i.e.* around 50±7 °C) is higher than the room temperature, evidencing that the epoxy polymer is partially cured. Accordingly, no further isothermal treatment is needed if the mechanical and barrier properties of the films are good enough to enable their use as protective coating.

Finally, Figure 8.4c shows the DSC curves for the Epoxy-DMSO film treated at 120 °C for 24 hours. In this case, the epoxy is free of DMSO, the film being fully cured. Thus, the $T_{g\infty}$ values obtained from the first and second heating curves, $T_{g\infty}$=92.2 °C and 92.4 °C, respectively, are very similar to that achieve for the Epoxy-xylene RT film ($T_{g\infty}$=91.4 °C, Figure 8.4a).

The DSC curves of coatings modified with CP showed the same $T_{g\infty}$ values that the epoxy system with zinc phosphate after complete curing process. However, the coatings without isothermal treatment present a broad fusion peak from 90 to 200 °C, which has been associated to the covalent interaction between the epoxy resin and PAni or PTE. CPs are amorphous materials able to interfere with the crystalline domains of polymer chains, as recently reported for systems based on mixtures of thermoplastic polyurethane (TPU) and PTE[28], affecting the fusion process.

The thermal stability of the epoxy resins formulated with DMSO and modified with CPs has been evaluated by TGA. Figure 8.5 compares the TGA curves for the epoxy resins modified with zinc phosphate, PAni-EB or PTE (Epoxy-DMSO/Zn, Epoxy-DMSO/PAni and Epoxy-DMSO/PTE resins, respectively) but without containing inorganic additives and pigments. Thus, these systems are not final paint coatings, as is reflected by the low amount of solid contents at 600 °C. All films were first cured at 120 °C for 24 h to ensure the elimination of DMSO and to obtain a cross-linked material. As expected, the

decomposition temperatures are very high in all cases: 421 °C, 433 °C and 437 °C for the Epoxy-DMSO/Zn, Epoxy-DMSO/PTE and Epoxy-DMSO/PAni resins, respectively. Interestingly, the addition of PAni-EB and PTE produced a small increment in the thermal stability of the epoxy resin, which has been attributed to the interaction of the amine and ester groups with the polymer chains. The solid content of the modified epoxy resins at 600 °C is lower than 15 % whereas the solid contents typically observed for epoxy paints (with additives and pigments) range from 30 % to 45 %.

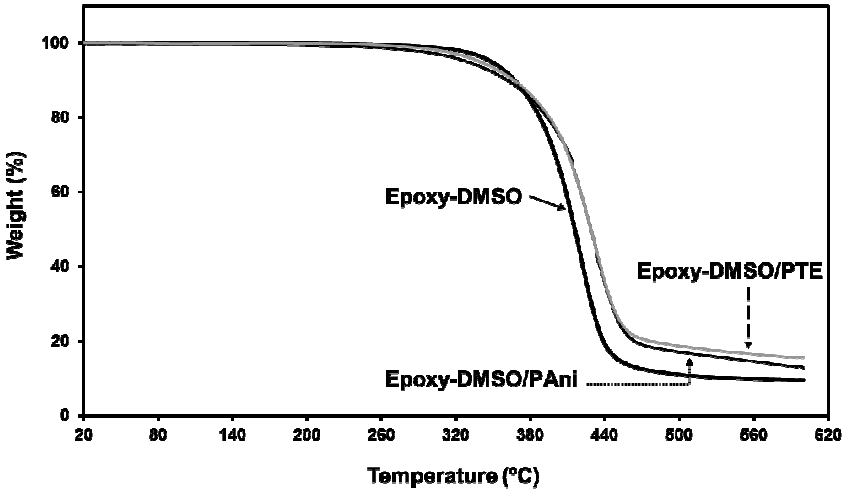

Figure 8.5. Thermogravimetric analyses of epoxy resins prepared using DMSO, and inorganic [$Zn_3(PO_4)_2$] or organic CPs (Pani-EB and PTE) anticorrosive pigments. All samples were previously cured at 120 °C for 24 h.

8.3.3. Mechanical properties of the Epoxy-DMSO coating compared to Epoxy-xylene

The Young's modulus, tensile strength and strain to break of the epoxy coatings prepared using DMSO as solvent differ significantly from those of conventional paints prepared in xylene. Figure 8.6 (a-c) shows the stress-strain curves for the coatings prepared at RT and HT. In general, Epoxy-xylene films have high tensile strength (σ_{max}=25-32 MPa) and very low elongation at break (ε_b=2.7-3.4 %) when deformed at room temperature, as is typically observed in epoxy systems.[29] In contrast, Epoxy-DMSO films present very low

tensile strength (σ_{max}=3-5 MPa) and very high elongation at break (ε_b=121-189 %), independently of the curing temperature. Therefore, DMSO solvent produces a significant reduction of the elastic modulus (*E*=5-7 MPa) and an enhancement of ductility, this behaviour being similar to that observed for some thermoplastics.[29]

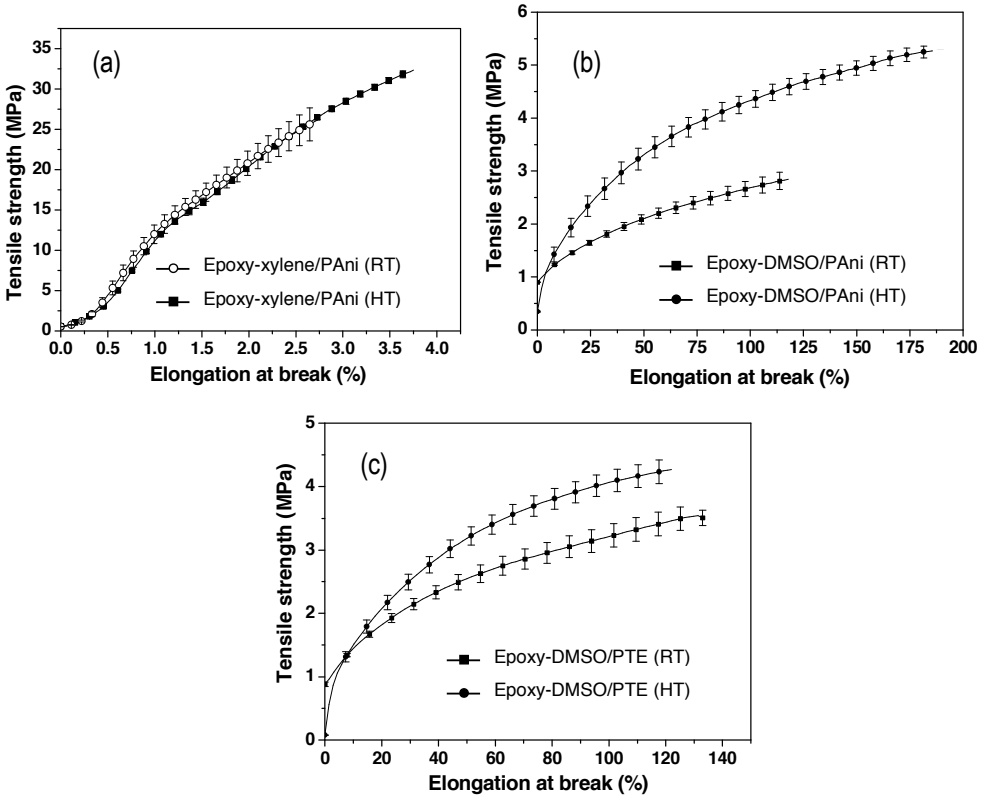

Figure 8.6. Stress-strain curves for the epoxy coatings dried at room temperature for 7 days (RT) and after fully cured at 120 °C for 24 hours (HT): (a) Epoxy-xylene with 0.3 wt.% of PAni-EB, (b) Epoxy-DMSO with 0.3 wt.% of PAni-EB and (c) Epoxy-DMSO with 0.3 wt.% of PTE. Deformation rate: 0.8 mm/min.

It should be mentioned that Epoxy-DMSO/Zn films were not assayed because of their extremely high brittle behaviour. Unfortunately, we were unable to cut the films to obtain the test samples. As this is the first anticorrosive epoxy paint prepared with zinc phosphate prepared with DMSO as solvent, the reasons of this brittle behaviour are not definitively

clear. However, we assume that it comes from the high amount of zinc phosphate in the paint formulation (10 wt.%), which is significantly higher than in Epoxy-DMSO/PAni and Epoxy-DMSO/PTE. These results indicate that PAni-EB, PTE and DMSO interact favourably with the epoxy system giving a plastic behaviour with less brittle properties than conventional epoxy paints prepared with xylene.

8.3.4. Comparison of Epoxy-DMSO/PTE and Epoxy-xylene/PTE anticorrosive performance

Several authors investigated the failure mechanism of different coating systems by multi-frequency ac impedance measurements.[16,22,30-33] This procedure allows to monitor the behavior of coated surfaces giving valuable information about both coating degradation and the coating resistance to protect the metal surface. The corrosion behavior of uncoated and epoxy coated steel panels was evaluated by electrochemical impedance spectroscopy (EIS) in 3.5 wt.% NaCl aqueous solution considering different immersion times (Figure 8.7). The corrosion potential (E_{OCP}), coating resistance (R_p) at high frequencies, and coating capacitance (C_c) derived from impedance curves are listed in Table 8.2.

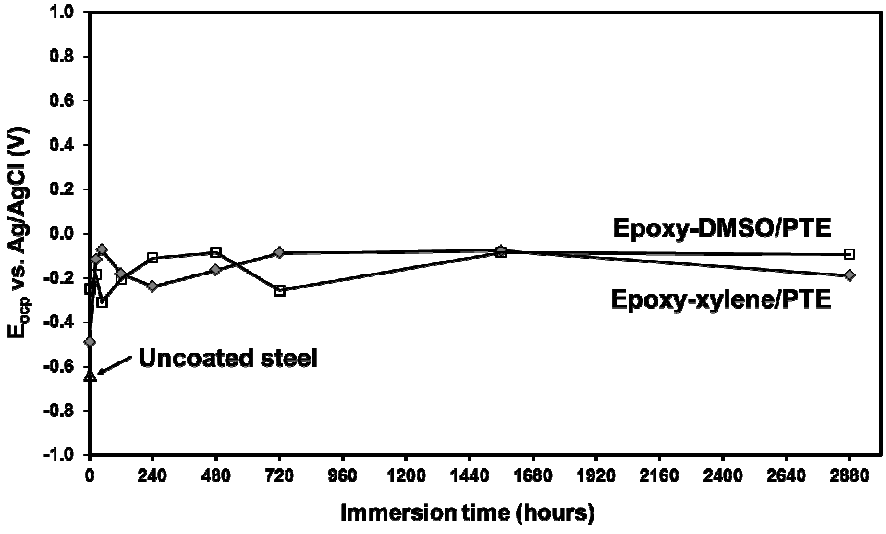

Figure 8.7. Evolution of the corrosion potential (E_{OCP}) with the immersion time.

The E_{OCP} of unprotected mild steel is very low and negative (-0.638 V), whereas the protected metal has more positive values. More specifically, Epoxy-xylene/PTE and Epoxy-DMSO/PTE showed similar corrosion potential during four months (2880 hours), as is reflected in Figure 8.7. Accordingly, both coatings exert the same protection compared to the uncoated steel, maintaining almost constant E_{OCP} values during the four months of exposure in NaCl 3.5 %.

Figure 8.8 shows the Nyquist plot at various immersion time for the uncoated steel and coated with Epoxy-DMSO/PTE and Epoxy-xylene/PTE. Uncoated carbon steel has a high inductive loop at the low-frequency region, which is due to the fast adsorption and desorption of oxides in the metal surface (Figure 8.8a). However, coated steel substrates show a highly resistive behavior with impedance values of about 10^9-10^{10} $\Omega \cdot cm^2$ at high frequencies (Figure 8.8b), these values being comparable to those obtained for other protecting coatings.[33] In organic coatings systems the pore resistance (R_p), which is associated to the coating resistance, usually decreases with time, as is evidenced in Table 8.2. Although epoxy systems present high chemical resistance to both solvents and water, they are porous materials and, therefore, aggressive electrolytes are able reach the metal surface in a short time. Fortunately, the anticorrosive additive offer an additional resistance to metal corrosion, acting as sacrificial anode or promoting a passive layer between the metal and coating interface. The two PTE-containing epoxy formulations studied in this section, which differ in the solvent, show similar protection. This result indicates that the solvent does not affect the permeability of the coating. Indeed, differences in coating resistance must be attributed to the thickness of the coatings, which is higher for the Epoxy-DMSO/PTE (107±12 μm) than for the Epoxy-xylene/PTE paint (72±8 μm).

EIS tests revealed that both coatings have only one time constant (σ) at initial exposure in NaCl (from 1 h to 20 days), evidenced by only one semi-circle. This feature indicates the excellent barrier protection and high impermeability of the epoxy coating. The coating resistance values (R_p) gradually decreased (from 20×109 to 3×106 $\Omega \cdot cm^2$) and the coating capacitance (C_c) gradually increased (from 1.2×10-10 to 3.0×10-9 $F \cdot cm^2 \cdot s^{n-1}$) with the immersion time (Table 8.2). As the NaCl diffusion inside the coating is unavoidable, a

second time constant (σ) appears after 20 days of immersion test (Figure 8.8c). Indeed, this is detected by a slight increase of a second semi-circle in the low frequency zone. This can be interpreted by the time required to initiate the development of other significant interface under the coating, like passive layers or oxide corrosion products from pitting or deposited substances. However, this is a good result taking to account that the coating resistance is still high after 4 months (~2×106 $\Omega \cdot cm^2$; data not shown). Comparison of the EIS results obtained for these same epoxy systems with those recently reported for PTE-containing alkyd systems indicates that the latter start to corrode earlier, the second time constant being observed after 7 days only.[34]

After four months in contact with sodium and chloride ions, the Nyquist curves show only two time constants (Figure 8.8d), evidencing that the coating systems still protect the metal. No pitting signal was visually observed inside the coating, indicating that the second semi-circle appeared after 20 days is not due to an aggressive oxide product formation. EIS results are in excellent agreement with outdoor industrial corrosive assays performed over an open brine tank (see next section).

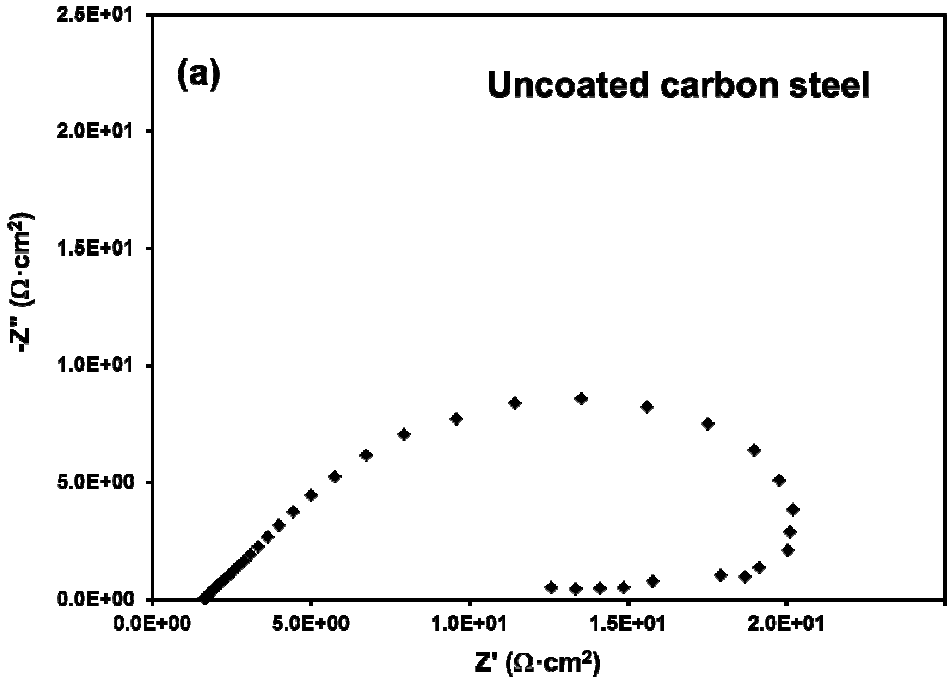

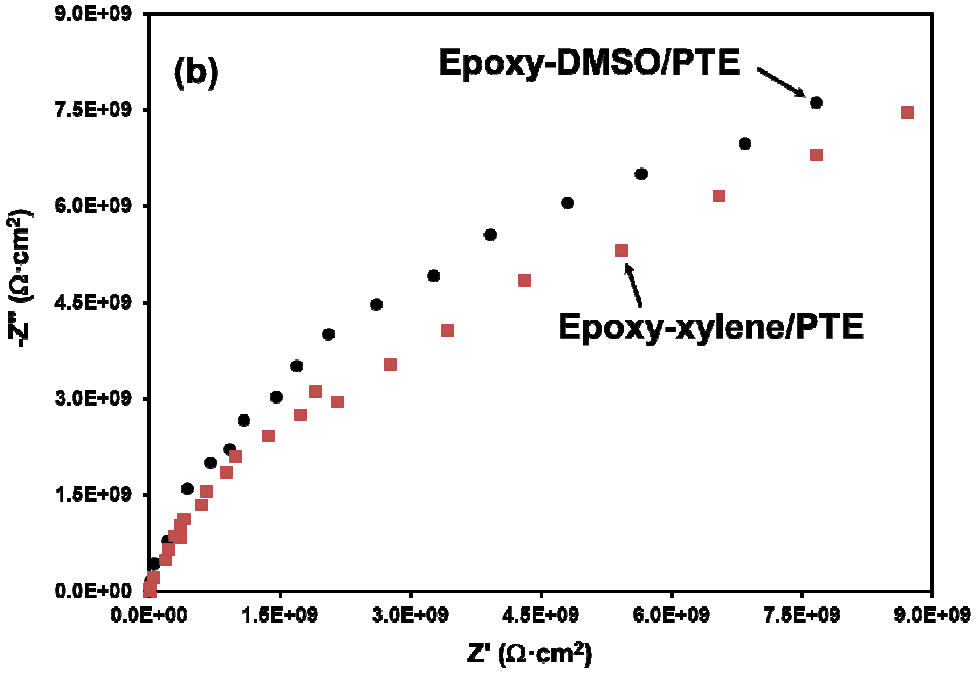
(b)
Epoxy-DMSO/PTE
Epoxy-xylene/PTE
-Z'' (Ω·cm²)
Z' (Ω·cm²)
9.0E+09
7.5E+09
6.0E+09
4.5E+09
3.0E+09
1.5E+09
0.0E+00
0.0E+00
1.5E+09
3.0E+09
4.5E+09
6.0E+09
7.5E+09
9.0E+09

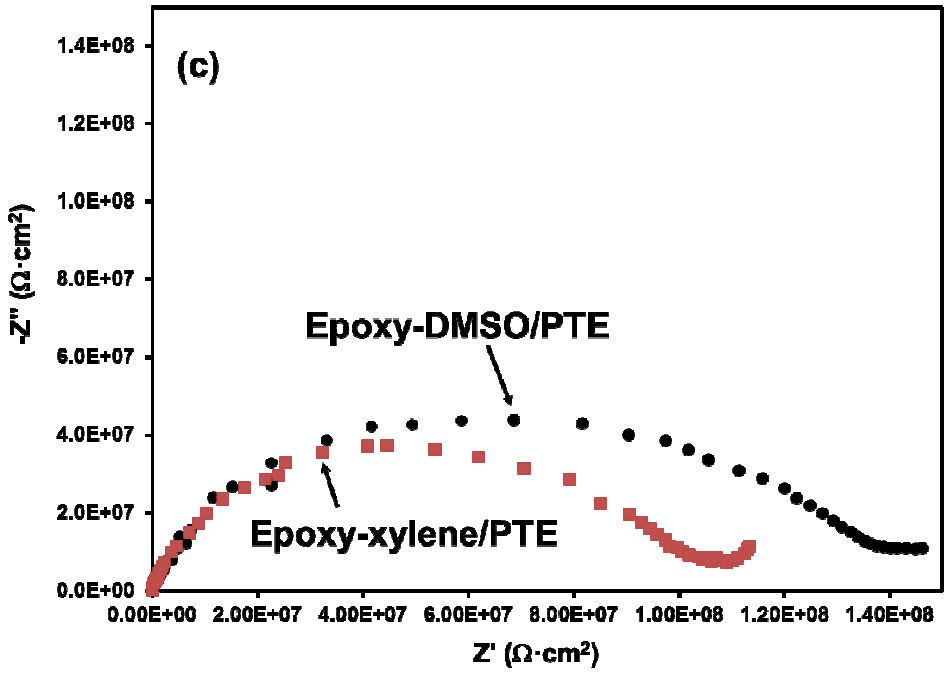
(c)
Epoxy-DMSO/PTE
Epoxy-xylene/PTE
-Z'' (Ω·cm²)
Z' (Ω·cm²)
1.4E+08
1.2E+08
1.0E+08
8.0E+07
6.0E+07
4.0E+07
2.0E+07
0.0E+00
0.00E+00
2.00E+07
4.00E+07
6.00E+07
8.00E+07
1.00E+08
1.20E+08
1.40E+08

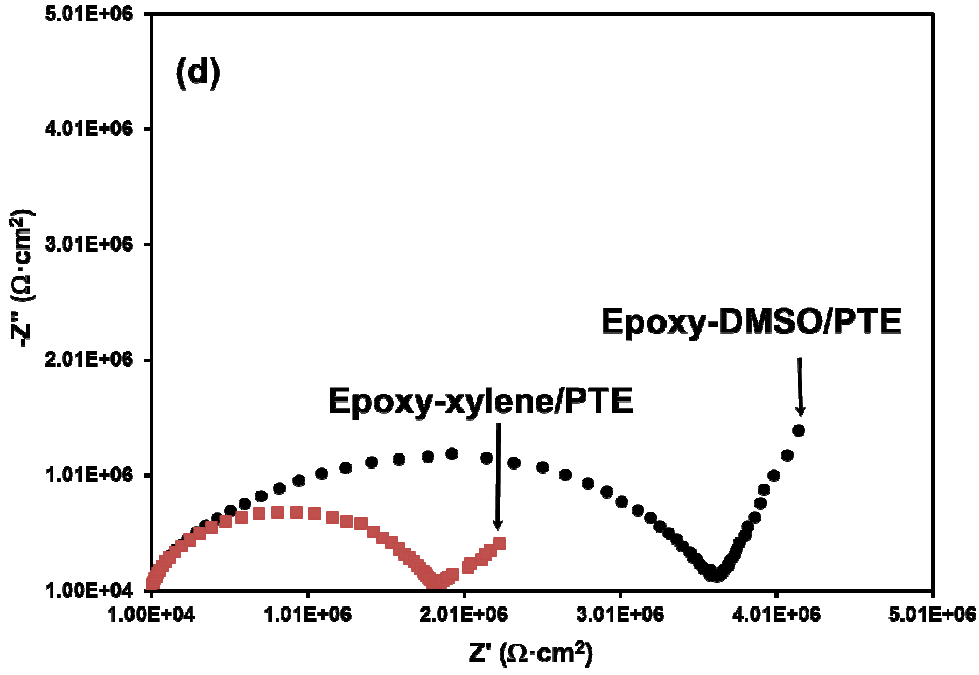

Figure 8.8. Nyquist plot of mild steel after 1 hour of immersion in NaCl 3.5 % (a) and mild steel coated with Epoxy-DMSO/PTE and Epoxy-xylene/PTE after 1 hour (b), 20 days (c) and two months (d) of immersion in NaCl 3.5 %.

It should be mentioned that Epoxy-DMSO/Zn films were not assayed because of its extremely brittle behaviour (one coat application). In spite of this, the performance of this formulation was checked in the outdoor assays (see next section). In regard to the Epoxy-DMSO/PAni, results (not shown) indicate that this coating offers lower protection than the PTE-containing systems (*i.e.* lower coating resistance and higher capacitance than Epoxy/PTE). However, these results are been omitted because the anticorrosive properties of Epoxy/PAni systems were extensively studied in previous works.[21,23,27,34]

Immersion time	1 hour		24 hours		48 hours		5 days	
Sample	Epoxy-xylene/PTE	Epoxy-DMSO/PTE	Epoxy-xylene/PTE	Epoxy-DMSO/PTE	Epoxy-xylene/PTE	Epoxy-DMSO/PTE	Epoxy-xylene/PTE	Epoxy-DMSO/PTE
E_{OCP} (V) [a]	-0.490	-0.248	-0.116	-0.184	-0.074	-0.309	-0.182	-0.204
R_p ($\Omega \cdot cm^2$)	19.8 G	21.9 G	3.57 G	3.06 G	2.63 G	2.29 G	0.98 G	0.89 G
C_C ($F \cdot cm^{-2} \cdot s^{n-1}$)	$1.20 \cdot 10^{-10}$	$5.43 \cdot 10^{-10}$	$4.87 \cdot 10^{-10}$	$5.49 \cdot 10^{-10}$	$9.95 \cdot 10^{-11}$	$6.27 \cdot 10^{-11}$	$5.75 \cdot 10^{-10}$	$1.72 \cdot 10^{-10}$
n	0.84	0.78	0.67	0.61	0.74	0.77	0.72	0.78

Immersion time	10 days		20 days		30 days		65 days	
Sample	Epoxy-xylene/PTE	Epoxy-DMSO/PTE	Epoxy-xylene/PTE	Epoxy-DMSO/PTE	Epoxy-xylene/PTE	Epoxy-DMSO/PTE	Epoxy-xylene/PTE	Epoxy-DMSO/PTE
E_{OCP} (V) [a]	-0.238	-0.110	-0.164	-0.085	-0.088	-0.256	-0.078	-0.085
R_p ($\Omega \cdot cm^2$)	200 M	257 M	103 M	138 M	35.8 M	39.0 M	5.57 M	1.65 M
C_C ($F \cdot cm^{-2} \cdot s^{n-1}$)	$3.34 \cdot 10^{-9}$	$9.73 \cdot 10^{-10}$	$5.53 \cdot 10^{-10}$	$8.19 \cdot 10^{-10}$	$2.59 \cdot 10^{-9}$	$5.26 \cdot 10^{-9}$	$4.93 \cdot 10^{-10}$	$3.01 \cdot 10^{-9}$
n	0.69	0.69	0.81	0.72	0.82	0.87	0.69	0.77

[a] The open circuit potential for uncoated mild Steel after one hour in NaCl 3.5 wt.% is -0.638 V.

Table 8.2. Data of EIS results obtained from Nyquist plots for Epoxy-xylene/PTE and Epoxy-DMSO/PTE coatings after exposure to NaCl 3.5 wt.% aqueous solution.

8.3.5. Performance of Epoxy-DMSO anticorrosive paint in outdoor corrosion tests

The phenomenology of blister formation and growth on coated mild steel exposed to outdoor industrial corrosion assays was evaluated. The high thickness of the coatings allowed an excellent protection for the three systems studied as long as 2 years of exposure. All epoxy systems imparted protection as barrier coatings, no failure being induced in the films. This behavior is fully consistent with EIS results, which reflected high coating resistances and low coating capacitances. Figure 8.9 shows the absence of any blistering in Epoxy-DMSO/PAni and Epoxy-DMSO/PTE after 2 year of exposure, indicating that they represent a good alternative to the less sustainable coating formulated with xylene and zinc anticorrosive additives.

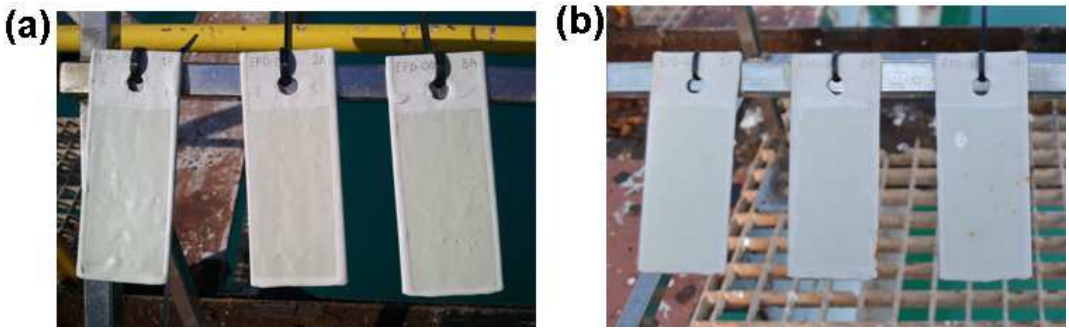

Figure 8.9. Digital photographs of coated samples exposed to outdoor assays at initial exposure (a) and after 2 years (b), above the brine tank at Solvay Martorell S.A. From left to right: Epoxy-DMSO/PTE, Epoxy-DMSO/PAni and Epoxy-xylene/Zn.

8.4. Conclusions

Solvent-borne products, which play a very dominant role in the protective coatings marketplace, are generally preferred to water-borne products. These preferences are due to considerations such as excellent performance, application and handling characteristics and aesthetic appearance. A key advantage of this work is the ability to make not only a two-component epoxy primers with drastically low VOC value (70 g/L) but also high

performance anticorrosive coatings free of toxic inorganic zinc components. The solvent used in the epoxy paint formulation offers less health and environmental hazards than the traditionally used solvents, such as aromatic hydrocarbons and alcohols. Although the epoxy coatings based on DMSO as solvent and PTE or PAni-EB as anticorrosive pigments have extremely slow surface dry due to the non-volatile component, they have excellent corrosion resistance properties. Moreover, the adhesion to metallic substrates remained for two years in outdoor corrosive ambient, which makes them useful in marine and heavy duty industrial applications. Furthermore, the resistance protection results provided by epoxy coatings formulated with DMSO are comparable to those achieved with coatings formulated with xylene.

While researchers in industrial settings must be free to choose their own solvent content, inside the maximum VOC limit content value of 290 g/L for multi-pack primers and intermediates established by European Community in January 1st, 2012; those of us who are motivated to reduce solvent-related environmental damage focus our research efforts on potential solutions to those problems. Therefore, the benefits of the present study must be measured against the objective of significantly reducing VOC emissions from the xylene-based epoxy protective primers, usually used outside installations, and to eliminate zinc as anticorrosive additive for epoxy primers for steel protection.

8.5. References

[1] D. Stoye and W. Freitag, in *Paints, Coatings and Solvents*, 2nd. Edition, Wiley & Sons-VCH, 1998, Chapters 2-3 and 14.

[2] F.H. Walker and M.I. Cook, in *Technology for Waterborne Coatings*, ACS Symposium Series 663; J. Edward Glass Ed., American Chemical Society: Washington, DC; 1997.

[3] M. Cook, F.H. Walker and D.A. Dubowik, “Developments in Two-Pack Water-Based Epoxy Coatings”, *JOCCA-Surf. Coat. Intern.*, 1999, **82**, 528-535.

[4] M. Lohe, M. Cook and A.H. Klippstein, "3-dimensional epoxy binder structures for water damp permeable and breathable coating and flooring systems", *Macrom. Symp.*, 2002, **187**, 493-502.

[5] T. Erdmenger, C. Guerrero-Sanchez, J. Vitz, R. Hoogenboom and U.S. Schubert, "Recent developments in the utilization of green solvents in polymer chemistry", *Chem. Soc. Rev.*, 2010, **39**, 3317-3333.

[6] R. Hofer and K. Hinrichs, in *Additives for the Manufacture and Processing of Polymers, in Handbook Environmental Chemistry, Vol. 12, Polymers: Opportunities and Risks II: Sustainability, Product Design and Processing*, ed. P. Eyerer, M. Weller and C. Hübner, Springer Verl., Berlin, Heidelberg, 2010, 97–145.

[7] A. Azapagic, A. Emsley and I. Hamerton, *Polymers: The Environment and Sustainable Development*, John Wiley & Sons, 2003.

[8] M. Lohe, M. Cook and A.H. Klippstein, Patent Number: EP1544230-A1; US2005154091-A1; JP2005200646-A; CN1637039-A; KR2005062456-A; CN100349948-C; US7528183-B2; US2009176931-A1; US7615584-B2; EP1544230-B1; DE60336737-E; KR1070716-B1.

[9] EU Regulations, Directive 2004/42/EC of the European Parliament and of the Council of 21 April 2004 on the limitation of emissions of volatile organic compounds due to the use of organic solvents in certain paints and varnishes and vehicle refinishing products and amending Directive 1999/13/EC. Official Journal of the European Union, DO L143/87, 30.4.2004.

[http://ec.europa.eu/environment/air/pollutants/stationary/solvents/legislation.htm; accessed 6 August 2012]

[10] EU Regulations, EC No 1907/2006 of the European Parliament and of the Council of 18 December 2006 concerning the Registration, Evaluation, Authorisation and Restriction of Chemicals (REACH), establishing a European Chemicals Agency.

[http://ec.europa.eu/enterprise/sectors/chemicals/documents/reach/review2012/registration_requirements_en.htm, accessed 6 August 2012]

[11] I. Soroko, Y. Bhole and A. G. Livingston, "Environmentally friendly route for the preparation of solvent resistant polyimide nanofiltration membranes", *Green Chem.*, 2011, **13**, 162-168

[12] W. M. Nelson, *Green solvents for chemistry: Perspectives and practice in Green Chemistry*, Oxford University Press, USA, 1st Ed., 2003, Chapter 3: pages 60-62 and Chapter 5: pages 116-132.

[13] M. Doble and A. Kumar, *Green Chemistry and Engineering*, Elsevier Inc., 2007, Chapter 5: pages 93-104.

[14] M. Warner and J. E. Hutchison, *Greener Approaches to Undergraduate Chemistry Experiments*, Print; M. Kirchhoff and M. Ryan, Eds.; American Chemical Society: Washington D.C., 2002; pp 32-34.

[15] Dimethyl Sulfoxide Producers Association, US Environmental Protection Agency, Report number 201-14721A, Leesburg, VA 20175, September 8, 2003.

[16]. P. Lima-Neto, A. P. Araújo, W. S. Araújo and A. N. Correia, "Study of the anticorrosive behavior of epoxy binders containing non-toxic inorganic corrosion inhibitor pigments", Prog. Org. Coat., 2008, **62**, 344-350.

[17] EU Regulations, Directive 2006/11/EC of the European Parliament and of the Council of 15 February 2006 on pollution caused by certain dangerous substances discharged into the aquatic environment of the Community. Official Journal of the European Union, DO L64/52-59, 4.3.2006.

[18] B. Kim, L. Chen, J. Gong and Y. Osada, "Titration behavior and spectral transitions of water-soluble polythiophene carboxylic acids" *Macromolecules,* 1999, **32**, 3964-3969.

[19] E. Armelin, C. Alemán, J.I. Iribarren, F. Liesa and F. Estrany, Patent Cooperation Treaty PCT/ES2010070820, 2010.

[20] UNE-EN-ISO 8504: Preparation of steel substrates before application of paints and related products - Surface preparation methods, International Organization of Standardization, 2nd Edition, 2000.

[21] E. Armelin, A. Meneguzzi, C.A. Ferreira and C. Alemán, "Polyaniline, polypyrrole and poly(3,4 ethylenedioxythiophene) as additives of organic coatings to prevent corrosion" *Surf. Coat. Technol.*, 2009, **203**, 3763-3769.

[22] M. Tiitu, A. Talo, O. Forsén and O. Ikkala, "Aminic epoxy resin hardeners as reactive solvents for conjugated polymers: Polyaniline base/epoxy composites for anticorrosion coatings", *Polymer*, 2005, **46**, 6855-6861.

[23] E. Armelin, C. Alemán and J. I. Iribarren, "Anticorrosion performances of epoxy coatings modified with polyaniline: A comparison between the emeraldine base and salt forms" *Prog. Org. Coat.*, 2009, **65**, 88-93.

[24] Okopol Institute for Environmental Strategies, Hamburg, Germany, in *Implementation and Review of Directive 2004/42/EC Final Report*, Part 1 and 2 of 10 November 2009. [http://ec.europa.eu/environment/air/pollutants/pdf/paints_report.pdf; accessed 6 August 2012]

[25] J. Coates, "Interpretation of Infrared Spectra, A Practical Approach" in *Encyclopedia of Analytical Chemistry*. R.A. Meyers (Ed.), John Wiley & Sons Ltd., Chichester, 2000, 10815-10837.

[26] F. A. Cotton, R. Francis and W. D. Horrocks Jr., "The infrared spectra of some dimethyl Sulfoxide complexes", *J. Phys. Chem.*, 1960, **64**, 1534-1536.

[27] E. Armelin, R. Pla, F. Liesa, X. Ramis, J.I. Iribarren and C. Alemán, "Corrosion protection with polyaniline and polypyrroleas anticorrosive additives for epoxy paint", *Corr. Sci.* 2008, **50**, 721-728.

[28] M. M. Pérez Madrigal, M. I. Giannotti, G. Oncins, L. Franco, E. Armelin, J. Puiggalí, F. Sanz, L. J. del Valle and C. Alemán, "Bioactive nanomembranes of semiconductor polythiophene and thermoplastic polyurethane: thermal, nanostructural and nanomechanical properties", *Polym. Chem.,* 2013, **4**, 568-583.

[29] W. D. Callister, Jr. *Materials Science and Engineering: An Introduction*, 7th edition, John Wiley & Sons Ltd., New York, 2007, Chapter 15, 524-543.

[30] O. Schneider and R.G. Kelly, "Localized coating failure of epoxy-coated aluminium alloy 2024-T3 in 0.5 M NaCl solutions: Correlation between coating degradation, blister formation and local chemistry within blisters", *Corr. Sci.,* 2007, **49**, 594-619.

[31] X. Liu, J. Xiong, Y. Lv and Y. Zuo, "Study on corrosion electrochemical behavior of several different coating systems by EIS", *Prog. Org. Coat.*, 2009, **64**, 497-503.

[32] A. Collazo, X. R. Nóvoa, C. Pérez and B. Puga, "The corrosion protection mechanism of rust converters: An electrochemical impedance spectroscopy study", *Electrochim. Acta*, 2010, **55**, 6156-6162.

[33] A. Sakhri, F.X. Perrin, E. Aragon, S. Lamouric and A. Benaboura, "Chlorinated rubber paints for corrosion prevention of mild steel", *Corr. Sci.*, 2010, **52**, 901-909.

[34] M. Martí, G. Fabregat, D. S. Azambuja, C. Alemán and E. Armelin, "Evaluation of an environmentally friendly anticorrosive pigment for alkyd primer", *Prog. Org. Coat.*, 2012, **73**, 321-329.

9

CONCLUSIONS

The main conclusions of this PhD Thesis are listed below:

1. PNMPy microspheres are successfully prepared using the LbL self-assembly templating technique. This process allows controlling the size of the microspheres through the diameter of PS microspheres, which are used as a template.

2. Hollow PNMPy microspheres are obtained by removing the PS template with tetrahydrofurane. The resulting hollow microspheres are free standing when the thickness of the PNMPy shell is of 30 nm (*i.e.* nanostructured layer).

3. PNMPy/PSS core-shell microspheres are incompatible with solvent-borne epoxy paints. This precludes the use of such nanostructured CP as anticorrosive additive of conventional organic primers.

4. Metallic zinc dust of marine epoxy primers can be partially replaced by 0.3 wt.% of PAni-ES without any detrimental effect in the protecting properties. Moreover, the adherence properties of the coating improve upon the incorporation of PAni-ES.

5. The partial substitution of zinc dust in marine epoxy primers by a small concentration of PAni-ES produces a change in the corrosion protection mechanism. In the new mechanism, the CP protects steel through an autocatalytic cycle based on the reversible transformation between its doped and neutral forms.

6. Among the alkyd primers investigated, the Alkyd-PTE/1 showed the best anticorrosive properties, evidencing that PTE is a very powerful corrosion inhibitor. Replacement of zinc phosphate by a low concentration of this eco-friendly additive results in an improvement of the corrosion protection, an enhancement of the adherence and a reduction of the permeability.

7. PTE induces the formation of spots dispersed on the surface of the metal, which consist on calcium carbonate particles released from the formulation of the paint. These spots are well adhered and act as a passivating layer. The formation of such protecting particles is not promoted by PAni-ES and PAni-EB.

8. In spite of its poor solubility, PAni-EB has been found to be more effective as anticorrosive additive in epoxy formulations than polythiophene derivatives with multiple carboxylate groups. This has been attributed to the fact that the electroactivity of PAni-EB is higher than those of such polythiophenes.

9. PTE has been found to be more effective as anticorrosive additive for epoxy paints than PT3AME and PT3MDE. Despite of the higher solubility of the latter, electrochemical properties of the former are more appropriated for such purpose.

10. The results presented in this PhD Thesis provide a significant advance towards the new environmental regulations to decrease, or even eliminate, the use of metal containing compounds as anticorrosive pigments.

11. Epoxy coatings based on DMSO as solvent and a CP as anticorrosive pigment have been formulated. These coatings present very low VOC values (70 g/L) and high performance anticorrosive coatings free of toxic inorganic zinc components, offering offers less health and environmental hazards than coatings based on traditional organic solvents.

12. Epoxy coatings based on DMSO as solvent and a CP as anticorrosive pigments have excellent corrosion resistance properties, excellent application and handling characteristics, and aesthetic appearance.

13. Moreover, the adhesion of epoxy coatings based on DMSO and PTE to metallic substrates remained for two years in outdoor corrosive ambient, which makes them useful in marine and heavy duty industrial applications. This resistance protection is comparable to that achieved with coatings formulated with xylene.

14. The overall of the results presented in this Thesis represents a significant advance in the field related with the application of CPs as anticorrosive additives.